CARBON AND OXYGEN ISOTOPE STUDIES IN MARBLES

CARBON AND OXYGEN ISOTOPE STUDIES IN MARBLES

By

Simon Mark Foster Sheppard, B.A.

A Thesis

Submitted to the Faculty of Graduate Studies

in Partial Fulfilment of the Requirements

for the Degree

Doctor of Philosophy

McMaster University

July, 1966

DOCTOR OF PHILOSOPHY — McMASTER UNIVERSITY

(Geochemistry) — Hamilton, Ontario.

TITLE: Carbon and Oxygen Isotope Studies in Marbles

AUTHOR: Simon Mark Foster Sheppard, B.A. (University of Cambridge)

SUPERVISOR: Professor H.P. Schwarcz

NUMBER OF PAGES: x, 185

SCOPE AND CONTENTS:

Fractionations of C^{13}/C^{12}, O^{18}/O^{16} ratios and Mg between co-existing dolomite and calcite have been determined from rocks of a variety of metamorphic grades in Vermont and the Grenville of Ontario. Working criteria for equilibrium are established. Temperature dependent fractionation expressions are derived (1) for O^{18} and C^{13} from the C- and O-isotope fractionations concordant with the Mg-calcite solvus thermometer, for T = 130° to 550°C, using natural dolomite-calcite assemblages; (2) for C^{13} from hydrothermal partial exchange experiments. Problems with partial exchange reactions are discussed. A thermodynamic analysis of the solvus relations shows that spinodal decomposition probably is important in high Mg-calcites. Quench phenomena in high grade assemblages are complex. The quench temperature may be much lower than the maximum temperature attained. The sizes of some equilibrium systems are delineated.

ACKNOWLEDGEMENTS

I wish to thank Professor Henry P. Schwarcz for his encouragement, directorship and the many tangible and intangible benefits derived from his counsel throughout the course of this work.

I am indebted to Dr. H.G. Thode for the use of his mass spectrometer laboratory and facilities, together with the many assistances extended by Mr. Jan Monster.

To Dr. Robert N. Clayton, special thanks for advice, and assistance with the calibration of the isotopic standards.

I acknowledge the use of Dr. B.J. Burley's laboratory where the hydrothermal experiments of this work were performed. The assistance provided by Mr. Peter M. Anderson especially is appreciated.

My thanks are extended to Drs. J.H. Crocket, R.D. MacFarlane, G.V. Middleton, D.M. Shaw and members of the department for helpful discussions and advice at various stages during the development of this work.

I am also grateful to the following for financial support during this study:

McMaster University

Government of Ontario (Graduate Fellowship)

International Nickel Company of Canada

National Research Council (Studentship)

Finally to Margaret, my thanks for her encouragements and unreserved acceptance of many secretarial tasks to hasten the progress of this thesis.

TABLE OF CONTENTS

TABLES

LIST OF ILLUSTRATIONS

I. HISTORICAL BACKGROUND

Calcite and dolomite are the principal minerals of important groups of rocks occurring in an extremely wide variety of physicochemical environments: sedimentary, metamorphic, hydrothermal and igneous. In any physicochemical analysis of such natural systems application of the concept of equilibrium is vital and fruitful. Intrinsically the system calcite-dolomite is of considerable interest because of the potential simultaneous thermometric equilibrium properties of the carbon and oxygen isotope and cation partition coefficients.

The theoretical basis for equilibrium isotope effects was established by Urey (1947) and Bigeleisen and Mayer (1947). This allows the unambiguous calculation of the equilibrium constant for an isotopic exchange reaction, provided that the characteristic vibrational frequencies for the isotopic species are known. Although this latter point is met rarely for condensed phases, the theory predicts the form of the temperature dependency as a function of the vibrational frequency.

The geothermometric properties of oxygen isotope fractionations between calcite and water were first exploited by McCrea (1950), Epstein *et al.* (1951, 1953), and Urey *et al.* (1951). At the same time, the modification of the Nier (1947) mass spectrometer by McKinney *et al.* (1950) increased the precision in determining the O^{18}/O^{16} and C^{13}/C^{12}

ratios using CO_2 gas from 0.1% to 0.01%. This step forward not only enabled the temperature of the ancient oceans to be determined to ±0.5°C, but allowed Clayton and Epstein (1958) to open up the field of high temperature isotopic geothermometry.

The two pioneering papers in high temperature isotopic geothermometry by Clayton and Epstein (1958) and Engel et al. (1958) established that isotopic equilibrium was attained and frequently preserved. These authors also appreciated that the isotopes could be used as tracers to study certain geological processes. Their encouraging results stimulated subsequent work in igneous and metamorphic systems (Taylor and Epstein, 1962a & b; James and Clayton, 1962; Taylor et al., 1963; Taylor and Epstein, 1963; Garlick, 1964; Schwarcz and Clayton, 1965; Sharma et al., 1965; Schwarcz, 1966).

Laboratory calibration of the isotopic geothermometers has played an integral part in this development (McCrea, 1950; Epstein et al., 1951, 1953; Clayton, 1959, 1961; O'Neil and Clayton, 1964; Northrop and Clayton, 1966; O'Neil and Epstein, 1966).

Despite the considerable number of isotopic studies on sedimentary calcite-dolomite assemblages (e.g. Clayton and Degens, 1959; Keith and Weber, 1964; Degens and Epstein, 1964; Weber, 1964) relatively little attention has been directed to metamorphosed calcite-dolomite assemblages or marbles (Schwarcz, 1966).

In the recent literature, two incompatible groups of data for the dolomite-calcite O-isotope fractionation have been contrasted, based on studies in sedimentary, metamorphic and hydrothermal environments

(Friedman and Hall, 1963; Epstein et al., 1964; Northrop and Clayton, 1966; O'Neil and Epstein, 1966):

1) 1-4‰ fractionations in high temperature rocks.

2) 0-2‰ fractionations in sedimentary rocks.

One or both of these groups must be disequilibrium fractionations. The sedimentary results are disequilibrium fractionations (Epstein et al., 1964; O'Neil and Epstein, 1966). However, there is a marked disparity between the high temperature fractionations, group 1, the results from studies on metamorphic marbles by Schwarcz (1966) and the experimentally determined O-isotope fractionation expressions by Northrop and Clayton (1966) and O'Neil and Epstein (1966).

Research Objectives

This research attempts to combine the three basic approaches to geochemistry; observational, experimental and theoretical, to these problems in calcite-dolomite systems from metamorphic environments:

1) To determine experimentally the carbon equilibrium isotope fractionation as a function of temperature.
2) To investigate the attainment and preservation of isotopic equilibrium and to evaluate the geothermometric properties of carbon and oxygen isotope fractionations.
3) To determine the concordant or discordant relations between the various carbonate geothermometers.
4) To delineate the size of equilibrium isotopic exchange systems for carbon and oxygen.

5) To elucidate the nature of petrological processes during the metamorphism of limestone.

6) To consider some aspects of the thermodynamics of the calcite-dolomite solvus relations.

II. INTRODUCTION

2.1 Definition of Terms

2.1.1 Carbonates

Unless otherwise stated specifically the name calcite will refer to magnesian calcite solid solutions having the calcite structure, space group $R\bar{3}c$. Similarly, dolomite will refer to the ordered Ca-Mg carbonates with the dolomite structure, space group $R\bar{3}$. For dolomite the superlattice reflections due to long-range ordering are sharp. In some instances, calcite may contain micro- or crypto-exsolution blebs of dolomite.

The following subscript abbreviations will be used:

Ct	=	Calcite
D	=	Dolomite
x	=	sample x
std	=	standard

2.1.2 δ Values

The results of carbon and oxygen isotope analyses of a sample x are expressed as the per mil deviation of the C^{13}/C^{12} or O^{18}/O^{16} ratio from that ratio in an arbitrary standard:

$$\delta_x = \left(\frac{R_x}{R_{std}} - 1 \right) 1000$$

where R_x = C^{13}/C^{12} or O^{18}/O^{16} in sample x

R_{std} = C^{13}/C^{12} or O^{18}/O^{16} in standard

The δ value for carbon is reported relative to the Chicago PDB standard (Craig, 1957), and that for oxygen relative to standard mean ocean water (SMOW) (Craig, 1961). The raw mass spectrometer data are corrected, δC^{13} for the O^{17} contribution and δO^{18} for the C^{13} contribution (Craig, 1957).

2.1.3 Fractionation Factors and Isotopic Equilibrium Constants

The isotopic fractionation factor, α, between two phases x and y is defined by

$$\alpha_{x-y} = \frac{R_x}{R_y}$$

In general at equilibrium

$$\alpha = K^{1/n}$$

where K is the isotopic equilibrium constant and n is the number of exchangeable atoms. Consider the isotopic exchange of oxygen between dolomite and calcite:

$$1/3\ CaCO_3^{18} + 1/6\ CaMg(CO_3^{16})_2 \rightleftharpoons 1/3\ CaCO_3^{16} + 1/6\ CaMg(CO_3^{18})_2$$

At equilibrium

$$K^{O^{18}}_{D-Ct} = \alpha^{O^{18}}_{D-Ct} = \frac{(O^{18}/O^{16})_D}{(O^{18}/O^{16})_{Ct}}$$

The fractionation factor, α, is a measured property. Thus, it is expedient to avoid equating it with the isotopic equilibrium constant until the fractionation is shown unambiguously to be the equilibrium value at that particular temperature.

For simplicity, the fractionation between x and y is expressed as 1000 ln α_{x-y} where α generally is of magnitude 1.00X and 1000 ln 1.00X $\simeq$ X. For small differences in δ, 1000 ln $\alpha_{x-y} \simeq \delta_x - \delta_y \equiv \Delta_{x-y}$.

Superscripts O^{18} and C^{13} are used to refer respectively to oxygen isotope fractionations and carbon isotope fractionations.

2.2 Theory

2.2.1 General Considerations, Temperature Dependence

The theory of equilibrium isotopic exchange has been developed by Urey (1947) and Bigeleisen and Mayer (1947). Only the results which are of importance are quoted here. This theory predicts that the exchange equilibrium constant should vary with temperature in such a way that:

1) ln K is proportional to 1/T at low temperature when $\frac{hc\omega}{kT} > 20$ (high frequencies) for all contributing vibrations.

2) ln K is proportional to $1/T^2$ at high temperature when $\frac{hc\omega}{kT} < 5$ (low frequencies) for all contributing vibrations.

3) ln K $\rightarrow$ 0 at infinite temperature, $kT \gg h\nu$, when the vibrational partition functions approach their classical value, $kT/h\nu$.

For most polyatomic oxygen and carbon compounds the vibrational frequencies are of the order of 1000 $cm.^{-1}$ and $hc\omega/k\,T < 5$ for $T > 300°K$. However, the CO_2 molecule has vibrational frequencies up to 2400 $cm.^{-1}$. OH bonds also form a notable exception with frequencies around 4000 $cm.^{-1}$. In reactions involving water the $1/T^2$ proportionality is not expected until $T > 1000°K$.

The expression for the temperature dependence of the equilibrium fractionation in many systems, e.g. $CaCO_3 - H_2O$ or $C^{13}O_3^{=}$ (aq) - $C^{12}O_2$ (g), has both a crossover point and a minimum (O'Neil and Clayton, 1964; Thode et al., 1965). These characteristics are explicable from theoretical considerations.

Many assumptions are involved in the above generalizations. In general, these become less satisfactory with increase in temperature. At present, calculation of the equilibrium isotopic exchange constant usually cannot be performed satisfactorily for condensed phases. In the meantime, this qualitative structure provides a framework within which to discuss and interpret the observed fractionations. The linear dependence of the fractionation on $1/T^2$ is an approximation of particular importance.

2.2.2 Pressure Dependence

Partition coefficients for the distribution of elements between coexisting phases are functions of temperature, pressure and composition (see § 4.4). Isotopic partitioning is, to a very good approximation, a function of temperature only at constant composition.

There is no overall chemical change in an isotopic exchange reaction; the two sides of such an equation have essentially identical molar volumes. Therefore, the pressure dependence is anticipated to be a second order effect only. With a pressure difference of 4kb. between otherwise identical experiments on bicarbonate-water exchange Hoering (1961) observed a difference of 0.2 ± 0.2‰.

Joy and Libby (1960) approached the problem by estimating the volumetric effect of isotopic substitution. Their estimate is based on assumptions which, at present, are difficult to evaluate. Bottinga (1963) and Garlick (1964) also discuss the influence of pressure and conclude that it is probably of little significance.

In a system such as calcite-dolomite there is an indirect effect of pressure on the fractionation. Increase in pressure increases the solubility of $MgCO_3$ in calcite (Goldsmith and Heard, 1961). The isotopic fractionation between dolomite and calcite is a function of this variable cation composition. This effect can be estimated from O'Neil's (1963) cationic radius-dependent equation (see § 2.2.3). At 500°C an increase in solubility of $MgCO_3$ by 1 mol %, approximately equivalent to 5kb., changes the fractionation by -0.01‰. It is concluded that the pressure dependence of the isotopic fractionation is a second order effect.

2.2.3 Chemical Effects

O'Neil (1963) determined the dolomite-pure calcite fractionation relation:

$$1000 \ln \alpha_{D\text{-}Ct}^{O^{18}} = 0.207 \, (10^6 \, T^{-2}) + 0.25 \qquad (1)^*$$

---

* Expressions (1) and (2) have not been modified using the revised α for the phosphoric acid reaction (Sharma & Clayton, 1965).

from his empirical expression:

$$1000 \ln \alpha^{O^{18}}_{carbonate\text{-}H_2O} = \frac{2.700\ (10^6\ T^{-2})}{r^{1/3}} - (r + 0.70) \quad (2)$$

where r is the cation radius in Angstroms. This expression was derived from the results of experimental studies in carbonate-water systems ($CaCO_3$ - , $SrCO_3$ - , $BaCO_3$ - , $CaBa(CO_3)_2$ - , and $CdCO_3$ - H_2O) which revealed that the fractionation was:

(1) proportional to exp (T^{-2})

(2) a function of the cationic radius

(3) independent of structure.

This empirical expression predicts that substitution of 1-2% of $FeCO_3$, $MnCO_3$, $SrCO_3$, etc. in either the calcite or dolomite structure will have only a secondary effect on the fractionation, assuming that $r = \Sigma N_i r_i$ where N_i is the mole fraction of cation i, radius r_i. Similarly, the fractionation between dolomite-pure calcite and dolomite-Mg-calcite is decreased by 0.05‰ at 500°C (calcite $MgCO_3$ = 5.6 mol %).

In some of the experimental methods the fractionation between mineral pairs is derived from a relation of the form:

$$\ln \alpha_{D\text{-}Ct} = \ln \alpha_{D\text{-}Fluid} - \ln \alpha_{Ct\text{-}Fluid}$$

where the isotopic nature of the fluid phase is assumed to be equivalent in the two separate runs. Various salts such as NaF, NH_4Cl, $CaCl_2$, and NH_4HCO_3 have been used. Taube's (1954) studies on the effect of various salts on isotopic exchange reactions showed that the ratio of the fractionation to the concentration is independent of the anionic species but strongly dependent on the cation present. Cation concentrations were of several molalities in Taube's experiments.

Similarly, Thode et al. (1965) found that the equilibrium constant for the exchange reaction:

$$C^{13}O_2 + HC^{12}O_3^- \rightleftharpoons C^{12}O_2 + HC^{13}O_3^-$$

was dependent on the concentration of Mg^{2+}. There is evidence that the system is quite complex, possibly due to the formation of various complexes in the solution.

These results recommend caution in equating the fluid phases of different runs. However, the effects in hydrothermal experiments are probably minor because:

1) usually the same salts are used.
2) the salt concentration is low (0.8 molar NaF, O'Neil (1963); 0.45 molar NH_4Cl, Northrop (1964)).
3) the solubility of the solid phase (carbonates, quartz, etc.) in the fluid solution is small, on the order of a few to tens of p.p.m..

2.3 Isotopic Studies in Natural Systems

2.3.1 Metamorphic Rocks

Clayton and Epstein (1958) and Engel et al. (1958) established that isotopic equilibrium is often preserved in mineral assemblages from moderate to high temperature environments. The observed fractionations between mineral pairs decreased with inferred increase in temperature, as predicted by the Urey-Bigeleisen-Mayer theory. Since the review of O-isotope geochemistry by Clayton (1963) more data from metamorphic minerals and rocks have filled out the picture. It will be convenient to summarize some of these general results for metamorphic rocks.

1) The isotopic composition of the minerals in a metamorphic rock are controlled by:

(a) the isotopic composition of the protolith.

(b) the degree of equilibration between the various phases.

(c) the quench temperature.

(d) the chemical composition of the minerals.

(e) the degree of exchange with other systems.

(f) the extent of decarbonation and/or dehydration, etc.

where factors (e) and (f) may drown the influence of (a).

2) Isotopic disequilibrium definitely occurs between minerals sometimes, and probably reflects the different rates of re-equilibration of the various minerals during the cooling history. Such effects appear to be more commonly associated with calcite and hydrated silicates, e.g. hornblende, biotite (Taylor and Epstein, 1962b; Schwarcz, 1966). Isotopic results in minerals with non-equivalent oxygen sites may be complex due to different rates of exchange between the oxygen atoms in different structural sites.

3) Isotopic equilibrium probably is preserved on other occasions between some minerals, e.g. quartz-magnetite (or ilmenite), quartz-muscovite, etc. (Taylor et al., 1963; Garlick, 1964).

4) Retrograde re-equilibration may be important under some circumstances, e.g. in high grade assemblages (James and Clayton, 1962; Garlick, 1964).

5) Evidence for a general decrease in rock O^{18}/O^{16} ratio with increase in metamorphic grade, i.e. approach to igneous rock isotopic composition, is variable. Evidence for this is presented by Silverman (1951), Schwander (1953), Taylor and Epstein (1962b), and Schwarcz and Clayton (1965). Garlick (1964) from his studies in central and southern Vermont, Duchess County, New York, Connecticut and Idaho concludes that there is no general evidence for a decrease in isotopic composition, although a regional depression is observed in some high grade areas.

6) Mineral isotopic homogenization over hundreds of metres in high grade pelitic schists generally is observed (Taylor et al., 1963; Taylor and Coleman, 1965).

7) Isotopic ratios largely inherited from the protolith have been observed in many non-pelitic rocks:

meta-iron formations of Quebec:	Sharma et al. (1965)
quartzites:	Taylor and Coleman (1965)
marbles:	Schwarcz (1966)
quartzites and schists:	Anderson and Clayton (1966)

These statements reflect the wide variety of isotopic effects observed in metamorphic rocks. Quench and exchange processes occurring in one assemblage may be different from those in another, but adjacent, assemblage. Hence, generalizations must be considered with caution. These results display the potential of the isotopic technique to decipher certain aspects of the metamorphic history of the minerals.

2.3.2 Studies of Carbonate Rocks

Sedimentary limestones are the protoliths of marbles. The C- and O-isotope composition of the initial sediments and the effect of diagenetic processes on them will influence the isotopic composition of the daughter marble to an extent which is dependent on the degree and nature of the metamorphic exchange and devolatilization processes.

In recent sediments the C- and O-isotope compositions of calcite are those expected for equilibrium with the environment of deposition (Craig, 1953; Clayton and Degens, 1959; Degens and Epstein, 1964). Coexisting calcite and dolomite give near zero fractionations. Degens and Epstein (1964) conclude that the dolomite is not in isotopic equilibrium with calcite, for both carbon and oxygen. With increase in age, the calcites become progressively enriched in O^{16}. A similar trend for dolomite is much less well defined. This is accounted for by the post-depositional O-isotope re-equilibration of calcite with subsurface waters, and the reluctance of dolomite to do the same. No significant change has been observed in the C-isotope composition of marine limestones over geological time (Craig, 1953; Keith and Weber, 1964). A few dolomite-calcite pairs have a $\Delta\ O^{18}_{D-Ct}$ value similar to the predicted equilibrium value of 5-10‰ (Weber, 1964; Gross and Tracey, 1966).

Although the average C-isotope composition of marine carbonates is: $\delta C^{13} = +0.6 \pm 3‰$ (Keith and Weber, 1964), associated organic carbon is usually some 15 to 30‰ enriched in C^{12} compared to carbonate carbon. Exchange between organic and carbonate carbon could occur during diagenesis or metamorphism. The average O-isotope composition of diagenetically altered limestones is: $\delta\ O^{18} = 23.8 \pm 2‰$ (Clayton, 1965).

In the calcite-dolomite system equilibrium isotopic effects were determined first, indirectly, by Clayton and Epstein (1958). They observed a consistent isotopic difference between quartz and dolomite of about 0.8‰. From associated quartz-calcite pairs, the dolomite-calcite fractionation was estimated. A 0.2-1.2‰ fractionation for $T \simeq 500°C$ was suggested by Epstein et al. (1964). O'Neil and Epstein (1966) consider that a fractionation of about 1.2‰ is consistent with their experimental fractionation studies. Nevertheless, this order of magnitude for the equilibrium fractionation at such a temperature must not be considered as being well established.

Schwarcz (1966) concluded that the isotopic behaviour of both C- and O-isotopes between calcite and dolomite may be rather complex. This was based on isotopic studies of marbles and calcareous schists from Vermont. Apparent discordant quench phenomena were observed between the O- and C-isotope fractionations. However, a relationship between Mg-calcite composition and $10^3 \ln \alpha^{C^{13}}_{D-Ct}$ was noted. Comparing Northrop and Clayton's (1966) O-isotope fractionation expression for dolomite-calcite, Schwarcz suggested that some natural O-isotope fractionations are larger than could have occurred during their metamorphism, and that others could not have crystallized in equilibrium. Inhomogeneities in isotopic composition were observed over a few feet.

The interpretation of all fractionations in this system at moderate to high temperatures must be approached with scepticism until equilibrium fractionations can be distinguished with confidence from disequilibrium fractionations.

2.4 Experimental Studies in Carbonate Systems

2.4.1 Introduction

Successful interpretation of fractionation data for coexisting minerals necessitates disentangling equilibrium from disequilibrium fractionations. Laboratory equilibration studies are invaluable, the more so in carbonate systems where different studies have resulted in conflicting interpretations.

Experimentally, there are two important types of reactions:

1) true exchange reactions - only isotopes and cations are exchanged between phases which are neither created nor destroyed during the process. For example:

$$CaMg_x(CO_3^{18})_{1+x} + CaMg(CO_3^{16})_2 \rightleftharpoons CaMg_x(CO_3^{16})_{1+x} + CaMg(CO_3^{18})_2$$

where $x \leqslant 0.8$.

2) synthesis reactions - a new phase is produced during the reaction. For example:

$$3CaCO_3 + MgCl_2 \xrightarrow{H_2O} CaCO_3 + CaMg(CO_3)_2 + CaCl_2$$

True exchange reactions, particularly if only isotopic exchange is involved, are unambiguous if the equilibrium fractionation is approached from both sides and 100% exchange achieved. Synthesis reactions, with unknown kinetic isotope effects, are best avoided. Large isotopic exchange has been observed in synthesis reactions but lack of reproducibility between runs and the difficulty of bracketing equilibrium are major problems to be contended with (Epstein *et al.*, 1964; Northrop and Clayton, 1966).

Isotopic exchange reactions accompanied with cation exchange show great enhancement compared to simple isotopic exchange reactions without cation exchange (Wyart et al., 1961; O'Neil and Taylor, 1965; Northrop, 1964). Exchange reactions in the system calcite-dolomite lend themselves readily to limited cation exchange.

There are three general classes of true exchange reaction experiments:

(1) Carbonate - H_2O

(2) Carbonate - CO_2

(3) Carbonate - Carbonate.

2.4.2 Carbonate-H_2O Systems

The first and also most extensively studied system over a wide temperature range (0° - 750°C) is $CaCO_3$-H_2O (McCrea, 1950; Epstein et al., 1953; Clayton, 1959, 1961; O'Neil, 1963; O'Neil and Clayton, 1964). Using similar hydrothermal techniques to Clayton (1959), where equilibrium was bracketed, other carbonate systems have been investigated: $SrCO_3$ - , $BaCO_3$ - , $CaBa(CO_3)_2$ - , $CdCO_3$ - H_2O (O'Neil, 1963); $CaMg(CO_3)_2$ - H_2O (Northrop and Clayton, 1966). For $CaCO_3$ - H_2O O'Neil and Clayton (1964) derived the equation:

$$1000 \ln \alpha^{O^{18}}_{Ct\text{-}H_2O} = 2.70 (10^6 T^{-2}) - 2.00 \qquad (3)$$

In systems containing dolomite isotopic exchange rates are very slow and equilibrium usually cannot be attained. Northrop and Clayton (1966) developed a partial exchange technique, subsequently referred to as PET, which theoretically enables the equilibrium fractionation to be calculated or determined by graphical extrapolation from a set of in-

complete exchange runs. This technique is used in this work (see § 6.3). For $CaMg(CO_3)_2$ - H_2O Northrop and Clayton (1966) derived the equation:

$$1000 \ln \alpha^{O^{18}}_{D\text{-}H_2O} = 3.20 (10^6 T^{-2}) - 2.00 \quad (4)$$

Certain problems with PET are not understood. For example, runs with different dolomite starting materials give different values for the fractionation. These problems are discussed further below (see § 6.4); meanwhile the results are presented with a cautionary note that the empirical fractionation may be different from the equilibrium value.

Carbonate-carbonate fractionations are determined by assuming that the fluid phase is isotopically equivalent in the two separate carbonate-H_2O runs (see § 2.2.3 for comments). Combining equations (3) and (4):

$$1000 \ln \alpha^{O^{18}}_{D\text{-}Ct} = 0.50 (10^6 T^{-2}) \quad (5)$$

It is noted that these empirical expressions are of the form predicted by the Urey-Bigeleisen-Mayer theory.

2.4.3 CO_2-Carbonate Systems

Direct equilibration between $CaCO_3$ and $CaMg(CO_3)_2$ with CO_2 was attempted by O'Neil and Epstein (1966) in the absence of water or salts. 100% exchange was not achieved. Equilibrium was apparently bracketed. CO_2-dolomite runs were restricted to 400° and 350°C. Decomposition of dolomite and sluggish reaction-rate problems prevented the use of higher and lower temperatures respectively. Dolomite-calcite fractionations are determined similarly to § 2.4.2. O'Neil and Epstein (1966) present the following equation, which they "[do] not consider to be accurate

enough for use in oxygen isotope thermometry":

$$1000 \ln \alpha^{O^{18}}_{D-Ct} = 0.56 (10^6 T^{-2}) + 0.45 \quad (6)$$

Northrop and Clayton (1966) applied PET to both CO_2-$CaCO_3$ and CO_2-$CaMg(CO_3)_2$. Unsatisfactory results with poor reproducibility were encountered. No fractionation expression was derived. They conclude that gas-solid exchange is complex.

2.4.4 Carbonate-Carbonate Systems

The direct determination of the isotopic fractionation between dolomite and calcite avoids problems associated with the fluid phase. Epstein et al. (1964) carried out two runs, using an exchange reaction only, in the presence of a single water rich H_2O-CO_2 fluid phase. Equilibrium was not approached from both directions. Limited dolomite exchange occurred.

Northrop and Clayton (1966) used dry mixtures of calcite and dolomite with a Li_2CO_3 flux; a small amount of decomposition occurs to provide the equilibrium P_{CO_2}. Exchange occurs but equilibrium fractionations apparently were not attained. Graf and Goldsmith (1955) have shown that chemical equilibrium is attained rapidly, few hours to a day, at $T \geqslant 500°C$.

2.4.5 Synthesis Reactions

Dolomite is easily synthesised from calcite by reacting it with $MgCl_2$ solution, under hydrothermal conditions. Dolomite-calcite mixtures were prepared in this way and the final fractionations measured by Epstein et al. (1964), and Northrop and Clayton (1966). The magnitude of the exchange may be very large but poor reproducibility and results inconsistent with equilibrium were obtained.

Dry mixtures of magnesite + calcite with Li_2CO_3 flux ran up against similar problems (Northrop and Clayton, 1966). However, a band of points indicating small dolomite - Mg-calcite fractionations (500°C, $\Delta\ O^{18}_{D-Ct} \simeq +0.10‰$; 750°C, $\Delta\ O^{18}_{D-Ct} \simeq +0.05‰$) were obtained, consistent with approach to equilibrium.

2.4.6 Summary and Conclusions

These investigations have been restricted primarily to the determination of the O-isotope equilibrium fractionation. At present there are many ambiguities in the results; inconsistencies exist both between the different methods and within a single method. These differences are not understood. Until these problems are resolved (see § 6.4 for a discussion) little confidence can be attached to equating even a consistent experimental fractionation with the equilibrium fractionation. Hence, the fractionation expressions (4), (5) and (6) should not be applied definitively.

Certain general outcomes from these experimental studies are advantageous to bear in mind when analysing the natural fractionation data:

1) Relative exchange rates: isotopic exchange is much more rapid in calcite than in dolomite, under equivalent conditions. In CO_2-carbonate systems, O-isotope exchange rates are greater than those for carbon (Northrop, 1964).

2) Retrograde effects: as a consequence of 1) above, calcite may tend to re-equilibrate with the fluid phase to a lower temperature than dolomite.

3) Crossover: a crossover in $10^3 \ln K^{O^{18}}_{D-Ct}$ is not indicated by any of the experimental results.

4) The dolomite-calcite O-isotope fractionation expressions are:

   (a) O'Neil (1963), theory.

$$1000 \ln \alpha^{O^{18}}_{D-Ct} = 0.207 \, (10^6 \, T^{-2}) + 0.25 \qquad (1)$$

   (b) Northrop and Clayton (1966), O'Neil and Clayton (1964), experimental.

$$1000 \ln \alpha^{O^{18}}_{D-Ct} = 0.50 \, (10^6 \, T^{-2}) \qquad (5)$$

   (c) O'Neil and Epstein (1966), experimental:

$$1000 \ln \alpha^{O^{18}}_{D-Ct} = 0.56 \, (10^6 \, T^{-2}) + 0.45 \qquad (6)$$

5) This summary of the experimental data is evidence that, at $T = 500°C$, $10^3 \ln K^{O^{18}}_{D-Ct}$ is on the order 0.0 to + 1.4‰.

III. GENERAL ANALYTICAL PROCEDURES

3.1 Preparation of CO_2

Carbon dioxide was extracted from all carbonates with 100% H_3PO_4 at a specific temperature using the methods of McCrea (1950):

$$3CaCO_3 + 2H_3PO_4 \longrightarrow Ca_3(PO_4)_2 + 3CO_2 + 3H_2O$$

$$\alpha_{CO_2\text{-carbonate}} = \frac{R_{CO_2}}{R_{carbonate}}$$

In such a reaction only 2/3 of the oxygen is liberated. At any given temperature the fractionation is reproducible so long as essentially 100% yield of the CO_2 is obtained. Recent work by Sharma and Clayton (1965) has examined the value of this fractionation factor, both as a function of temperature and carbonate composition. They find that:

$$\alpha_{CO_2\text{-D}} = 1.01090 \qquad 1000 \ln \alpha^{O^{18}}_{CO_2\text{-D}} = 10.84‰$$

$$\alpha_{CO_2\text{-Ct}} = 1.01008 \qquad 1000 \ln \alpha^{O^{18}}_{CO_2\text{-Ct}} = 10.02‰$$

$$\frac{\partial \alpha}{\partial T} = -0.032‰ \ ^{\circ}C^{-1}$$

Prior to 1965, a single value for the fractionation factor was used for all carbonates, viz. 1000 ln $\alpha^{O^{18}}_{CO_2\text{-carbonate}}$ = 10.00. All results prior to 1965 discussed in this thesis have been corrected for this effect.

It is noted that the phosphoric acid fractionation factor was not determined for any Mg-calcites. If, to a first approximation, it is assumed that the variation of the fractionation factor between calcite and dolomite is linear, then use of the $CaCO_3$ fractionation factor is in error by:

$$\delta O^{18}_{Ct} = + 0.08‰ \text{ for a Mg-calcite with } MgCO_3 = 5 \text{ mol \%}.$$

For samples where the coexisting dolomite and calcite were intimately mixed, e.g. in all the hydrothermal experiments of this work, physical separation was impractical. The technique, exploiting the differential rate of reaction of dolomite and calcite with phosphoric acid, as developed by Epstein et al. (1964), was used. The calcite-dolomite mixture ground to -200 mesh was reacted with the phosphoric acid. After one hour 90% to essentially 100% of the calcite, depending on the $MgCO_3$ composition, has reacted together with less than 5%of the dolomite. The CO_2 was extracted after one hour, three hours and at least 72 hours, giving the CO_2 from the calcite, the mixture, and the dolomite respectively. After 72 hours a little less than 100% yield of CO_2 from dolomite may be obtained, but no significant difference in isotopic composition between this and the 100% yield was detected. In general, dolomite reactions were continued for 95 hours or more. This method was found to be quite satisfactory giving a precision of ± 0.2‰ or better, when certain precautions were taken. Results are optimum when: (1) the ratio of dolomite to calcite

is 1:1; (2) the isotopic composition of the carbonates are similar; (3) the $MgCO_3$ content of the calcite is small, < 2 to 3 mol % $MgCO_3$. Northrop and Clayton (1966) also report satisfactory results with this method.

3.2 Mass Spectrometry

Samples were analysed on a 6", 90° sector type, double collecting mass spectrometer of the type described by Nier (1947) and subsequently modified by McKinney et al. (1950). It has no mixing correction. This instrument is used routinely for SO_2 by Thode and coworkers (e.g. Thode et al., 1961). When changing from SO_2 to CO_2 the mass spectrometer was always baked out for 24 hours or more, flushed with purified dry argon, and the glass reservoir system flamed out. No significant memory effect has been detected. Reproducibility was routinely about ±0.1‰ or a little better for both carbon and oxygen. At least two separate mass spectrometric analyses were done upon each carbonate sample.

Carbon dioxide from a Grenville metamorphic calcite was used as the working standard, having a C^{13} and O^{18} isotopic composition close to that from all analysed natural marbles.

3.3 Sample Preparation

Wherever possible dolomite and calcite were separated by physical means, using a Franz magnetic separator or heavy liquids on crushed samples, sieved to -100 to +200 mesh. These methods were found to be satisfactory for all samples from the biotite zone upwards. The fine grained and intimately mixed nature of samples from the chlorite zone in general prevented a clean physical separation. Chemical separation had

to be resorted to for such natural samples and for all those from the calcite-dolomite hydrothermal experiments (Epstein et al., 1964). This method is discussed in § 3.1.

3.4 Phase Identification

3.4.1 Staining

Alizarin Red S has been found to be a thoroughly reliable stain for calcite and Mg-calcite under all conditions (Friedman, 1959). The stain forms a strongly coloured complex with calcium ions. The rate of reaction with dolomite is very much slower. Therefore removal of excess solution after a minute or so prevents the staining of the dolomite. In a stained thin section a few percent of either phase usually can be detected.

Stains for dolomite are less satisfactory. The detection of iron in dolomite, using hot potassium ferricyanide solution, proved unreliable in some metamorphosed marbles. The limit of identification of iron in this method is 5×10^{-5} mg. (Feigl, 1958). Some ferromagnesian silicates are stained.

3.4.2 Optical Methods

Refractive index oils to distinguish dolomite from calcite have been used extensively to check on the purity of physical mineral separates. The method is rapid and reliable.

3.4.3 X-Ray Methods

The X-ray powder diffraction methods developed by Goldsmith and Graf (1955, 1958) were used to determine the $MgCO_3$ content of the Mg-calcites from the natural and synthetic samples. A 114.59 mm. Philips Debye-Scherrer powder camera was used with Mn-filtered FeKα radiation. The distances between the (521) and between the (552, 633) back reflections were measured. With these two measurements and the calibration curves of Goldsmith (1962), two determinations of the $MgCO_3$ content were made per photograph. No internal standard is necessary in this method. This has a distinct advantage because of the low relative intensities of these back reflections: (521), $I/I_i = 4$; (552, 633), $I/I_i = 2$, relative to $I_{112} = 100$. Temperatures were read off the revised calcite-dolomite solvus curve, determined experimentally by Graf and Goldsmith (1955, 1958) and Goldsmith and Heard (1961) or an extrapolation of this solvus curve towards lower temperatures. Neither corrections for $FeCO_3$ or $MnCO_3$ in solid solution nor the effect of pressure on solid solubility were attempted (see § 5.1.3 and § 5.1.4).

IV. CONDITIONS FOR EQUILIBRIUM

4.1 Introduction

The equilibrium concept is vital to the analysis of the physical, chemical and isotopic properties exhibited by a mineral assemblage. The concept of equilibrium, and in particular partial equilibrium, is reviewed now briefly before discussing suitable working criteria for determining whether a given assemblage preserves equilibrium relations for a chosen property.

4.2 Thermodynamic Symbols

a_i	Activity of component i
G	Gibbs free energy
G_m	Gibbs free energy of mixing
G°	Standard Gibbs free energy
H_m	Enthalpy of mixing
N_i	Mole fraction of component i
n_i	Moles of component i
P	Pressure
T	Temperature
γ_i^α	Activity coefficient of component i in phase α
μ	Chemical potential
i, j, .	Subscripts: refer to components
$\alpha, \beta, .$	Superscripts: refer to phases

4.3 General Equilibrium Conditions

The general conditions for complete equilibrium: thermal, mechanical and chemical, are of the form: for given T, P and n_i, G is a minimum. There are other alternative statements to this which are dependent on different sets of independent variables. All these statements for stable or metastable equilibrium are equivalent.

4.4 Chemical Equilibrium

Here, the equilibrium distribution of a species between coexisting phases and its properties are of particular importance. Polyphase systems, each one being in equilibrium, can be described by a fundamental equation. For $G = G(P, T, n_i)$:

$$dG = \Sigma^{\alpha} VdP - \Sigma^{\alpha} SdT + \Sigma^{\alpha} \Sigma_i \mu_i \, dn_i \qquad (7)$$

where Σ_i is the summation over the components and Σ^{α} that over the phases.

Consider a two phase system, α and β, in thermal equilibrium, $T^{\alpha} = T^{\beta}$. It is necessary to make the restriction that the system has attained thermal equilibrium in order to exclude the creation of entropy from internal heat transfer. Let dn_j^{α} moles of component j be transferred from phase α to β, the pressure and chemical potential of all other components in each phase remaining constant. From equation (7)

$$dG = \mu_j^{\alpha} \, dn_j^{\alpha} - \mu_j^{\beta} \, dn_j^{\alpha}$$

At equilibrium

$$dG = 0$$

$$\mu_j^{\alpha} = \mu_j^{\beta} \qquad (8)$$

Equation (8) is the most general condition for chemical equilibrium of component j distributed between two phases in thermal equilibrium.

4.5 Partial Equilibrium

As emphasized by Guggenheim (1959, p. 41), this condition for chemical equilibrium of component j is independent of the activities of other components and the condition for mechanical equilibrium. Such a system, which has attained thermal equilibrium and equalization of some, but not all, intensive properties, is said to be in partial equilibrium. The Nernst distribution equation can be applied to component j in such a system:

$$\frac{N_j^{\alpha}}{N_j^{\beta}} = \frac{\gamma_j^{\beta}}{\gamma_j^{\alpha}} K(P,T). \qquad (9)$$

The complete equilibrium state is no more than the special case when all the intensive properties have been equalized between the phases.

This concept of partial equilibrium is of relevance in systems in which: (1) complete equilibrium was never established but, nevertheless, some components attained their equilibrium partitioning; (2) the once established equilibrium state suffered a partial retrogradation, preserving some equilibrium conditions for one temperature, and some other conditions for another temperature.

The slow rate of attainment of certain chemical equilibria compared to the more rapid attainment of others, whether prograde or retrograde, is a characteristic feature of many natural systems, e.g. any

equilibrium system with certain components perfectly mobile. Hence, the importance of the concept of partial equilibrium in geological systems.

It is inherent in this approach that until the preservation of complete equilibrium has been shown with some confidence, application of the Nernst distribution law, (9), to one species, component, or, in a slightly modified, form, to one isotope at a time, can possibly elucidate the nature of the equilibrium.

4.6 Relation Between Chemical and Isotopic Equilibrium

It is necessary to introduce the concept of chemical equilibrium for systems with more than one phase. Chemical equilibrium can be considered to be composed of two parts: (1) a 'coarse condition' dependent on the equilibrium partitioning of chemical components, and (2) a 'fine condition' dependent on the equilibrium partitioning of the isotopes. Strictly, the establishment of chemical equilibrium requires both 'coarse and fine' equilibrium. However, the term chemical equilibrium often is used to refer to the 'coarse' condition only. This is reasonable usage insofar as the free energy associated with an equilibrium isotopic exchange reaction is very small: 7‰ fractionation at 300°K corresponding to about 4 cals/mole, compared with the larger free energy values for most chemical reactions of a few tens of K cals/mole.

Isotopic exchange usually involves the transfer of atoms, simple ions or complex ions, accompanied by the rupture of some bonds and formation of others. Isotopic exchange is often enhanced by chemical reactions (Wyart and Sabatier, 1961; O'Neil and Taylor, 1965, 1966). In those

experiments with cation exchange, O-isotope exchange was rapid. O'Neil and Taylor suggest that a solution - redeposition mechanism, rather than a solid state diffusion mechanism, is indicated to account for the very high exchange rates. It is of considerable interest that breaking and making of bonds in the $(Si, Al)O_4^{-4,-5}$ tetrahedron can be such a rapid process. Any process or mechanism allowing such interchange of O-isotopes might be expected to be accompanied by cation exchange and equilibration. Attainment of O- and C-isotope equilibrium probably is an excellent criterion that major cation equilibrium was achieved too, but not vice versa.

The isotopic equilibrium constant for a mineral pair is determined by the temperature alone, to a first approximation. This temperature can be determined once the relations between $10^3 \ln K_{x-y}$ and temperature are known. However, even if the resulting temperature is geologically reasonable, this by itself is not a sufficient test for equilibrium.

Determination of the fractionation between three or more minerals may provide information on: (1) whether equilibrium is preserved between all minerals; (2) the temperature of quench; (3) the nature of operative processes; (4) the isotopic composition of coexisting water (Clayton and Epstein, 1958). Concordant temperatures from three or more mineral fractionations are excellent criteria for equilibrium. Consistent fractionations for a set of dolomite-calcite pairs from a sufficiently small volume of rock through which uniformity in the physicochemical conditions can be assumed with confidence, coupled with variations in the isotopic composition of the carbonates, is an alternative and satisfactory criterion for equilibrium. This criterion will be applied in a later section (see

§ 8.2). The effect of differential exchange processes producing consistent fractionations can be detected so long as the carbonate isotopic compositions are different. In dolomite-calcite systems concordancy between Mg-, O- and C-isotope fractionations is an alternative and attractive criterion for equilibrium.

There is no reason to assume that the different exchange processes between any two phases should freeze-in together at the same temperature. If discordant freeze-in occurs, it is imperative that discordant equilibrium partitioning, i.e. partial equilibrium, can be distinguished from discordant disequilibrium partitioning. Equilibration of only the surfaces of coexisting minerals, local equilibrium, is a special case of the latter. The fractionation data may be able to resolve these problems when the relevant exchange equilibrium constants are known as a function of temperature.

Before predictions concerning the relative conditions for the quenching of the various exchange reactions can be made, more information on the kinetics and mechanisms of the exchange processes is required. Data from the rocks, interpreted through the concept of partial equilibrium, remain our main source of information. The interpretation of a set of discordant temperatures within the framework of the geological history of the sample is another major problem to be faced (Clayton, 1963).

V. SOLVUS GEOTHERMOMETRY

5.1 The Solvus Geothermometer

5.1.1 Experimental Studies

Subsolidus phase relations in the binary system $CaCO_3$-$CaMg(CO_3)_2$ have been described by Graf and Goldsmith (1955, 1958), Harker and Tuttle (1955) and Goldsmith and Heard (1961). These experimental studies have been restricted to temperatures greater than 500°C. Above this temperature, chemical equilibrium is attained in convenient laboratory time, even under dry conditions. The agreement between these several studies is satisfactory. The pertinent results are presented in Figure 1. In these experiments, the applied pressure was a little greater than the decomposition pressure of the carbonate at each temperature. The solvus shown in Figure 1 is polybaric. The effect of pressure on the solvus relations is reported by Goldsmith, in Goldsmith and Heard (1961, p. 55), to increase the solubility of $MgCO_3$ in calcite by approximately 1% per 5kb. total pressure in the range 1 to 15kb..

Dolomite occupies a very restricted field of compositions below 900°C or so. This is consistent with the ordered structure of this intermediate phase in the system $CaCO_3$-$MgCO_3$.

The relations between the magnesium content of a calcite and its X-ray spacings have been described by Goldsmith and Graf (1958). The method for determining the Mg-calcite composition is discussed above,

§3.4.3. Apart from pressure, however, there are two immediate problems to be evaluated before a temperature can be derived from the composition of a natural Mg-calcite:

(1) with what confidence can the experimentally determined solvus be extrapolated to temperatures less than 500°C?

(2) what is the effect of other ions, notably Fe, Mn and Sr, on the X-ray spacings of calcite?

5.1.2 Extrapolation of the Magnesian Calcite Solvus Limb

Figure 1 displays the marked asymmetry of the solvus. The Mg-calcite limb of the solvus very closely approximates a logarithmic function. A least squares analysis of the data of Graf and Goldsmith (1958) and Goldsmith and Heard (1961) gives the relation:

$$\log MgCO_3 = 1.586 \times 10^{-3} T - 0.055 \qquad (10)$$

where T is the temperature in degrees Centigrade (Fig. 2). Relation (10) predicts that a Mg-calcite in equilibrium with dolomite at 25°C contains 0.97 mol % $MgCO_3$. Temperatures derived from the extrapolated portion of the equation are considered to be satisfactory, especially in relation to greater uncertainties in the pressure.

5.1.3 Effects of Fe, Mn, Sr and Ba on the X-Ray Spacings

Other divalent ions, notably Fe, Mn, Sr and Ba, may substitute for Ca and Mg in the calcite structure. The studies of Goldsmith and Graf (1960), Goldsmith et al. (1962), Rosenberg (1963) and Chang (1965) indicate that the maximum solubility of these ions in calcite at a given temperature increase in the order:

Fig. 1. -- The subsolidus phase relations in the binary system: $CaCO_3$-$MgCO_3$.

Pressure increases from 2 to 8 kb in going from 500° to 1200°C. The dashed line A marks the limit of detectable order in dolomite. (After Goldsmith and Heard, 1961).

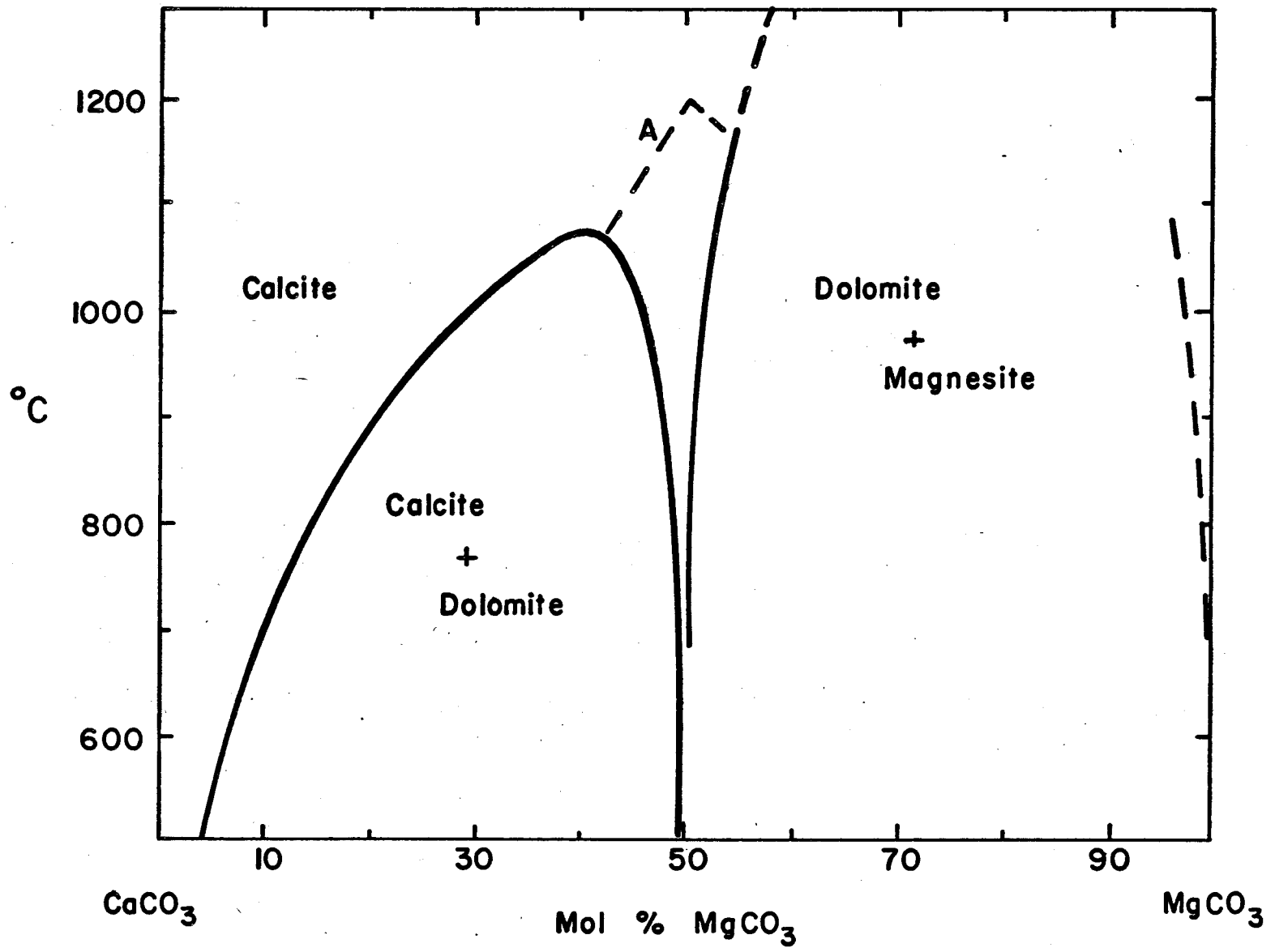
1200
1000
800
600
°C
A
Calcite
Calcite
+
Dolomite
Dolomite
+
Magnesite
10
30
50
70
90
CaCO3
Mol % MgCO3
MgCO3

Fig. 2 -- The Mg - Calcite solvus limb and its extrapolation below 500°C.

The least squares regression line fitted to the data of Graf & Goldsmith (1958) and Goldsmith & Heard (1961) between 500° and 1100°C. The dashed part of the line is the extrapolation to temperatures below 500°C.

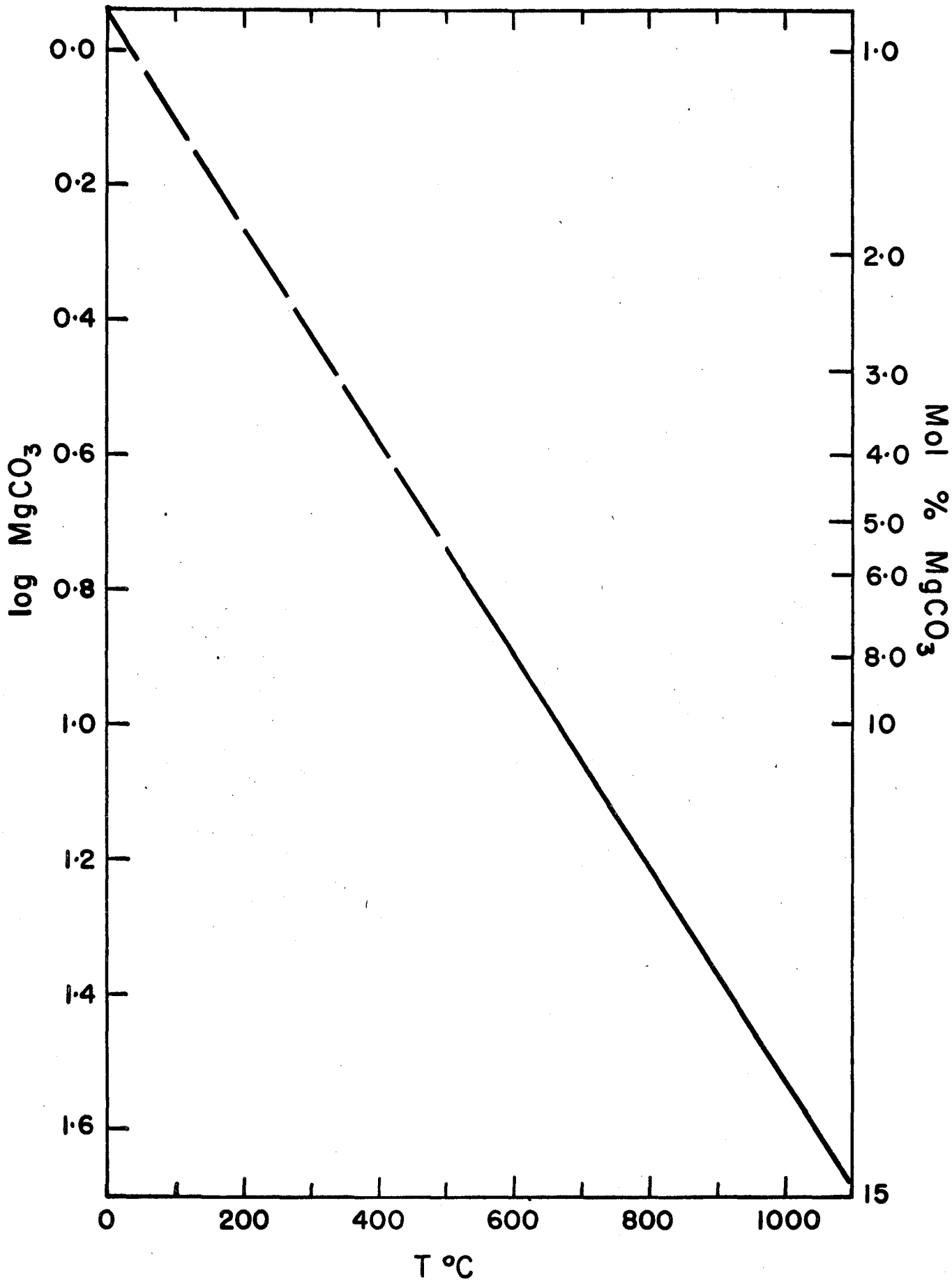
0·0
0·2
0·4
0·6
0·8
1·0
1·2
1·4
1·6
log MgCO3
1·0
2·0
3·0
4·0
5·0
6·0
8·0
10
15
Mol % MgCO3
0
200
400
600
800
1000
T °C

$$Ba^{2+} \ll Mg^{2+} < Sr^{2+} < Fe^{2+} \ll Mn^{2+}$$
$$(-0.35) \quad (0.33) \quad (-0.13) \quad (0.25) \quad (0.02)$$

The figure in parentheses is the ionic radius of Ca^{2+} minus that of the cation. This order of increasing solubility is, perhaps significantly, one of decreasing difference in ionic radius from that of Ca^{2+} with the exception of the switching of positions of Sr^{2+} and Fe^{2+} (see § 5.4.5.2). Only the substitution of divalent ions is considered here.

These ions influence the lattice parameters. Substitution of Sr and Ba increase the lattice constants, a_o and c_o, whilst Mn, Fe and Mg decrease them (Goldsmith and Graf, 1958; Goldsmith et al., 1962; Chang, 1965). For a given concentration the relative magnitude of the change is in the order:

$$Ba^{2+}(+) < Mn^{2+}(-) < Fe^{2+}(-) < Sr^{2+}(+) < Mg^{2+}(-)$$

where the (+) refers to an increase and the (-) to a decrease of the lattice parameters.

The partial analyses of some representative calcites from both Vermont and the Grenville are given in Table I. They compare favourably with some average analyses of Grenville marbles given in Shaw et al. (1963, Table 10) using spectrochemical methods. Fe is the most abundant of the ions having a marked effect on the lattice parameters of calcite.

The influence of Fe substitution on the X-ray spacings can be assessed from Figure 3. This illustrates the solvus relations in part of the system $CaCO_3$-$MgCO_3$-$FeCO_3$. Solvi at 300°C and 600°C are drawn after Goldsmith et al. (1962), Rosenberg (1963) and the extrapolated

Table I

Partial Chemical Analyses of Some Selected Calcites*

Sample No.	$FeCO_3$	$MnCO_3$	$SrCO_3$
GCS	0.12	0.02	0.017
GLSK	0.06	0.06	0.066
G5-1	0.61	0.10	0.076
G4-5-3	0.19	0.03	0.007
G4-54-1	0.01	0.06	0.007
Vt4-11B**	0.34	0.01	0.019
Vt4-35-1a	0.65	0.06	0.038
Vt4-35-1b	0.70	0.86	0.038
Vt4-35-5	0.30	0.21	0.001
Vt4-37-5	0.99	0.52	0.013

* Analyst: J.R. Muysson

** Average of the 9 samples: Vt4-11B-1, -6, -7, -8, -9, -17, -11, -12, -14

Fig. 3. -- The influence of $FeCO_3$ substitution in calcite on the X-ray spacing d_{633}.

Solvi at 300° and 600°C are given for part of the system $CaCO_3$-$MgCO_3$-$FeCO_3$ as full lines. The dashed lines are isopleths, lines of constant Δd spacing for the difference between d_{633} of the carbonate and that of pure calcite. (Data from Goldsmith et al., 1962 and Rosenberg, 1963).

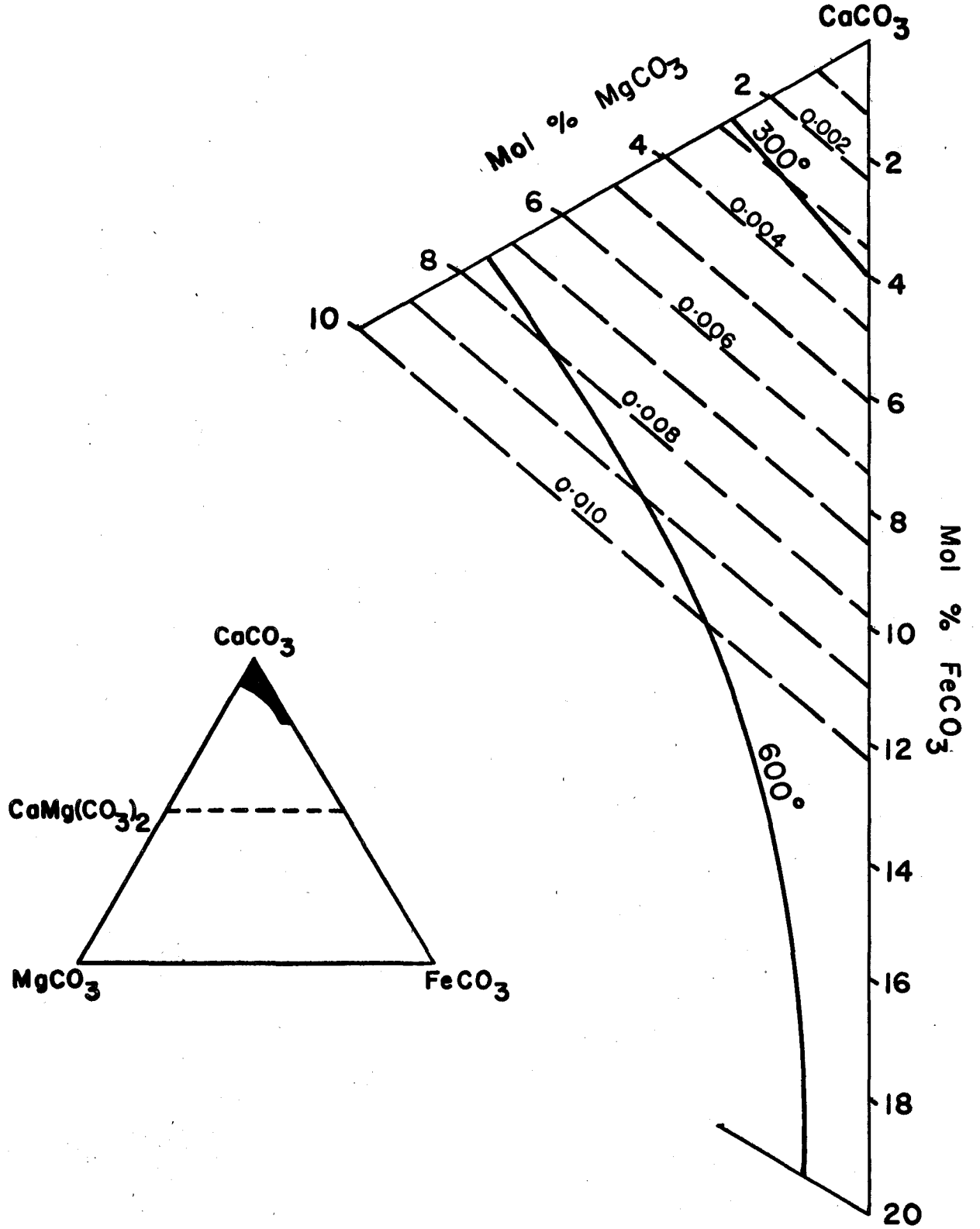
CaCO3
Mol % MgCO3
2
4
6
8
10
0·002
300°
0·004
0·006
0·008
0·010
600°
2
4
6
8
10
12
14
16
18
20
Mol % FeCO3
CaCO3
CaMg(CO3)2
MgCO3
FeCO3

Mg-calcite limb, expression (10). Isopleths, lines of constant Δ d spacing, for the difference between d_{633} of a carbonate and that of pure $CaCO_3$ are superposed. Knowing the $FeCO_3$ content, the error in the $MgCO_3$ determination can be read off Figure 3. Taking a $FeCO_3$ content of 1 mol % at 600°C, the error in the $MgCO_3$ determination is +0.25 mol %. This is equivalent to +8°C. For a given $FeCO_3$ value, the error in $MgCO_3$ decreases with decrease in temperature (Fig. 3). The influences of the other ions are probably significantly less than this. Therefore, these ions can be neglected with confidence when present up to 1-2 mol %.

5.1.4 Pressure Estimates

The $MgCO_3$ content of calcite can be determined by the X-ray method to ±0.2 mol % or better. Lack of knowledge of the pressure at the time of quench is primarily responsible for uncertainties in the temperature determination. The experimental data to 700°C are for pressures up to 2kb.. This is undoubtedly low compared with regional metamorphic pressures in the higher grade areas of Vermont and the Grenville Province.

The presence of kyanite at a temperature of about 550°C, determined with the quartz-magnetite isotopic thermometer by Garlick (1964), in Central Vermont and in the Chester dome area, indicates a pressure of: $P \geqslant 4$ to 5kb. (Newton, 1966; Weill, 1966; Holm and Kleppa, 1966). The older experimental data indicates: $P \geqslant$ 11kb. (Clark, 1961; Bell, 1963). The newer experimental results for the univariant kyanite-sillimanite phase boundary in the andalusite-kyanite-sillimanite system are geologically more satisfactory. If the geothermal gradient was as low as 15°C/km, an upper limit of about 10kb. is given.

In the Grenville Province knowledge of the pressure is uncertain. In the Denbigh area sillimanite is ubiquitous in the pelitic schists together with minor staurolite and rare kyanite (Evans, 1964). The temperature in this area was probably in the range 500° to 700°C, indicating $P \leqslant 4$ to 7kb. (Newton, 1966).

Neglecting the pressure correction, uncertainties in T_s, arising from the precision of determining Mg in calcite, are on the order of ±15°C at 500°C; ±25°C at 300°C. The enhanced solubility of Mg in calcite under high pressures increases T_s relative to T by 40°C for $P \simeq 7$kb, and 60°C for $P \simeq 10$kb. Samples from the amphibolite facies are most strongly influenced by this pressure effect, assuming that the quench takes place under the maximum pressure. Since the pressure at the time of quench is known so imperfectly, solvus temperatures are presented here with no pressure correction. Relative temperatures for closely related samples (P constant) are probably good to ±25°C, if the back reflections are sharp.

5.2 Solvus Geothermometry

The $MgCO_3$ content of the calcites coexisting with dolomite were determined for all samples analysed isotopically below (§ 7). The description of the geological setting of these samples from Vermont and the Grenville is deferred to chapter VII. Table II presents the solvus derived temperatures (T_s) from the calcites together with the metamorphic grade. The metamorphic grade was inferred from the mineral assemblages in nearby pelitic schists (see Appendix II for sample description and Figures 14 and 20 for the sample locations). The relation between the grade and T_s is illustrated in Figure 4. This emphasizes two charac-

Fig. 4. -- Variation of solvus temperature with metamorphic grade.

- ● Indicates T_s derived from maximum $MgCO_3$ content of calcite.
- O Indicates T_s derived from lower $MgCO_3$ content in calcites with split (521) and (522, 633) peaks. Samples in the chlorite and biotite zones are approximately in their relative position within the zone.

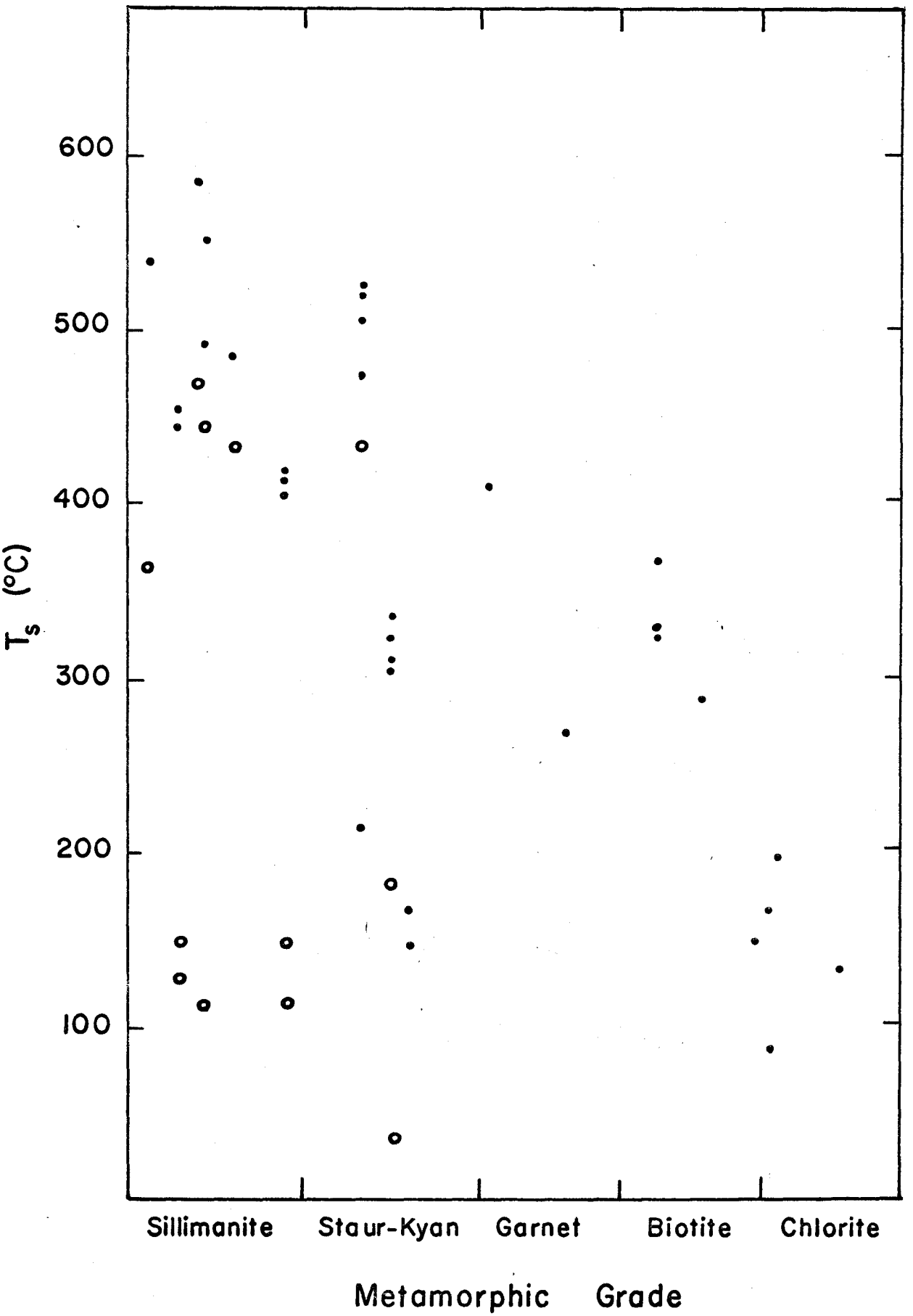
600
500
400
300
200
100
T_s (°C)
Sillimanite
Staur-Kyan
Garnet
Biotite
Chlorite
Metamorphic Grade

Table II

Solvus Geothermometry

Sample	Metamorphic Grade	Mol % $MgCO_3$	T_s °C
Vt 3-51	Chl	1.4	130
Vt 3-48	Chl	1.2	85
Vt 4-29	Chl	1.6	165
Vt 3-65	Chl	1.8	195
Vt 3-47	Bi	1.5	145
Vt 4-23	Bi	2.5	285
Vt 4-11B-6	Bi	2.8	)
-8	Bi	2.8	)
-9	Bi	3.0	) 325
-12	Bi	2.8	)
-15	Bi	2.9	)
Vt 3-83-3	Bi	2.8	320
Vt 4-12-1	Bi	3.4	365
Vt 3-76	Gt or SK(R)	3.9	405
Vt 3-74	SK(R)	1.6	165
Vt 3-75	SK(R)	1.5	145
Vt 4-37-1	SK(R)	1.0	35
-2	SK(R)	2.6	300
-3	SK(R)	2.7	305
-4	SK(R)	2.8, 1.7	320, 180
-5	SK(R)	3.0	335
Vt 4-35-1a	SK(R)	5.5, 4.9	500, 470
-1b	SK(R)	5.7(b)	515
-2a	SK(R)	5.9, 4.2	520, 430
-2b	SK(R)	5.9, 4.2	520, 430
-5	SK(R)	1.9	210

Notation: Chl = chlorite, Bi = biotite, Gt = garnet
SK = staurolite-kyanite, (R) = retrograde
(b) = broad peak

Table II continued

Solvus Geothermometry

Sample	Metamorphic Grade	Mol % $MgCO_3$	T_s °C
G Ch-14	L. Amph.	2.3(b)	265
G 4-54-1	U. Amph.	4.0, 1.3	415, 110
G 4-55	U. Amph.	3.8, 1.6	400, 160
G 4-6	U. Amph.	4.0, 1.5	415, 145
M 16	U. Amph.	5.1, 4.2	480, 430
G 4-5-3	U. Amph.	5.2, 1.3	485, 110
G 4-3	U. Amph.	6.5, 4.4	545, 440
GLSK	U. Amph.	7.4, 4.8	580, 465
G 5-1	U. Amph.	4.6, 1.4	450, 125
-1b	U. Amph.	4.4, 1.5	440, 145
G 3-11-1	Gran	6.2, 3.3	535, 360

Notation: L. Amph. = lower amphibolite facies
U. Amph. = upper amphibolite facies
Gran = granulite facies
(b) = broad peak

teristic features of the system:

1) A good correlation between the maximum value of T_s and the metamorphic grade, except from some high grade assemblages.
2) The coexistence of two Mg-calcites in some samples from the amphibolite facies.

The correlation presumably reflects a systematic relation between the temperature of the metamorphic high at a given point and the quench temperature. No sample gave T_s greater than that expected for its metamorphic grade, in contrast to the observations of Schwarcz (1966).

The five coexisting calcite-dolomite pairs from the Kent Quarry core, Vermont, Vt 4-11B -6, -8, -9, -12, -15, are samples taken from within a 60 foot section of this core. These Mg-calcites quenched in at essentially identical temperatures: $MgCO_3$ = 2.85 mol %, σ = 0.09 mol % $MgCO_3$, T_s = 325° ± 25°C. The percentage of calcite to total carbonate ranges from 95% to 12% and there are minor variations in the content of other phases, notably quartz, phlogopite, chlorite, and actinolite. Apparently these minor variations of the environment have had little direct influence on the quench phenomena. Two other samples from the South Dorset area in the neighbourhood of the Kent Quarry (Fig. 21) give similar solvus temperatures: Vt 3-83-3, T_s = 320° ± 25°C; Vt 4-12-1, T_s = 370° ± 25°C.

5.3 Peak Broadening

Many Mg-calcites from the high grade rocks display considerable peak broadening of the high-angle back reflections. This has been interpreted as the coexistence of two or more calcites with differing Mg con-

tents. It is not a grain size phenomenon. Goldsmith et al. (1955) attribute this effect to a once homogeneous Mg-calcite which has locally segregated into low Mg-calcite-dolomite regions within the higher Mg-calcite host. Although such a system is in disequilibrium as a whole it can be subdivided into subsystems which possibly established equilibrium with respect to Mg-partitioning at different temperatures.

This peak broadening is particularly pronounced for the high 2θ reflections, d_{521} and $d_{552,633}$, which, unfortunately, are of low intensity (§ 3.4.3). The broadening may represent a whole series of Mg-calcites but often two weak maxima are observed. A microdensitometer was unsuccessfully employed to determine the relative intensities across the broadened peak. Future application of the electron probe microanalyser, X-ray scanning and cathodo-luminescence to this problem is desirable. Long and Agrell (1965) have demonstrated Fe impoverishment in calcite immediately adjacent to exsolved dolomite blebs.

Many of the more Mg-rich calcite separates ($MgCO_3 > 4$ mol %) gave weak dolomite d_{211} reflections. Optical study of the stained calcite separates detected < 1 to 2% of dolomite. This is probably insufficient dolomite to account for the reflection. Exsolved dolomite is the probable major source (Goldsmith, 1960). Exsolution blebs of dolomite were observed in some thin sections and most calcites from the high grades were cloudy due possibly to very fine exsolved dolomite (Goldsmith, 1960; Shaw et al., 1965, Figs. 4 and 5). These features are indicative of complex quench processes and hence introduce uncertainties into temperatures derived from such samples.

Chemical analyses for $MgCO_3$, determined for a few selected high grade calcites, using an atomic absorption spectrophotometer, are compared in Table III with the X-ray determinations for $MgCO_3$. The chemical analyses are consistently higher. Exsolved dolomite is possibly responsible in part. Because of the problems of accurately assessing the location of dolomite - all exsolved, or exsolved plus discrete dolomite - and their quantities these differences reported in Table III are not yet resolved. However, the temperatures, T_{sc}, corresponding to the higher Mg contents are not unreasonably high for the grade of metamorphism.

It is proposed as a working hypothesis that the maximum $MgCO_3$ content of the calcite reflects the preservation of equilibrium, albeit sometimes on a very local scale, at a temperature similar to the metamorphic maximum, except for some amphibolite facies samples. A few high grade samples, e.g. Vt 4-35-5, Vt 3-74, Vt 3-75 (Fig. 4) apparently recrystallized at a low temperature. Some samples, e.g. G 4-54-1, G 4-6, G 4-55, may have quenched at a temperature 100° to 150°C less than the probable metamorphic maximum. Other high grade samples give T_s similar to but less than the maximum metamorphic temperature inferred from other geological criteria (§ 9.4) and possibly from the chemical analysis (Table III). These solvus temperatures would be lower if the pressure correction is significant.

This interpretation has assumed implicitly that the exchange reactions for Mg between calcite and dolomite tend to be equilibrium processes up to the time of quench. This assumption may not be justified for many of the amphibolite facies samples where quench phenomena are

Table III

Comparison of the Determination of Mol % $MgCO_3$ in Calcite by X-Ray Method and Chemical Analysis

Sample No.	X-Ray (mol % $MgCO_3$)	Chemical (mol % $MgCO_3$)	T^*_{sx} (°C)	T^*_{sc} (°C)	Remarks
GLSK	7.4 4.8	9.84	585 465	660	D blebs in Ct** Ct cloudy
G 5-1	4.6 1.4	9.24	450 125	645	Ct cloudy with occasional bleb of D
G 4-5-3	5.2 1.3	8.84	485 110	630	Ct centres cloudy, margins clear
G 4-54-1	4.0 1.3	7.71	415 110	595	Ct cloudy

Analyst: J.R. Muysson

* T_{sx} : Solvus temperature from X-ray data

T_{sc} : Solvus temperature from chemical analysis

** Illustrated in Shaw et al. (1965, Fig. 5)

complex. Hence, the temperature derived from the $MgCO_3$ content may not be a measure of the preservation of an equilibrium factor of state. However, the observed trend shown in Figure 4 is consistent with a close approach to equilibrium partitioning of Mg at a temperature similar to or less than the metamorphic maximum.

5.4 Partial Thermodynamic Analysis of the Calcite-Dolomite System

5.4.1 Introduction

At equilibrium in the assemblage calcite-dolomite a Mg-calcite of uniform composition coexists with dolomite as shown in Figure 1. The experimental studies demonstrate the rapid rate of reactions in this system for $T \geq 500°C$. So, the observed variable $MgCO_3$ composition of the Mg-calcites are inferred to be a manifestation of the quench processes in a one-time homogeneous Mg-calcite. This raises the related questions: (1) why are some high Mg-calcites, $MgCO_3 > 4$ mol %, quenched in at all in natural samples?; (2) are Mg-calcites of certain compositions more prone to exsolution phenomena than others? The factors influencing such phenomena as exsolution in condensed systems are intricate. While the kinetics of the nucleation process and the subsequent growth of the phase are important these will not be discussed here. Rather, attention is directed to the thermodynamic stability or instability of Mg-calcites of different compositions under metamorphic and surface P,T conditions and its bearing on the observed Mg-calcite relations. In the binary calcite-dolomite system a considerable amount of thermodynamic information can be derived from the solvus relations.

This analysis shows that Mg-calcites from low to intermediate metamorphic grades are thermodynamically stable or metastable under surface P,T conditions. Some high Mg-calcites from the highest grade rocks may be unstable under surface conditions and tend to decompose spontaneously into a lower Mg-calcite plus dolomite assemblage.

5.4.2 General Statement of Problem

In order to delineate the stable, metastable and unstable regions in the calcite-dolomite system it is necessary to evaluate the activities or activity coefficients of the components as a function of temperature, pressure and composition, and hence derive the Gibbs free energy of mixing for this system. As a by-product of the analysis, a feeling will be obtained for the magnitude of the departures from the ideal model.

The success of this analysis requires that the Gibbs free energy of mixing be a continuous function throughout the whole system. The nature of this assumption will now be examined.

The asymmetric solvus curve, Figure 1, betokens appreciable positive deviation from Raoult's Law, $\gamma_i > 1$, ΔH_m positive, and the inapplicability of the regular solution model. Binary solution models for non-ideal solutions necessitate certain approximations. Since the mathematical expressions for the excess functions or activity coefficients used in these models are continuous functions, the binary system calcite-magnesite, with components $CaCO_3$ and $MgCO_3$ and intermediate compound $CaMg(CO_3)_2$, is not amenable to such treatment. For this reason the system calcite-dolomite is chosen as the binary system.

Dolomite is an ordered phase, space group $R\bar{3}$, while Mg-calcite, space group $R\bar{3}c$, lacks long-range ordering. This necessitates the occurrence of a structural change somewhere between the end members $CaCO_3$ and $CaMg(CO_3)_2$. The nature of this disordering transformation is critical. A first order transformation requires a discontinuity in the free energy function and invalidates this analysis. Goldsmith and Heard (1961), in their analysis of the subsolidus phase relations in this system, discuss the nature of this transformation in some detail. They conclude that:

1) Experimental studies indicate only a continuous simple solvus curve between calcite and dolomite. The transformation takes place in the region of the crest of the solvus, $T \simeq 1100°C$, Figure 1, where the experimental detection of a classical transformation is difficult.

2) A similar simple continuous solvus relation has been observed in the analogous $CdCO_3$-$CdMg(CO_3)_2$ system, a lower temperature 'equivalent' of the calcite-dolomite system.

These arguments favour a second order or higher transformation with a continuity of state between calcite and dolomite, the two phases becoming identical at the critical point.

It is convenient to choose $CaCO_3$ and $Ca_{0.5}Mg_{0.5}CO_3$ as the thermodynamic components. All phase compositions can be expressed in terms of these two components. The validity of the thermodynamic analysis with these components does not require that a Mg-calcite is physically composed of domains of $CaMg(CO_3)_2$ (ordered) in a $CaCO_3$ host.

5.4.3 Restricted Analysis*

The solubility of $CaCO_3$ in dolomite is very limited, especially for $T < 900°C$. Hence, the activity of component 'dolomite' in phase dolomite follows Raoult's Law, to an extremely good approximation. This introduces a critically important simplification into the thermodynamics with little loss of generality.

For coexisting calcite and dolomite at equilibrium

$$a_D^D = a_D^{Ct} \simeq N_D^D \qquad \text{(Raoult's Law)}$$

and

$$\gamma_D^{Ct} \simeq \frac{N_D^D}{N_D^{Ct}} \qquad (11)$$

Table IV tabulates the values of γ_D^{Ct} for composition-temperature points on the solvus limb. The effect of pressure is neglected. For metamorphic temperatures the departures from the ideal solution model are seen to be quite appreciable. Although this analysis is restricted to composition-temperature points located on the solvus curve, the approach provides a good test for the approximations used in the more general model given below, § 5.4.4.

5.4.4. General Analysis

The Gibbs free energy of a solution is given by

$$G = \sum_i N_i \mu_i$$

---

* See § 4.2 for thermodynamic symbols.

Table IV

Comparison of Activity Coefficients Calculated from the Restricted Model and General Model for Composition-Temperature Points on the Mg-Calcite Solvus

T°C	N_D^{Ct}	N_D^D	$\gamma_D^{Ct})_{restricted}$	$\gamma_D^{Ct})_{general}$
1000	0.678	0.912	1.35	1.44
900	0.469	0.942	2.01	2.15
800	0.328	0.960	2.92	3.14
700	0.224	0.975	4.35	4.72
600	0.159	0.984	6.2	7.4
500	0.110	0.990	9.0	11.1
400	0.076	0.993	13.1	16.6
300	0.053	0.995	18.9	23.4
200	0.036	0.997	27.4	33.8
100	0.025	0.998	39.9	40.8
0	0.017	0.999	58.7	50.9

For a binary solution at constant temperature and pressure

$$G = RT \sum_i N_i \ln a_i + N_1 G_1^\circ + N_2 G_2^\circ \qquad (12)$$

where G_1° and G_2° are the Gibbs free energies for the components in their standard states. They are constants for a given temperature and pressure. The molar Gibbs free energy of mixing is defined by

$$\left.\begin{aligned} G_m &= RT \sum_i N_i \ln a_i \\ &= RT \sum_i N_i \ln N_i + RT \sum_i N_i \ln \gamma_i \\ &= G_m^{ideal} + G_m^{excess} \end{aligned}\right\} \qquad (13)$$

The free energy of mixing for the solution is a measure of the relative stability of the solution with respect to the stability of the two separate phases.

The polynomial series, as given by Guggenheim (1959, p. 249), are used to evaluate the activity coefficients:

$$\ln \gamma_1 = N_2^2 \left\{ A_o + A_1(N_2 - 3N_1) + A_2(N_2 - N_1)(N_2 - 5N_1) \right\} \qquad (14)$$

$$\ln \gamma_2 = N_1^2 \left\{ A_o - A_1(N_1 - 3N_2) + A_2(N_1 - N_2)(N_1 - 5N_2) \right\} \qquad (15)$$

The marked asymmetry of the solvus discounts the regular solution model, $A_o \neq A_1 = A_2 = 0$. Hardy (1953) and Lerman (1965) considered a more general model with $A_o \neq A_1$, $A_2 = 0$. This reduces the number of unknown coefficients in equations (14) and (15) to two. By definition the coefficients A_o and A_1 are independent of composition but are dependent on

temperature and pressure. The pressure dependence of A_o and A_1 will be neglected as a first approximation, although the solvus data used is polybaric (§ 5.1.1). At equilibrium

$$\left.\begin{aligned} a_D^D &= a_D^{Ct} \\ a_{Ct}^D &= a_{Ct}^{Ct} \end{aligned}\right\} \qquad (16)$$

From equations (14, 15 and 16) a pair of simultaneous equations in terms of mole fractions, A_o and A_1 can be derived at constant temperature and pressure (Lerman, 1965):

$$\ln(N_{Ct}^D/N_{Ct}^{Ct}) = A_o(N_D^{Ct^2}-N_D^{D^2}) + A_1\left\{(1-4N_{Ct}^{Ct})N_D^{Ct^2} - (1-4N_{Ct}^D)N_D^{D^2}\right\} \qquad (17)$$

$$\ln(N_D^D/N_D^{Ct}) = A_o(N_{Ct}^{Ct^2}-N_{Ct}^{D^2}) - A_1\left\{(1-4N_D^{Ct})N_{Ct}^{Ct^2} - (1-4N_D^D)N_{Ct}^{D^2}\right\} \qquad (18)$$

Table V and Figure 5, after Lerman (1965, Fig. 11), present the solutions for A_o and A_1 as a function of temperature using the equilibrium solvus relations, Figure 1 and equation (10), and equations (17) and (18). The activity coefficients are then calculated from equations (14) and (15) with $A_2 = 0$. The activity coefficient, γ_D^{Ct}, for the composition-temperature point on the solvus curve are presented in Table IV for comparison with the restricted approach solution, § 5.2.3. The agreement is considered satisfactory. The success of the restricted model lies in the insignificant deviations from Raoult's Law for a_D^D at temperatures below 800°-900°C. On the other hand, the general model has demanded a simplified form of the activity coefficient expressions (14) and (15) in terms of no more than two constants, A_o and A_1, at constant P and T.

Fig. 5. -- Coefficients A_o and A_1 as functions of temperatures.

The solid curves are calculated from the solvus data of Goldsmith & Heard (1961). The dashed parts use the extrapolated solvus data for $T < 500^{\circ}C$. (After Lerman, 1965).

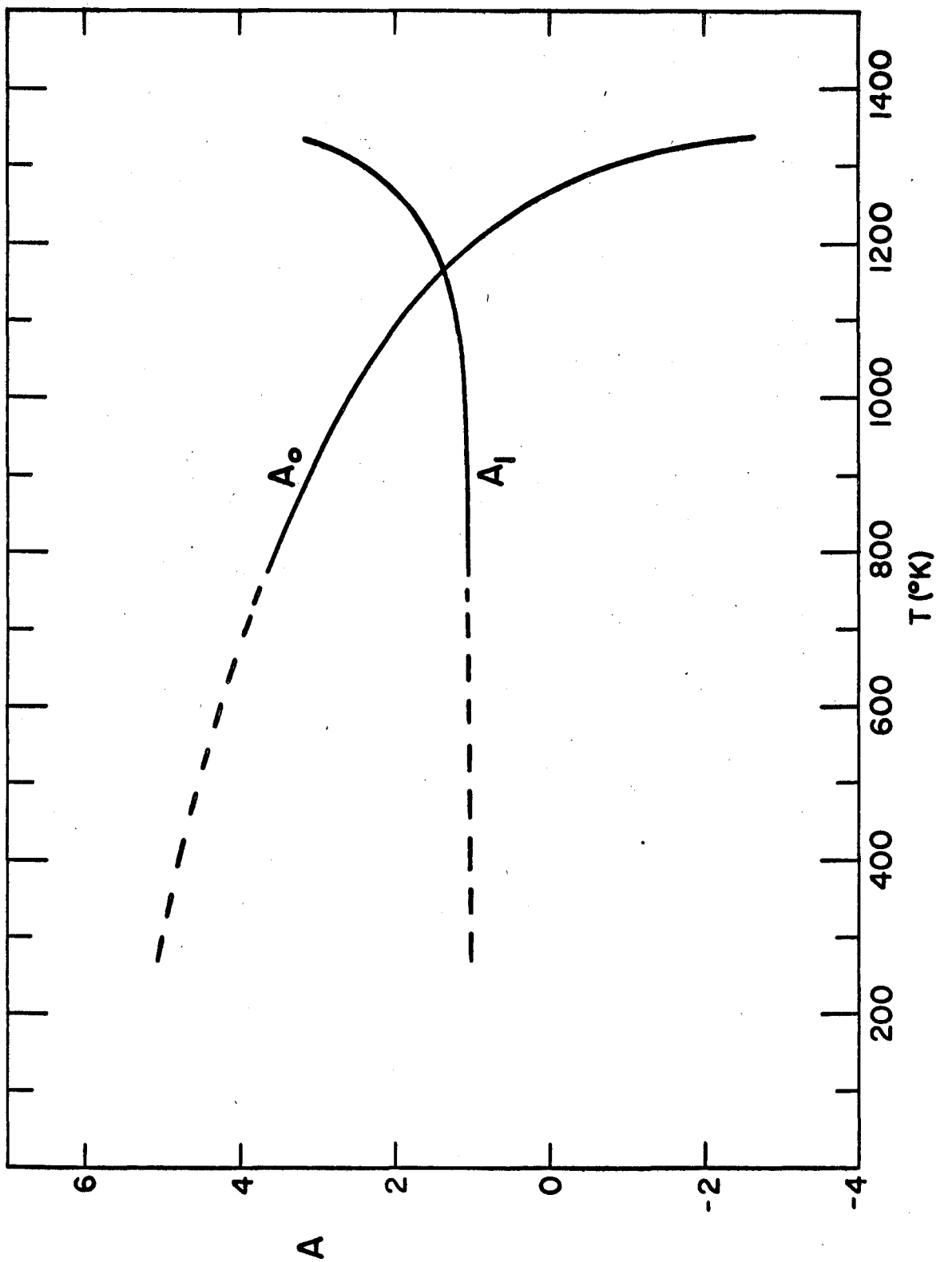
A
6
4
2
0
-2
-4
T (°K)
200
400
600
800
1000
1200
1400
A_0
A_1

Table V

Solutions for Constants A_o and A_1 (after Lerman, 1965)

T°K	N_{Ct}^{Ct}	N_{D}^{Ct}	N_{Ct}^{D}	N_{D}^{D}	A_o	A_1
1333	0.212	0.782	0.114	0.886	-2.431	3.068
1304	0.30	0.70	0.10	0.90	-0.827	2.334
1259	0.40	0.60	0.08	0.92	0.259	1.874
1173	0.56	0.44	0.06	0.94	1.434	1.381
1073	0.70	0.30	0.04	0.96	2.164	1.135
913	0.84	0.16	0.02	0.98	2.962	1.084
773	0.91	0.09	0.01	0.99	3.611	1.017
298	0.98	0.02	0.00_2	0.99_8	5.0	1.0

Although the values for $\gamma_D^{Ct}\big)_{restricted}$ are more reliable, the general analysis is adequate as a first approximation.

The Gibbs free energy of mixing is derived from equations (13) using these activity coefficient data; G_m, γ_D and γ_{Ct} as functions of composition and selected temperatures are shown in Figures 6 and 7.

The variations of G_m, μ_{Ct}, μ_D and $\partial^2 G_m / \partial N_D^2$, with composition are given schematically in Figure 8, P and T constant. The pertinent features arising from these relations are:

1) Stable equilibrium: defined by the minimum value for the total Gibbs free energy for the system. It is given by the common tangent to the points a and b, the coexisting equilibrium calcite-dolomite assemblage. These points a and b are not necessarily at the minima of the free energy of mixing curve.

2) For stability (Prigogine and Defay, 1954)

$$\left(\frac{\partial^2 G}{\partial N^2}\right)_{PT} > 0$$

3) The boundaries between the metastable and unstable regions, points c and d, are determined by

$$\left(\frac{\partial \mu_1}{\partial N_D}\right)_{PT} = \left(\frac{\partial^2 G}{\partial N_D^2}\right)_{PT} = 0$$

Within the metastable region

$$\left(\frac{\partial^2 G}{\partial N^2}\right)_{PT} > 0$$

and the phase is stable to compositional fluctuations. The

Fig. 6. -- Gibbs molar free energy of mixing for Mg-calcites.

Free energy curves are given for four selected temperatures: 500°, 400°, 300° and 25°C. The curves are dashed in the unstable region. The 25°C curve is after Lerman (1965).

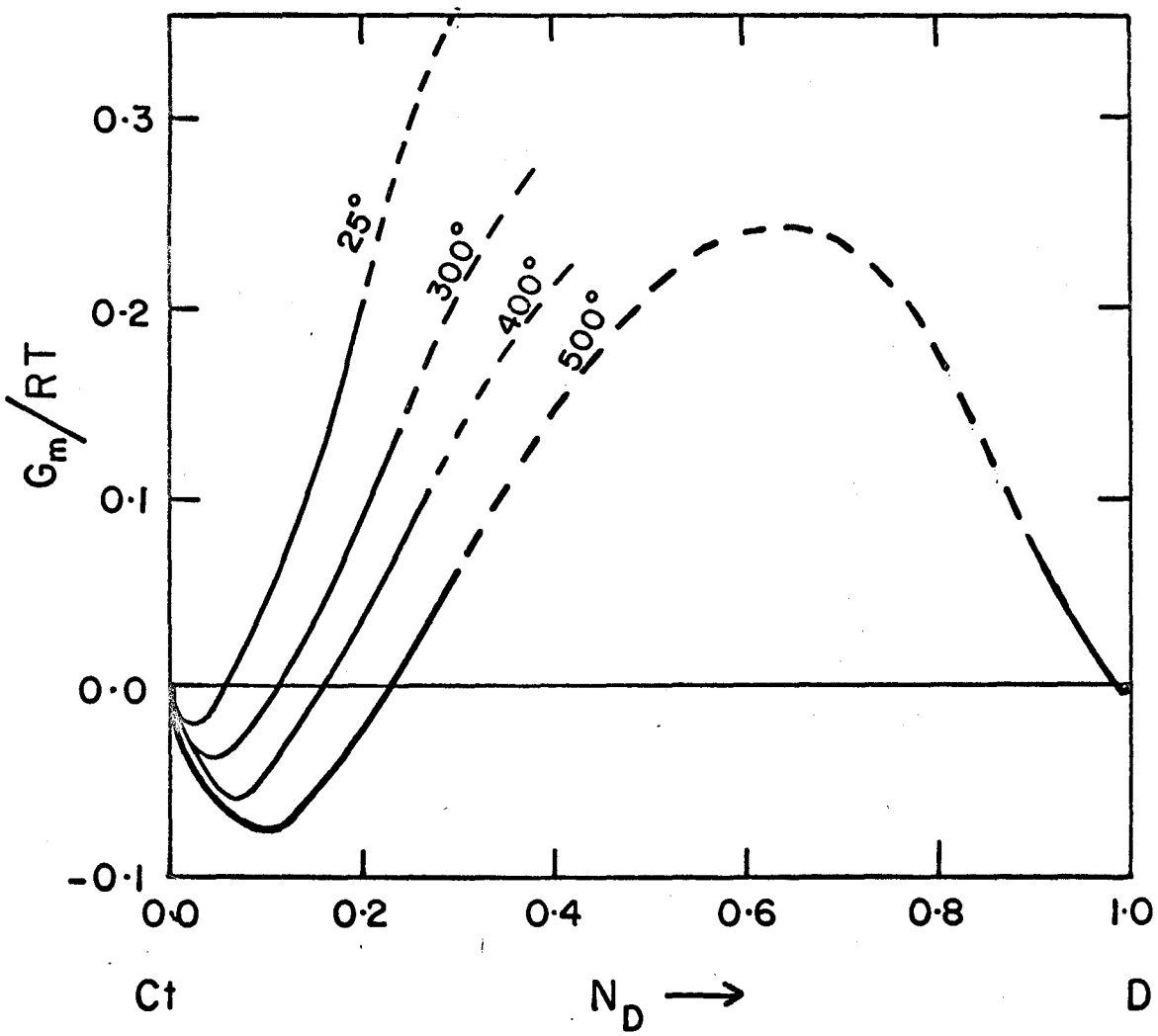
0·3
0·2
0·1
0·0
-0·1
G_m/RT
25°
300°
400°
500°
0·0
0·2
0·4
0·6
0·8
1·0
Ct
$N_D \longrightarrow$
D

Fig. 7. -- Variation of the activity coefficients with composition.

Subscripts: Ct indicates component $CaCO_3$.

D indicates component $Ca_{0.5}\ Mg_{0.5}\ CO_3$

The variation of $\ln\gamma$ is given for two selected temperatures: 500° and 25°C. The 25°C curves are after Lerman (1965).

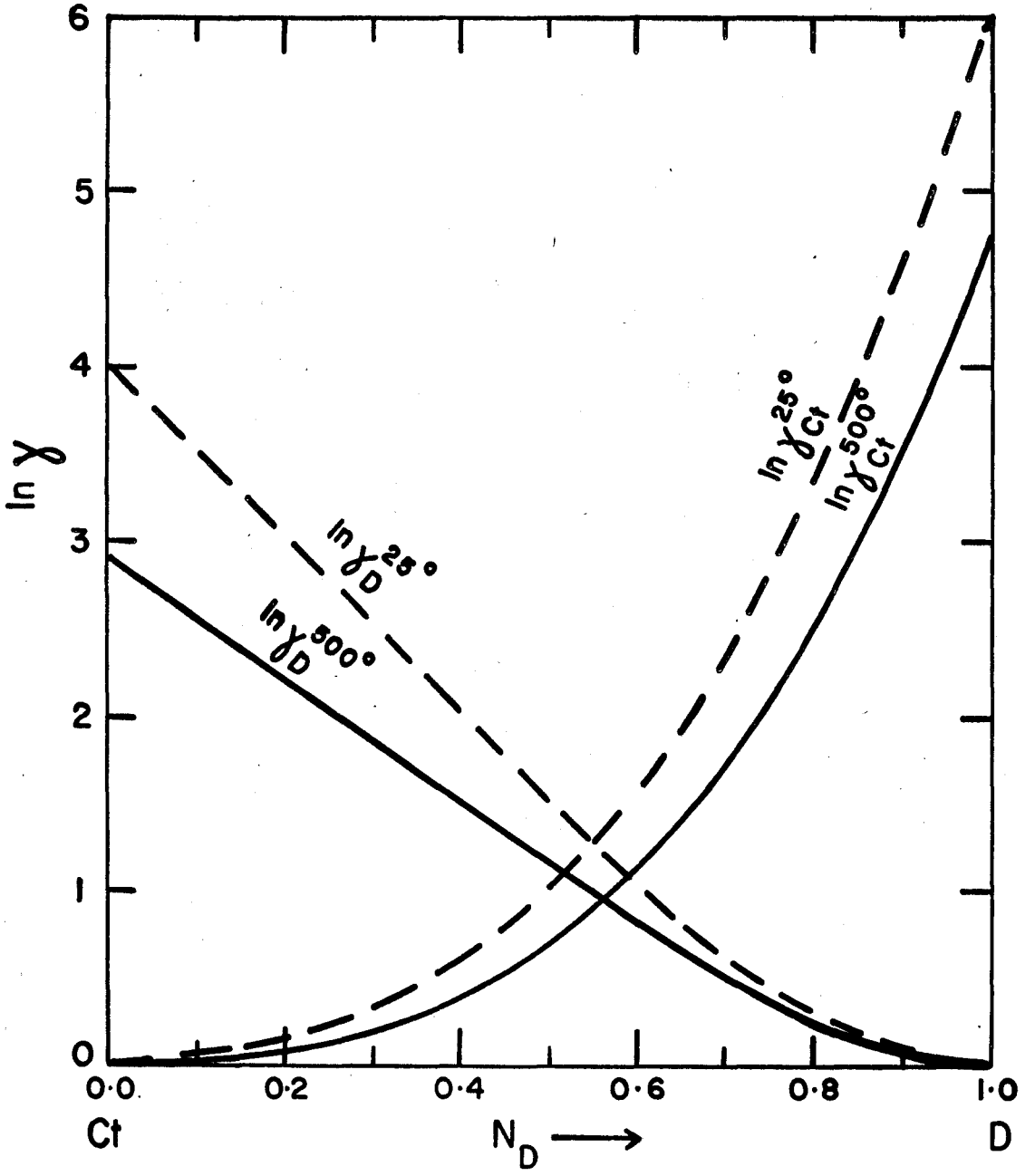
6
5
4
3
2
1
0
ln γ
$\ln\gamma_D^{25°}$
$\ln\gamma_D^{500°}$
$\ln\gamma_{Ct}^{25°}$
$\ln\gamma_{Ct}^{500°}$
0·0
0·2
0·4
0·6
0·8
1·0
Ct
N_D ⟶
D

Fig. 8. -- Schematic representation of the variation of:
(a) the Gibbs free energy of mixing,
(b) the chemical potentials of $CaCO_3$ and $Ca_{0.5}Mg_{0.5}CO_3$,
(c) $(\partial^2 Gm/\partial N_D^2)_{P,T}$,
with composition in the binary system $CaCO_3$-$Ca_{0.5}Mg_{0.5}CO_3$

8(a) Common tangent to a and b joins the coequilibrium calcite - dolomite assemblage. Points c and d are points of inflexion.

To the left of a	Mg-calcite is stable
Between a and c	Mg-calcite is metastable
Between c and d	Mg-calcite is unstable

8(b) At equilibrium

$$\mu_D^{ct} = \mu_D^D$$

$$\mu_{ct}^{ct} = \mu_{ct}^D$$

8(c) At the spinodal points c and d

$$\left(\frac{\partial^2 G}{\partial N_D^2}\right)_{PT} = 0$$

between c and d

$$\left(\frac{\partial^2 G}{\partial N_D^2}\right)_{PT} < 0$$

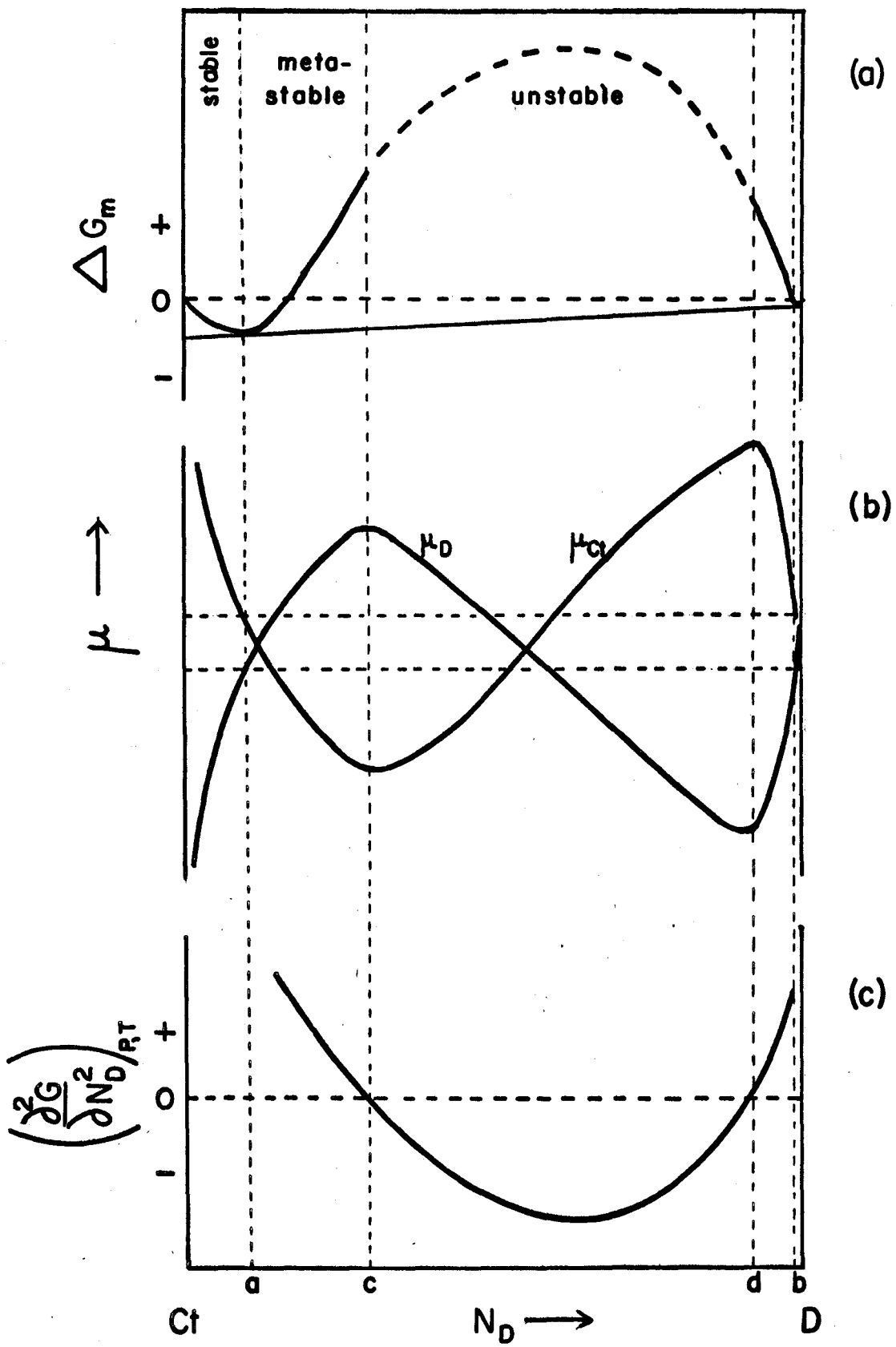
stable
meta-
stable
unstable
(a)
ΔG_m
+
0
−
(b)
$\mu \longrightarrow$
μ_D
μ_{Cl}
(c)
$\left(\frac{\partial^2 G}{\partial N_D^2}\right)_{P,T}$
+
0
−
a
c
d
b
Cl
$N_D \longrightarrow$
D

phase will remain in this metastable equilibrium state until nuclei of a more stable phase are introduced.

4) The points of inflection, c and d, are known as the spinodal points. They occur at the boundary between the metastable and unstable regions. In the unstable region

$$\left(\frac{\partial^2 G}{\partial N_D^2}\right) < 0$$

and the phase is unstable to compositional fluctuations. In this region a high Mg-calcite decomposes spontaneously to a coexisting low Mg-calcite-dolomite assemblage; this is spinodal decomposition due to diffusional instability (Prigogine and Defay, 1954). In the unstable region homogeneous nucleation is dominant. The spinodal point composition has been calculated using the condition

$$\left(\frac{\partial^2 G}{\partial N_D^2}\right)_{P,T} = 0$$

$$= RT \left\{ 1/N_{Ct} + 1/(1-N_{Ct}) + 12 A_1 N_{Ct} - 2(A_o + 3 A_1) \right\} \qquad (19)$$

The variation of the spinodal point composition with temperature is reported in Table VI and shown for Mg-calcites in Figure 9. Comparison of this with the solvus curve in the metamorphic temperature range indicates that all metamorphic Mg-calcites from low to intermediate grades are metastable or stable at 25°C. However, spinodal decomposition may be responsible for the exsolution phenomena in the

Fig. 9. -- Variation of the spinodal point composition with temperature.

Curve A is the Mg - calcite solvus limb.

Curve B is the spinodal point composition curve.

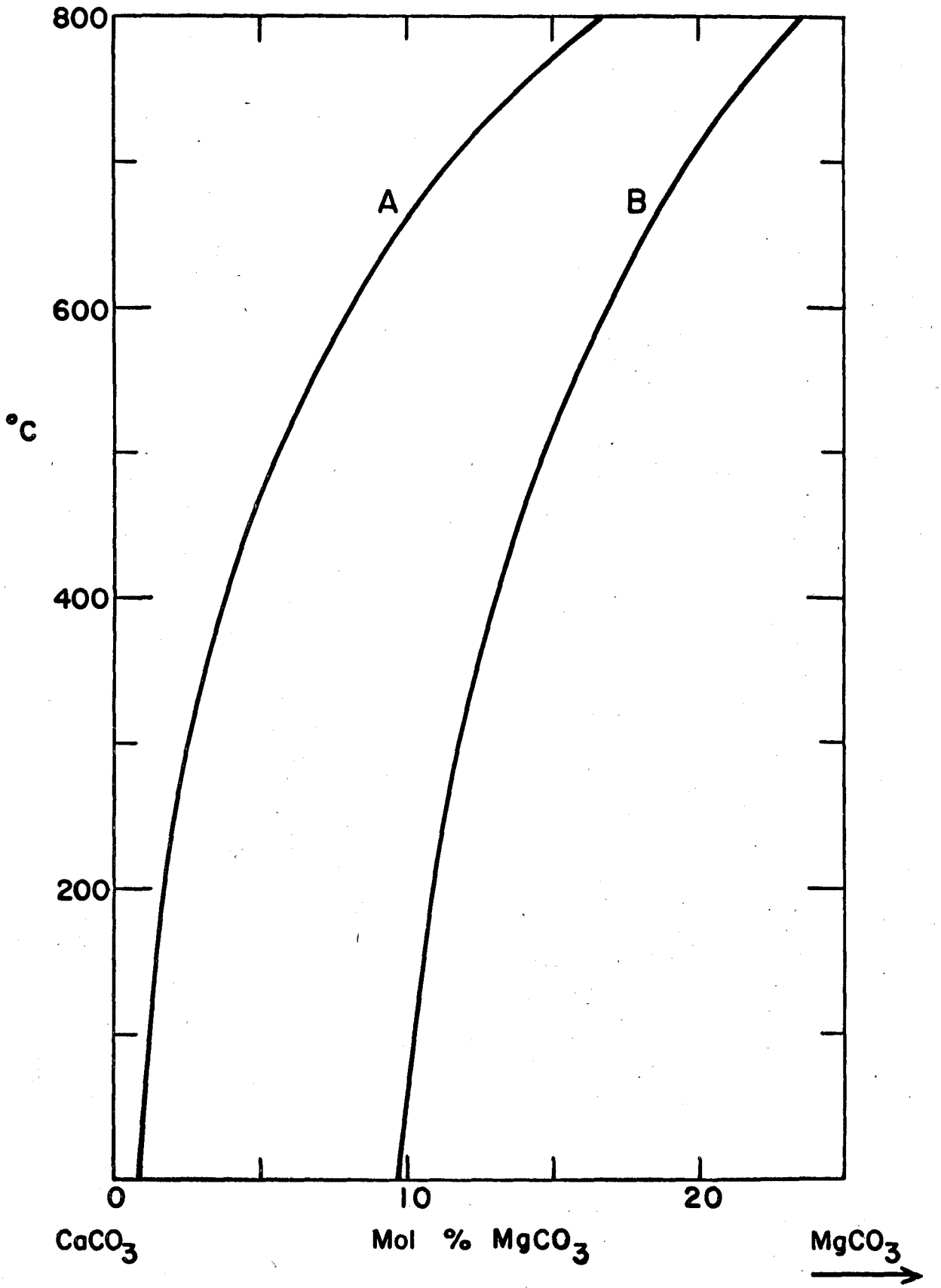
800
600
400
200
°C
A
B
0
10
20
CaCO3
Mol % MgCO3
MgCO3

Table VI

Calculated Values for the Spinodal Composition vs. Temperature

T°C	N_D^{Ct} (Solvus)	Spinodal Point mol % $MgCO_3$
800	0.328	23
600	0.159	17
400	0.076	13
200	0.036	11
25	0.02	10

higher grade assemblages. This effect becomes more critical for marbles from higher pressure as well as temperature regions since the $MgCO_3$ solubility is increased by pressure. Spinodal decomposition may not take place until the sample is in a near surface P,T environment.

This analysis predicts that at 25°C calcites with more than about 10 mol % $MgCO_3$ are thermodynamically unstable. Therefore, Mg-calcites in nature with larger concentrations should be very rare or absent. Excluding some very recent fossils, fossil calcites and metamorphic calcites invariably are observed to contain less than about 10 mol % $MgCO_3$ as demonstrated by Chave (1954), Goldsmith et al. (1955) and Lowenstam (1963). The influence of other cations on the spinodal composition is unknown but is presumed to be small for low concentrations.

5.4.5 Cation Distribution in Carbonates

Many properties of crystals such as the kinetics of phase transformation are dependent upon the types and concentrations of various defects which are present. For this reason the possible nature of the distribution of Mg in calcite and dolomite is considered briefly. Mg-calcites lack long-range ordering as super-lattice reflections are absent (Goldsmith and Heard, 1961). However this does not exclude the possibility of either short-range ordering, as distinct from a random array, or clustering.

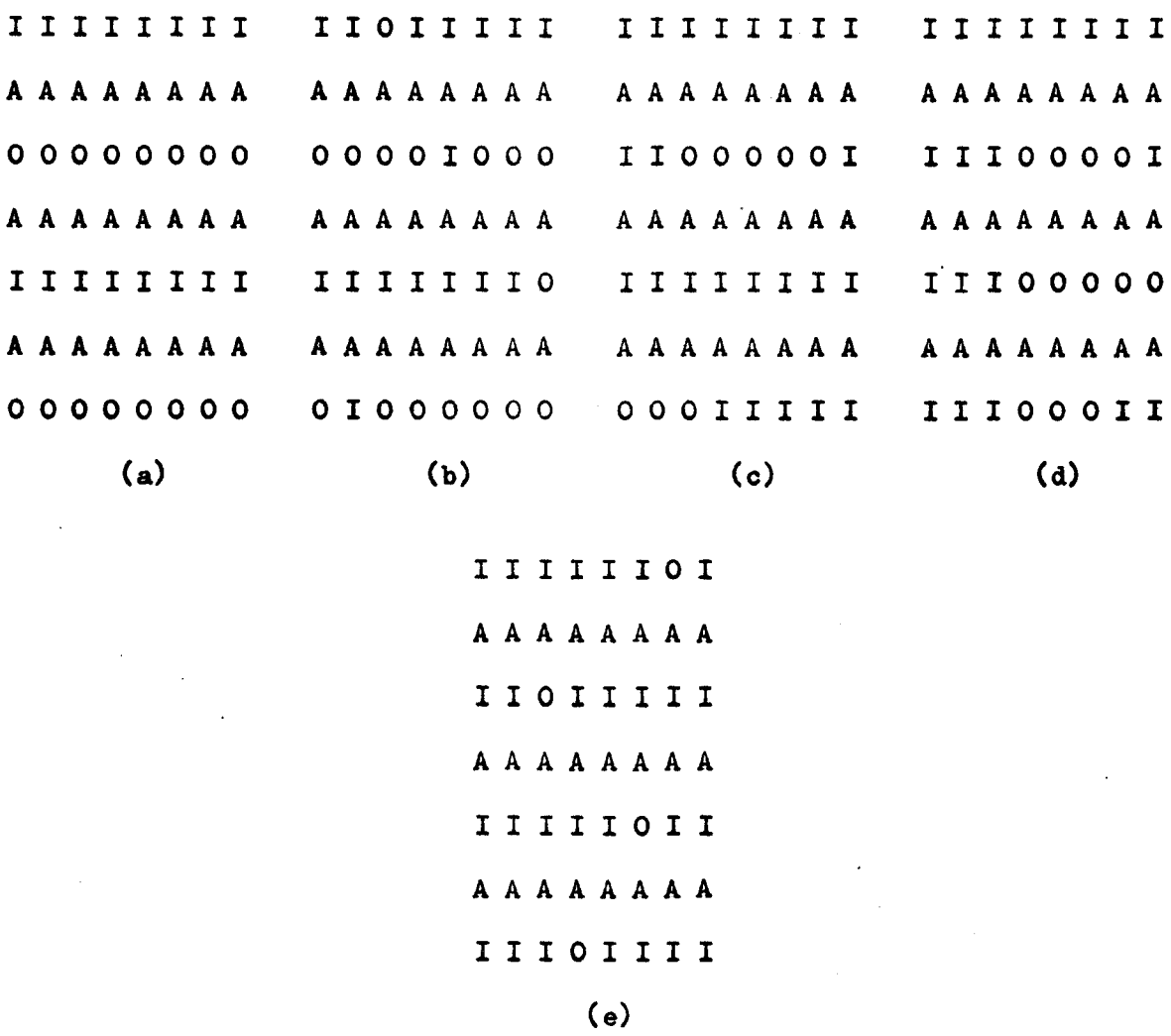

Figure 10. Schematic representation of order, and point and domain disorder, where I and O are two different cations.

(a) Ordered compound like dolomite.

(b) Point disorder in dolomite type structure.

(c) and (d) Domain disorder.

(e) Point disorder in calcite type structure.

5.4.5.1 Dolomite

Goldsmith and Graf (1958) and Goldsmith and Heard (1961) have discussed the X-ray characteristics of dolomite in terms of certain disordering models, which are not necessarily independent of each other. These authors present the X-ray criteria for the models. Ordered dolomite consists of alternating basal planes of Ca and Mg ions as shown in Figure 10(a). In summary these models are:

Point Disorder: Ca atoms occupy Mg sites and Mg atoms occupy Ca sites. The probability of Mg being at either site approaches 0.5 (see Fig. 10(b)). The cation arrangement may be random or have short-range order. Point or substitutional disorder occurs in dolomite when Ca:Mg $\neq$ 1:1. Also it can occur in dolomite with Ca:Mg = 1:1.

Domain Disorder:

The Mg or Ca cations in excess of the 1:1 ratio for ideal dolomite reside in certain locations as shown in Figure 10(c) and (d), producing small out-of-step regions or domains. The special two-dimensional case of this is mixed layering or layer disordering. Domain disordering is equivalent to subunits of calcite or magnesite within the dolomite host, i.e. clustering.

In dolomites, various combinations of these types of disordering have been observed over a temperature and compositional range by Goldsmith and coworkers (e.g. Goldsmith and Heard, 1961).

5.4.5.2 Calcite

These models for dolomite provide a useful framework for the discussion of the possible distribution of Mg in calcite. At present, very little is known about the nature of this distribution.

For Mg-calcites there are two models for clustering: (1) preference for like nearest neighbours in three dimensions; carried far enough this would result in domains of $MgCO_3$ in the calcite host (Fig. 10(d)); (2) preference for like nearest neighbours within cation layers but unlike neighbours between layers; this would result in domains of $CaMg(CO_3)_2$ within the calcite host (Fig. 10(c)). An alternative model for the non-random distribution of Mg in calcite is short-range ordering. Figure 10(e) represents point disorder in the calcite type structure.

It is of interest to summarize some of the characteristics of short-range ordering and clustering as observed in alloy systems and apply these results to the Mg-calcite problem to suggest a tentative model for the description of the Mg distribution in calcite. Ordering phenomena in binary alloys tend to be simpler than those in mineral systems because of their higher symmetry. In summary, the relevant characteristics of binary alloys, after Averbach et al. (1954), are:

Short-Range Order: ΔH_m negative or positive; strain energy very critical, and hence difference in ionic radii important; chemical bonding effects secondary; precipitation sluggish; heterogeneous nucleation dominant.

Clustering: ΔH_m positive; chemical bonding effects critical; differences in ionic radii small; clustering provides embryos for precipitation reactions, therefore, exsolution is relatively rapid; homogeneous nucleation dominant.

Strain energy, introduced through differences in atomic size, tends to be lowered by the occurrence of a non-random cation arrangement and/or immiscibility. This may be important in the calcite system (see the cation solubility order, § 5.1.3). In this system, with ΔH_m positive, a non-random cation arrangement is to be expected. The laboratory studies of Goldsmith (1960) indicate that the precipitation of dolomite in high Mg-calcite occurs with ease. The thermodynamic analysis above also supports this and indicates that homogeneous nucleation is dominant in the unstable region. These few observations tentatively favour the clustering of $CaMg(CO_3)_2$ in calcite. This effect would become more dominant as the concentration of Mg increases.

5.5 Conclusions

A good correlation exists between the solvus derived temperature and the metamorphic grade for many samples. Low to intermediate grade Mg-calcites give well defined back reflections. Many high grade calcites give broad or split-peak back reflections with the highest Mg-calcite correlating with the metamorphic grade. The few chemical analyses available on high grade cloudy calcites give $MgCO_3$ contents appreciably higher than those determined by the X-ray technique (Table III). Exsolved dolomite is, at least in part, responsible. The higher solvus temperature

derived from the chemical analysis gives a geologically reasonable temperature, even without applying a correction for pressure. The influence of other cations on T_s is of second order. T_s may be too high by 40° to 60°C if the pressure at the time of quench was as high as 7 to 10kb. A thermodynamic analysis of the solvus relations is consistent with the observed quench phenomena in the high Mg-calcites. Spinodal decomposition may be important here. Finely divided dolomite can cause clouding in calcite (Goldsmith, 1960). This is consistent with, but does not prove, the proposed clustering of CaMg in the calcite host and the importance of homogeneous nucleation of dolomite.

VI. EXCHANGE REACTION STUDIES

6.1 Introduction

These equilibration experiments were aimed at determining the equilibrium carbon isotope fractionation between calcite and dolomite as a function of temperature. In the general review of previous isotopic experimental work in carbonate systems, § 2.4, the important significance of true exchange reactions was emphasized. Only exchange reactions were performed in this work except for some preliminary synthesis runs where calcite-dolomite mixtures were produced from the reaction of calcite with $MgCl_2$ solutions. These latter experiments were abandoned because of poor reproducibility.

6.2 Preliminary Carbonate-Carbonate Exchange Reactions

Cold seal hydrothermal bombs are not convenient for carrying out isotopic exchange reactions of the type:

$$CaC^{13}O_3 + C^{12}O_2 \rightleftharpoons CaC^{12}O_3 + C^{13}O_2$$

Therefore, alternative exchange reactions were explored of the following type:

$$CaC^{12}O_3 + Na_2C^{13}O_3 \rightleftharpoons CaC^{13}O_3 + Na_2C^{12}O_3$$

$$CaMg(C^{12}O_3)_2 + Na_2C^{13}O_3 \rightleftharpoons CaMg(C^{13}O_3)_2 + Na_2C^{12}O_3$$

Ideally this method has the advantage that at the end of a run the two carbonates can be separated easily. However, the formation of double carbonates such as $Na_2Mg(CO_3)_2$ precluded these reactions.

6.3 Calcite-Dolomite Exchange Reactions

6.3.1 Introduction

The direct determination of the isotopic fractionation between dolomite and calcite avoids the problem of analysing the fluid phase. At the conclusion of such runs the coexisting dolomite and calcite, which cannot be physically separated, are separated chemically, exploiting the different reaction rates of calcite and dolomite with phosphoric acid. This technique and its limitations are discussed above, see § 3.1.

Exchange reactions between calcite and dolomite were studied:

$$\text{Calcite} + \text{Dolomite} \longrightarrow \text{Mg-calcite} + \text{Dolomite}$$

Coupled with the chemical exchange, the isotopic exchange:

$$Ca_{1-x}Mg_xC^{13}O_3 + \tfrac{1}{2}CaMg(C^{12}O_3)_2 \rightleftharpoons Ca_{1-x}Mg_xC^{12}O_3 + CaMg(C^{13}O_3)_2$$

where $x \leqslant 0.4$.

In these reactions the equilibrium composition of the Mg-calcite coexisting with the dolomite depends upon the temperature (Fig. 1). These exchange reactions have the advantage that (1) a limited degree of cation exchange takes place without creating or destroying any phase and (2) the isotopic fractionation between Mg-calcite coexisting with dolomite is determined directly.

6.3.2 Experimental Methods

All the carbonate exchange reactions were carried out using conventional hydrothermal apparatus. Cold seal bombs (O.D. = 2.0", I.D. = 0.5") (Tuttle, 1949) holding three gold capsules (d = 6 mm., l = 3.8 cm.) were run at the selected temperature and 1000 bars water pressure. The pressure is read directly off a gauge connected to the bomb. The temperature was measured by a chromel-alumel thermocouple placed in a well in the bomb wall close to the sample. The temperature is recorded to ±5°C. Nevertheless, there are two cautions to be observed regarding the character of cold seal bombs: (1) the sample temperature probably is not known to better than ±25°C, because the bombs are externally heated, (2) the length of the gold capsule is such that a significant temperature gradient may exist along it, especially during the higher temperature runs. Quenching was completed in a few minutes at constant pressure using a cold air blast until $T < 400°C$, followed immediately by a cold water bath. These exchange reactions were run for a few days to five weeks. Some small cold seal bombs were used for exploratory runs.

In each charge an intimate mixture of calcite and dolomite of known composition was sealed in a gold capsule with a known quantity of water plus salts. The isotopic compositions of the starting materials were chosen so that the exchange reactions for two of the three charges would approach the equilibrium fractionation from a distance, but from opposite sides, while the third charge had an initial composition quite close to the anticipated equilibrium value. The composition of the water plus salt was dictated by the following considerations:

1) H_2O - water was added to aid the exchange reactions.

2) $CaCl_2$ - above about 100°C dolomite is incongruently soluble in water (Morey, 1962; Rosenberg and Holland, 1964). Addition of small quantities of Ca^{++} ions prevents this decomposition of dolomite. In was felt important to prevent the formation of other phases such as magnesite in order to restrict the partial equilibration studies to simple exchange reactions.

3) NH_4HCO_3 - dolomite decomposes to brucite plus calcite in water at high temperatures and low P_{CO_2}. The minimum quantity of NH_4HCO_3 was added sufficient to prevent brucite formation.

4) NH_4Cl - exchange rates are increased in carbonate systems by the addition of NH_4Cl (Clayton, 1959; O'Neil, 1963; Northrop, 1964).

A description and the isotopic composition of the starting materials are given in Tables VII and VIII respectively. The composition of a typical initial charge is given in Appendix I. In all runs, with $T > 320°C$, the fluid phase probably can be considered as an aqueous rich single phase (Takenouchi and Kennedy, 1964). X-ray examination of the solid phases at the conclusion of all runs revealed only Mg-calcite and dolomite. No magnesite nor brucite was detected.

Incomplete isotopic exchange was achieved in all runs. This is a problem that is characteristic of laboratory studies in systems with dolomite (Epstein et al., 1964; Northrop and Clayton, 1966; O'Neil and

Table VII

Description of the Starting Materials

Sample		Description
Calcites:	A-calcite	A very finely-divided, reagent grade $CaCO_3$ (B.D.H.)
	H-calcite	A very finely-divided $CaCO_3$ synthesized from Tivoli travertine.
	L-calcite	A very finely-divided $CaCO_3$ synthesized from Canadian Liquid Air tank CO_2.
Dolomites*:	H-dolomite	A white metamorphic dolomite from Haley, Ontario; a well crystallized dolomite with well-defined order reflections.
	B-dolomite	A natural hydrothermal dolomite from Bamle, Norway; from the same hand specimen as that used by Northrop.**
Others:	$CaCl_2$	A calcium chloride solution: 4.22 gm. of reagent grade $CaCl_2\ 2H_2O$ in 100 cc. H_2O.
	NH_4HCO_3	A reagent grade NH_4HCO_3 (B.D.H.)
	NH_4Cl	A reagent grade NH_4Cl (Fisher)
	H_2O	Laboratory distilled water.

* Partial chemical analyses are given in Table IX.

** The author thanks Dr. D.A. Northrop for this sample.

Table VIII

Isotopic Composition of the Starting Materials

Material		δO^{18}_{SMOW} (‰)	δC^{13}_{PDB} (‰)
Calcites:	A-calcite	13.65	-7.07
	H-calcite	9.04	+8.80
	L-calcite	5.10	-28.07
Dolomites:	H-dolomite	27.67	+2.94
	B-dolomite	11.50	-8.00
Others:	NH_4HCO_3	3.51*	-25.80

* Using $\alpha_{CO_2\text{-}NH_4HCO_3} = 1.01008$

Epstein, 1966). The technique developed by Northrop and Clayton (1966) was used, whereby the equilibrium fractionation is obtained by graphical extrapolation of a set of incomplete exchange reaction runs.

The kinetics of isotopic exchange reactions in heterogeneous systems are complex. The rate of exchange of ions between coexisting phases is a function of the surface area, which changes with time, extent of solution, degree of recrystallization, nature of starting material, presence of other ions, temperature, etc. Northrop and Clayton have modified the more simple analysis for homogeneous exchange reactions (e.g. see Bunton et al., 1955; Frost and Pearson, 1961). This method is based on the assumption that the amount of exchange is directly proportional to the distance that the system is from isotopic equilibrium. It is assumed that the reaction rate is independent of the relative numbers of the different isotopic species present, i.e. there is negligible isotope effect.

Three charges of identical constitution except for their isotopic compositions were run together in a single bomb in order to have identical thermal histories. The fractionation data were then analysed using Northrop and Clayton's relation:

$$\ln \alpha_i = \ln \alpha_e + B (\ln \alpha_f - \ln \alpha_i)$$

where $1000 \ln \alpha_i$ = initial fractionation (observed)

$1000 \ln \alpha_f$ = final fractionation (observed)

$1000 \ln \alpha_e$ = equilibrium fractionation (determined)

B = constant.

The initial and final isotopic analyses of each charge in a set was plotted as ($\ln \alpha_f - \ln \alpha_i$) against $\ln \alpha_i$. The method predicts that this plot should give a straight line of slope B and with an intercept of $\ln \alpha_e$. Northrop and Clayton (1966, p. 179) state that "the fact that so many different sets of samples run under widely varying conditions yielded linear plots is a good indication that this method is valid". The accuracy of the method is greatly enhanced by an increase in the percentage of exchange. The percentage of exchange is measured by $\frac{-100}{B}$, if some exchange occurs throughout the whole crystal.

These authors found that the exchange behaviour of different initial dolomites was different, which was not unexpected. However, different values for the equilibrium fractionation were obtained from these different dolomites at the same temperature. A similar result was found in one run in this work. At present these important differences between the extrapolated fractionations are not understood completely. No chemical analyses of starting materials were presented by Northrop and Clayton. Partial chemical analyses of both the dolomites used in this work, Haley and Bamle, are given in Table IX. The Bamle dolomite was taken from the same hand specimen as used by Northrop; its relatively high iron content is noted.

6.3.3 Experimental Results

The dolomite-Mg-calcite fractionations determined from the sets of partial exchange reactions are given in Table X and in Figure 11 for each temperature studied. To a good approximation, the sets of charges have yielded linear plots. The $MgCO_3$ content of the Mg-calcite was

Table IX

Partial Chemical Analyses of Dolomite Starting Materials

Sample	$FeCO_3$	$MnCO_3$	$SrCO_3$
Haley Dolomite	0.00	0.02	0.023
Bamle Dolomite	5.69	0.15	0.003

Analyst: J.R. Muysson

Table X

Experimental Data for Sets of Dolomite-Calcite Samples*

Run	D	Temp. (°C)	Time (hrs.)	Solvus Temp. (°C)	$10^3 \ln \alpha_i$	$10^3 \ln \alpha_f$	$10^3(\ln \alpha_f - \ln \alpha_i)$	δO^{18}_{Ct} (‰)
CtD II	H	335	803	~25	-5.24	-3.57	1.67	7.64
					31.36	28.13	-3.23	7.27
					1.00	1.32	0.32	9.51
CtD III	H	500	346	485	-3.58	-1.01	2.57	1.50
					31.24	14.70	-16.54	0.36
					1.46	1.46	0.00	1.76
CtD I	H	590	240	570	-2.66	-0.69	1.97	0.82
					31.19	7.77	-23.42	0.50
					2.08	0.98	-1.10	1.53
CtD IV	H	610	113	580	-2.83	-0.67	2.16	0.80
					2.10	0.39	-1.71	2.58
CtD V	B	590	113	565	-13.62	-7.36	6.26	-0.44
					20.22	6.55	-13.67	-0.70
					-8.72	-4.53	4.19	+0.38

* See Appendix I for (1) constitution of typical initial charge and (2) NH_4HCO_3 correction.

Fig. 11. -- The determination of the dolomite - calcite C-isotope fractionation by partial exchange from 335° to 610°C.

Y axis is: $1000 \ln \alpha_{initial}$

X axis is: $1000 (\ln \alpha_{final} - \ln \alpha_{initial})$.

1 Unit = $1000 \ln\alpha = 5$

● H - dolomite

○ B - dolomite

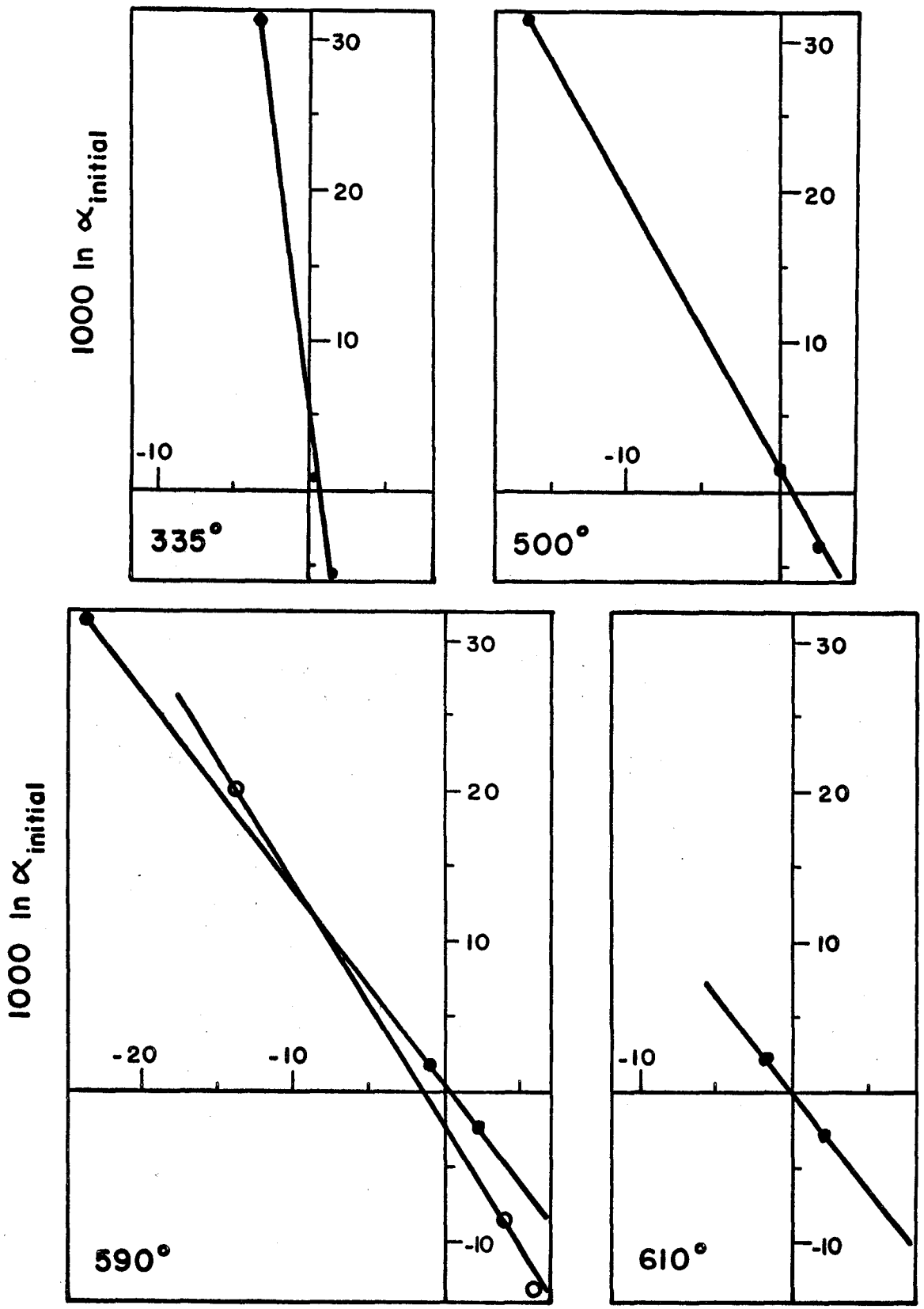
1000 ln $\alpha_{initial}$
30
20
10
-10
335°
500°
-20
590°
610°
1000 ($\ln \alpha_{final} - \ln \alpha_{initial}$)

determined for each run and this provides a convenient guide as to whether equilibrium Mg partitioning was attained for the temperature, using the line in Figure 2. Cation equilibration was attained in all runs excepting the lowest temperature run at 320°C. Excepting this same run, recrystallization of the calcite was conspicuous. Some calcite crystals were as large as 1 mm. across. Recrystallization of the dolomite, if any, was less apparent and difficult to judge adequately because of the presence of intimately mixed finer grained calcite. Absence of the very fine fraction, however, was noticeable. No quench products were observed in these runs.

The results of these exchange runs are presented in Table XI and in Figure 12. The temperature dependence of this fractionation in the range of 335° to 610°C can be described by the equation:

$$1000 \ln \alpha^{C^{13}}_{D-Ct} = 3.93 (10^6 T^{-2}) - 5.04 \qquad (20)$$

6.3.4 Discussion

The combination of obtaining a satisfactory linear plot for each set of charges, Figure 11, and a linear relation between the determined fractionations plotted against $10^6 T^{-2}$, shown in Figure 12, might lend confidence to the method and the results. The fractionations given by equation (20) are large in comparison with those determined from natural calcite-dolomite assemblages, to be discussed below (§ 9.2). The equivalent runs CtD I and CtD VB, using the Haley and Bamle dolomite respectively, gave different values for the apparent equilibrium frac-

Table XI

The Dolomite-Calcite Carbon Isotope Fractionation Determined From Sets of Incompletely Exchanged Dolomite-Calcite Samples

Run	Dolomite	Temperature (°C)	Time (hrs.)	$10^3 \ln \alpha_e^{C^{13}}$	- 1/B
CtD II	Haley	335	803	5.6	0.13
CtD III	Haley	500	346	1.4	0.54
CtD I	Haley	590	240	0.4	0.76
CtD IV	Haley	610	113	0.0	0.79
CtD V	Bamle	590	113	-2.4	0.62

Fig. 12. -- The experimentally determined dolomite - calcite fractionation between 335° and 610°C.

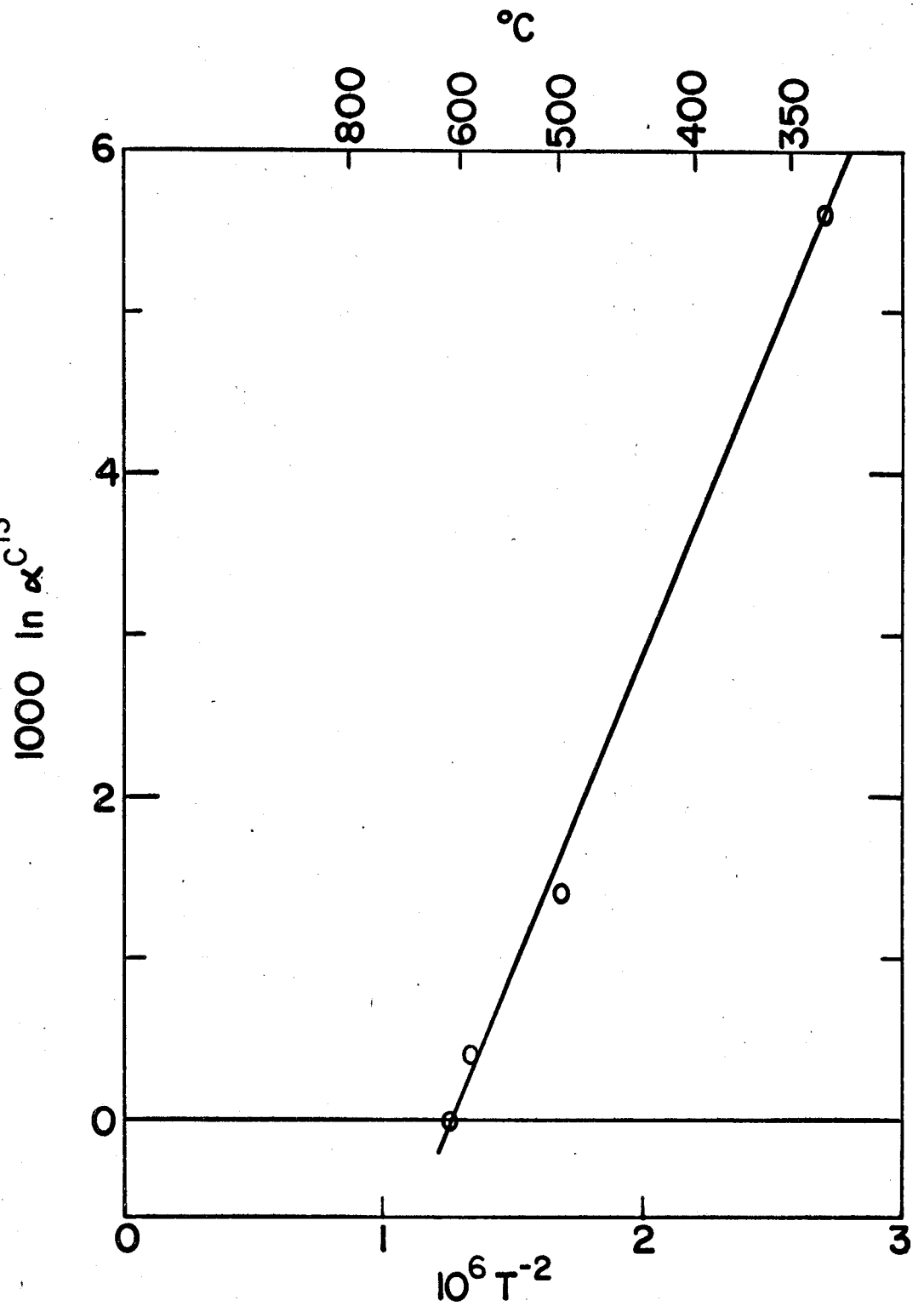
°C
800
600
500
400
350
6
4
2
0
1000 ln $\alpha^{C^{13}}$
0
1
2
3
$10^6 T^{-2}$

tionation at 590°C. A similar such discrepancy observed in O^{18} partial exchange studies by Northrop and Clayton (1966) was noted previously. These results cast doubt on the adequacy of this method, despite the linearity of the plots shown in Figures 11 and 12, when incomplete exchange occurs. Although the fractionation is approached from both directions in each run, little confidence can be attached to the equating of the intercept, $\ln \alpha_e$, with the equilibrium fractionation between homogeneous dolomite coexisting with homogeneous calcite until the above problem is resolved.

6.4 Experimentally Determined Fractionations Expressions - Problems

Resolution of the conflict between the experimental and natural fractionation results necessitates an explanation of the following observations:

1) Studies with dolomites of different isotopic composition lead to different values for the equilibrium fractionation. This applies to all methods used: dolomite-H_2O, CO_2-dolomite, dolomite-calcite and for both oxygen and carbon isotopes.
2) The empirical fractionation expression for both carbon and oxygen isotopes closely follows the form predicted by the Urey-Bigeleisen-Mayer theory:

$$\ln K = AT^{-2} + B.$$

Point (1) was noted by Northrop (1964, p. 64) for his CO_2-carbonate data. However, it is also critical in his dolomite-H_2O experiments and in the dolomite-calcite experiments of this work. One possible explanation is that, although the Northrop-Clayton expression

apparently is followed, $\ln \alpha_e$ is not independent of either B or the isotopic composition of the initial carbonates. B is not a simple measure of the percent of exchange in these partial exchange reactions.

Haul and Stein (1955) using C^{13}, and Northrop and Clayton (1966) and O'Neil and Epstein (1966) using O^{18} have shown that the exchange rate in the system carbonate-CO_2 is initially fast but is followed by a slower rate, as presumably exchange proceeds into the solid by a diffusion controlled mechanism. Exchange rates were observed to be faster in calcite than in dolomite and faster for oxygen than carbon (Northrop and Clayton, 1966). The fractionations for calcite appear to be closer to the presumed equilibrium values. The final O-isotope composition of the calcites in the dolomite-calcite experiments, Table X, signifies that O-isotope equilibrium between the calcite and the water rich fluid phase was approached. The isotopic composition of the initial fluid phase is not known. It is assumed here that in experimental systems with dolomite the rate of exchange of the isotopic species in dolomite is the rate determining step.

Partial exchange reactions between dolomite and some source of oxygen or carbon can be considered to occur in two ways:

1) Partial exchange to some extent throughout the whole crystal.
2) Partial exchange with the outer shell but, because of the very slow exchange rates within the crystal, no exchange with the crystal core.

Type 1) is only the special case of type 2). At the surface, local equilibrium presumably is attained with the source. 'Outer shell' is used here to include more than just the surface layer. O'Neil and Epstein (1966) have shown that exchange extended through several layers into the crystal.

In Figure 13 the function $-B^{-1}$, using the C^{13} results of Table XI and the O^{18} results for the Bamle and Lee dolomites given by Northrop and Clayton (1966, Table 3) is plotted against the difference between the empirical fractionation and the probable equilibrium fractionation, derived in § 9.2 from the natural dolomite-calcite fractionations. A good correlation between these parameters is noted. This figure shows that α_e depends on the isotopic composition of the starting materials until $-B^{-1} \simeq 0.75$. The topological relations of the Bamle and Lee dolomite curves, Figure 13, are in sympathy with this argument, with $\delta O^{18}_{Lee} = 24.0‰$; $\delta O^{18}_{Bamle} = 11.8‰$. Similarly, in Northrop's CO_2-carbonate partial exchange runs the Bamle dolomite gave consistently larger values for the fractionation than the Lee, for both oxygen and carbon isotopes, with $\delta C^{13}_{Lee} = +0.70‰$; $\delta C^{13}_{Bamle} = -7.70‰$. The greater dispersion of Northrop and Clayton's data shown in Figure 13 is a consequence of the less regular relationship between 1000 ln $\alpha^{O^{18}}_{D-H_2O}$ vs $10^6 T^{-2}$. The reason for this irregularity is not clear. It could be due to the partial decomposition of dolomite observed in many of their runs or to the effect of the length of the experiment on the resulting fractionation.

The results of runs CtD I and CtD IV carried out at similar temperatures for different times, 240 hours and 113 hours respectively, give evidence that the value of the determined fractionation is more sensitive to temperature than to time.

Fig. 13. -- The variation of $-B^{-1}$ with 1000 ($\ln \alpha_{experiment} - \ln \alpha_{rock}$) for the Bamle, Lee and Haley dolomites.

Line B is drawn through the dolomite - calcite O-isotope fractionation data derived from the Bamle dolomite - water fractionation results of Northrop and Clayton (1966).

Line L is similar to Line B but is drawn through the Lee dolomite - water fractionation results of Northrop and Clayton (1966).

Line H is similar to Lines B and L but is drawn through the C-isotope results of this work with the Haley dolomite.

1000 ($\ln \alpha_{exp} - \ln \alpha_{rock}$) is the difference between the experimentally determined dolomite-calcite fractionation and the probable equilibrium fractionation for the same temperature derived from the natural fractionation data (see (22) and (23), § 9.2.)

⊙ B - dolomite

o L - dolomite

• H - dolomite

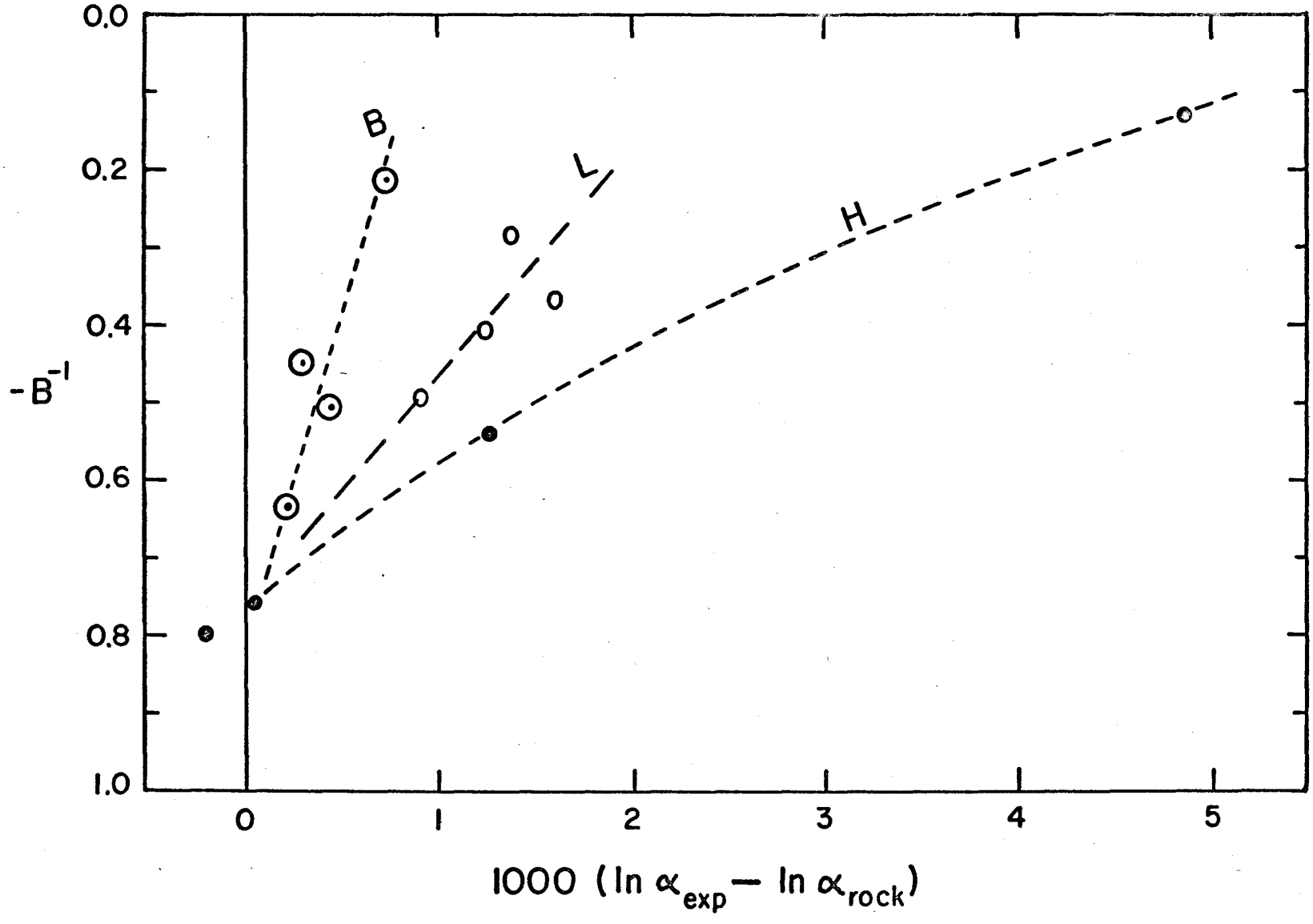
0.0
0.2
0.4
0.6
0.8
1.0
$-B^{-1}$
B
L
H
0
1
2
3
4
5
1000 ($\ln \alpha_{exp} - \ln \alpha_{rock}$)

The observation that all the experimental fractionation expressions give, to a good approximation, a linear relation against $10^6 T^{-2}$ also favours a process where the fractionation between those parts of the system undergoing exchange is primarily determined by the temperature of the experiment, with the time dependence being small compared with the length of the run.

The following model is proposed as being, in principle, consistent with the above observations and Figure 13.

1) The rate of exchange of the isotopic species in dolomite, or calcite in the absence of dolomite, is the rate determining step.
2) Partial exchange occurs with an outer shell, whilst the crystal core may remain unaltered.
3) Partial exchange processes are described by the Northrop-Clayton expression. B^{-1} is not necessarily the proportion exchanged.
4) The core size and composition introduces a factor into the determined fractionation. This factor may be rather insensitive to time.

The derivation of a more explicit expression for such a model has not been attempted. This model should be tested in more detail.

VII. REGIONAL METAMORPHIC FRACTIONATION STUDIES

7.1 Introduction

The exploratory studies on marbles from Vermont by Schwarcz (1966) forecast more complex relations than those anticipated from a simple model of attainment and preservation of the equilibrium state for a temperature at or near the thermal high. Therefore, the sampling programme was shaped by the following questions:

1) is equilibrium generally attained in metamorphic carbonate systems?
2) if equilibrium was attained, what are the relationships between the effective quench temperatures of the C-isotopes, O-isotopes, $MgCO_3$ solubility in calcite and the metamorphic grade?
3) if equilibrium is either attained but subsequently destroyed, or never attained at all, can anything be deduced about the nature of the processes?
4) how sensitive are the phases to retrograde effects?
5) can anything be deduced about the nature and role of the possible pore fluid phase?
6) what is the effect of decarbonation on the isotopic composition of the carbonates?

Samples were collected over comparatively large areas of regional metamorphic rocks, both in Vermont and in the Grenville Province.

Southwestern Vermont: 15 x 80 sq. miles.

Southeastern Vermont: 12 x 25 sq. miles.

Grenville Province : 100 x 160 sq. miles.

This scale of sampling was dictated largely by the need for coexisting carbonate pairs from as wide a range of metamorphic environments as possible. However, there are many dangers to such sampling methods; in particular, it is easy to lose sight of the geological setting of a particular sample locality.

7.2 Southwestern Vermont

The Vermont Valley runs north-south, bordered to the east by the Green Mountain massif and on the west by the Taconic Range. The general geology of this area is described here after Bain (1933), Dale (1912), Doll (1961), Fowler (1950), Hewitt (1961), Skehan (1961), Thompson (1952), and Zen (1960).

The Green Mountains are a manifestation of a major north-south trending anticlinorium overthrust to the west, Figure 14. The structure and metamorphic features observed in the Vermont Valley and Taconic Range, which jointly comprise the Middlebury synclinorium, are tightly coupled to the history of this basement structure. The crystalline basement complex was metamorphosed to lower or upper amphibolite facies in the pre-Cambrian. Deep erosion preceded the deposition to the west of the Cambro-Ordovician miogeosynclinal sediments in the Vermont Valley, predominantly carbonates, with minor sandstones and shales. The eugeosynclinal sediments in the Taconic sequence, sands and shales with minor

Fig. 14. -- General metamorphic map of southern Vermont with sample locations (After Doll, 1961).

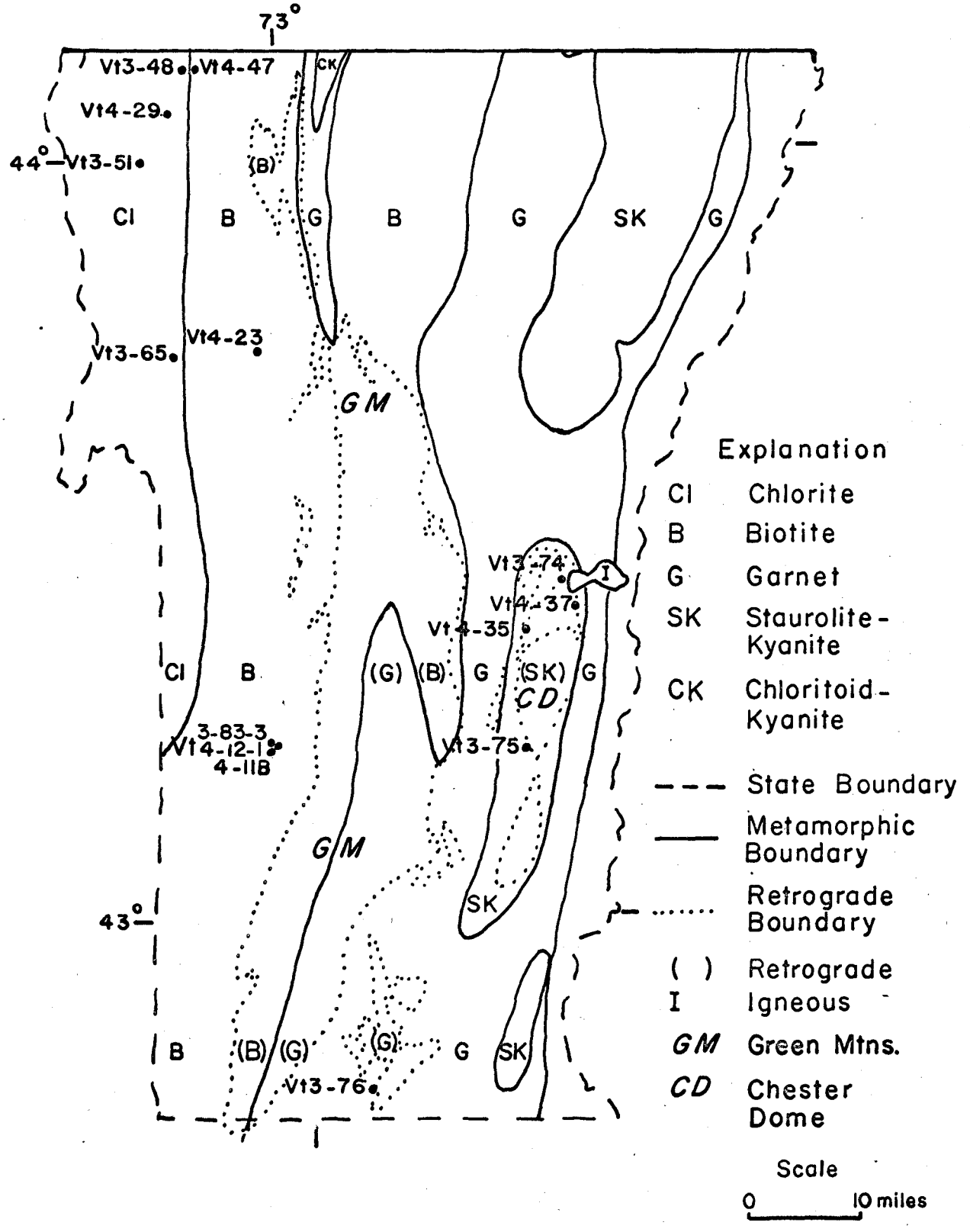
73°
44°
43°
Vt3-48
Vt4-47
CK
Vt4-29
Vt3-51
(B)
Cl
B
G
B
G
SK
G
Vt3-65
Vt4-23
GM
Vt3-74
I
Vt4-37
Vt4-35
Cl
B
(G)
(B)
G
(SK)
G
CD
3-83-3
Vt4-12-1
4-118
Vt3-75
GM
SK
B
(B)
(G)
(G)
G
SK
Vt3-76
Explanation
Cl Chlorite
B Biotite
G Garnet
SK Staurolite-Kyanite
CK Chloritoid-Kyanite
State Boundary
Metamorphic Boundary
Retrograde Boundary
( ) Retrograde
I Igneous
GM Green Mtns.
CD Chester Dome
Scale
0 10 miles

carbonates and volcanics, are allocthonous. The relationship between the Vermont Valley and Taconic sequences, the Taconic Problem, is not of direct consequence here except insofar as it restricts the main carbonate outcrops to the Vermont Valley.

The Taconic orogeny commenced towards the late Ordovician and presumably is directly related to the upward (?) and westward movement of the Green Mountain core. This was accompanied by a regional rise in temperature causing metamorphic zonation broadly coincident with the Green Mountain axis (Fig. 14). The grade increases from west to east towards this axis. The Middlebury synclinorium was metamorphosed to greenschist facies - chlorite and biotite zones - while, in contrast, the pre-Cambrian complex suffered retrogradation towards the greenschist facies. At the northeast border of this area, Lincoln Mountain, the amphibolite facies was attained (Cady et al., 1962).

The metamorphic zones deduced from the mineral assemblages in the pelitic schists are given on the map of Vermont (Doll, 1961) and in Figure 14. Igneous activity during the Taconic orogeny, and after, in this area is conspicuously absent, except for very sparse camptonite dikes.

Rocks in the Middlebury synclinorium were severely deformed. The intensity of isoclinal and recumbent folding increases with increase in metamorphic grade. In the Equinox area there is evidence for two episodes of folding - jointing and cleavage have been rotated following folding (Hewitt, 1961). The marbles generally display flowage folding rather than shear folding. The latter is characteristic in the phyllites.

Folding was accompanied by the development of slip cleavage in the argillaceous rocks. Fracture cleavage is common in the more competent dolomite beds.

The sequence of formations in the Vermont Valley is given in Table XII, after Thompson (1952) and Hewitt (1961), together with the dominant lithology and estimated thickness. The Vermont Valley sequence is characterized by the paucity of pelitic schists on the high grade eastern side of the main marble belt, except to a lesser extent towards the north end of the Green Mountains (this is not indicated in Table XII). Many calcite-dolomite samples come from the Shelburne formation. Chlorite, phlogopite, actinolite, sericite, pyrite and quartz are common minor phases in the marbles. Retrograde effects in the Middlebury synclinorium are not important. Several inliers of the pre-Cambrian basement crop out in the synclinorium.

The localities of all analysed carbonate samples from southwestern Vermont are shown in Figure 14. The isotopic data are presented in Table XIII. In all these samples the carbonates and quartz constitute 90% or more of the rock, except Vt 60 and Vt II 36 analysed by Schwarcz (1966). However, it is noted that all samples from the chlorite zone and a few from the low biotite zone, Vt 3-48, 3-51, 3-65, 4-29, 69, and 3-47, are dark grey to black meta-limestones. Irregular fractures are commonly filled with calcite or quartz veins. The other marble samples are more thoroughly recrystallized and are white to grey.

Table XII

Formations of the Vermont Valley Sequence

(after Thompson, 1952; Hewitt, 1961)

Period	Formation	Dominant Lithology	Thickness (Ft) (estimate)
M. Ordovician	Hortonville	slates or phyllites	600
	Whipple	grey to black limestones, bands of phyllite	300
L. Ordovician	Beldens, Burchards, Bascom, Shelburne	white and grey marbles, some bands of sandstone and phyllites	1400
U. Cambrian	Clarendon Springs	dolomite, sandy dolomite	100
	Danby	and quartzites	250
L-M. Cambrian	Winooski	dolomite	350
	Monkton	quartzite	300
	Dunham	dolomite	900
	Cheshire	quartzite	300-700
	Mendon	quartzites, quartz-phyllites greywacke	
	——— angular unconformity ———		
Pre-Cambrian	Mt. Holly Complex	schists, gneisses amphibolites, marbles	?

Table XIII

Isotopic Data for Samples from Southwestern Vermont

Sample No.	δO^{18}_{D} (‰)	δO^{18}_{Ct} (‰)	$10^3 \ln \alpha^{O^{18}}_{D-Ct}$	δC^{13}_{D} (‰)	δC^{13}_{Ct} (‰)	$10^3 \ln \alpha^{C^{13}}_{D-Ct}$
Vt 3-51	25.21	23.75	1.43	0.25	-0.70	0.95
Vt 3-48	21.74	20.88	0.85	-0.56	-0.56	0.00
Vt 4-29	24.16	23.13	1.01	-2.01	-2.72	0.71
Vt 3-65	24.08	22.27	1.77	2.36	1.60	0.76
Vt 3-47	22.81	21.60	1.19	-2.03	-2.68	0.65
Vt 4-23	23.00	22.30	0.68	1.32	0.62	0.70
Vt 3-83-3	23.94	22.71	1.21	-0.34	-1.14	0.80
Vt 4-12-1	22.62	21.43	1.17	+0.02	-1.11	1.13
Vt 4-11B-6	23.04	22.49	0.54	1.26	0.67	0.59
Vt 4-11B-8	23.04	22.50	0.53	0.64	0.18	0.46
Vt 4-11B-9	22.83	22.32	0.48	0.79	0.05	0.74
Vt 4-11B-12	23.03	22.50	0.52	0.66	0.04	0.62
Vt 4-11B-15	22.63	22.09	0.53	1.16	0.64	0.52

Samples were only collected from the chlorite and biotite zone in this area of Vermont. Vt II 36 a calcareous schist from the garnet zone is included here (Schwarcz, 1966).

Various relations between these data are presented in Figures 4, 15, 16, 17, 18 and 19. Analysis is deferred to the immediate end of this descriptive section, see § 7.5 et seq.

7.3 Southeastern Vermont

To the east of the Great Mountain basement complex early Paleozoic meta-shales, sandstones and volcanics predominate, extending into New Hampshire. A series of gneiss-cored domes occurring along an axis approximately parallel with the Green Mountain axis, but 15 miles or so to the east, have been plastically remobilized and uplifted into the overlying metamorphic rocks, Figure 14. The Chester dome, the largest of the outcropping domes in Vermont, is of interest here (Doll, 1961; Skehan, 1961; Thompson, 1952). This dome is composed mainly of pre-Cambrian gneisses, which are less heterogeneous than the Green Mountain gneisses.

The mantling Paleozoic schists are intensely deformed and exhibit major thinning around the domes of probable tectonic origin (Thompson, 1952). The folding and flowage structures are consistent with an upward movement of the domes. Contiguous metamorphic zonation is essentially concentric about the domes with the node, staurolite-kyanite zone, centered on the dome core. The pre-Cambrian complex has suffered retrogradation, from possible sillimanite zone or higher to staurolite-kyanite.

Much of the overlying Cavendish formation also exhibits retrograde features; garnet porphyroblasts in the Gassetts schist have chlorite haloes. All samples from the Chester dome area are from the Cavendish formation. The relatively thin marble unit is sandwiched between the pre-Cambrian gneisses (metavolcanics ?) and Cavendish schists. Dolomitic marbles predominate but extensive decarbonation in some places has produced diopside-actinolite assemblages. However, dolomite-quartz is a common assemblage in the Cavendish marbles and implies a high CO_2 activity.

Vt 3-76 is from the Sherman Marble, a member of the Cavendish formation associated with the Ray Pond or Sadawaga dome to the S.S.W. of the Chester dome. Schists lie both below and above this marble. Garnet zone or possibly staurolite-kyanite zone metamorphism was attained (Skehan, 1961). Decarbonation in some siliceous dolomitic marbles and retrogradation are characteristic here also.

Minor ultramafic intrusives are found in and around the Chester dome but antedate the metamorphism. The Mount Ascutney alkalic stock, hornblende-biotite diorite and syenite, on the N.E. edge of the dome outcrops ½ to 2 miles from sample localities Vt 3-74 and 4-37-1,2,3,4,5. It is post-metamorphic.

The analyses of these samples are presented in Table XIV and Figures 15 to 19. Data for sample localities in the Chester dome area given by Schwarcz (1966) are included in the figures.

Table XIV

Isotopic Data for Samples from Southeastern Vermont

Sample No.	δO^{18}_{D} (‰)	δO^{18}_{Ct} (‰)	$10^3 \ln \alpha^{O^{18}}_{D-Ct}$	δC^{13}_{D} (‰)	δC^{13}_{Ct} (‰)	$10^3 \ln \alpha^{O^{13}}_{D-Ct}$
Vt 4-35-1a	14.09	15.13	-1.03	-1.77	-2.37	0.60
Vt 4-35-1b	12.83	15.01	-2.16	-2.53	-2.84	0.31
Vt 4-35-2a	13.82	14.84	-1.00	-1.61	-2.25	0.64
Vt 4-35-2b	12.85	14.92	-2.04	-2.28	-2.65	0.37
Vt 4-35-5	19.22	18.13	1.07	1.84	1.09	0.75
Vt 4-37-1	19.14	17.92	1.20	1.57	-1.13	2.70
Vt 4-37-2	15.80	17.13	-1.31	1.53	1.23	0.30
Vt 4-37-3	15.08	14.80	0.28	-0.07	-0.44	0.37
Vt 4-37-4	17.65	16.32	0.33	1.88	1.42	0.46
Vt 4-37-5	16.34	17.66	-1.30	1.68	1.25	0.43
Vt 3-74	19.40	17.69	1.68	1.27	0.31	0.96
Vt 3-75	18.47	16.48	1.96	0.08	-1.07	1.15
Vt 3-76	18.89	17.82	1.06	1.72	1.22	0.50

Fig. 15. -- Variation of 1000 ln $\alpha^{C^{13}}_{D-Ct}$ with metamorphic grade.

- ● Marbles
- o Silicate marbles (Mg-silicates > 5%)
- \+ Marbles. (After Schwarcz, 1966)
- ⊕ Calcareous schist (After Schwarcz, 1966)

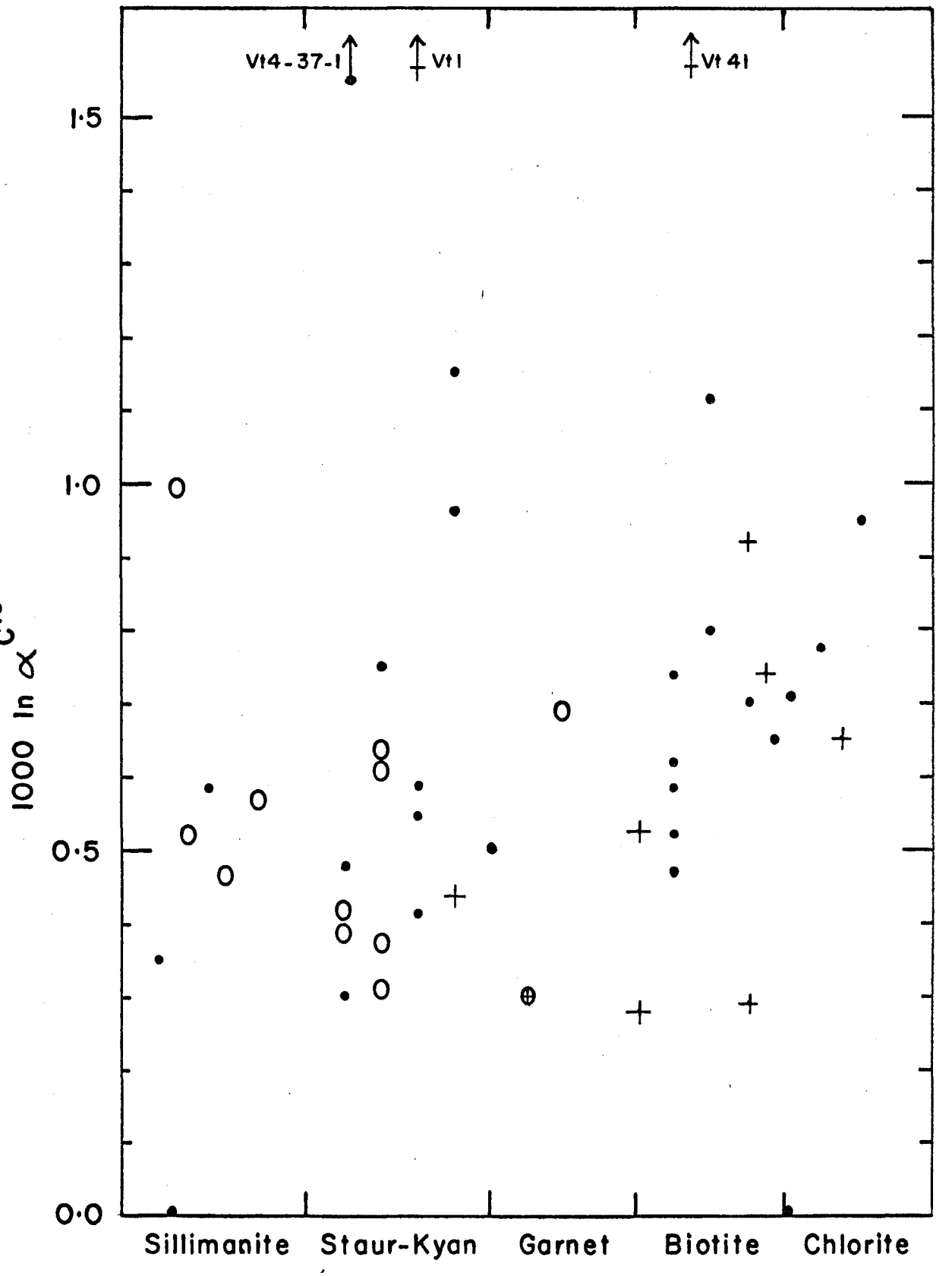
Vt4-37-1
Vt1
Vt41
1·5
1·0
0·5
0·0
1000 ln $\alpha_{C^{13}}$
Sillimanite
Staur-Kyan
Garnet
Biotite
Chlorite

Fig. 16. -- Variation of 1000 ln $\alpha^{O^{18}}_{D-Ct}$ with metamorphic grade.

- • Marbles
- O Silicate marbles (Mg-silicates > 5%)
- \+ Marbles. (After Schwarcz, 1966)
- ⊕ Calcareous schist (After Schwarcz, 1966).

Note change in scale on 1000 ln $\alpha^{O^{18}}$ axis at 0.0.

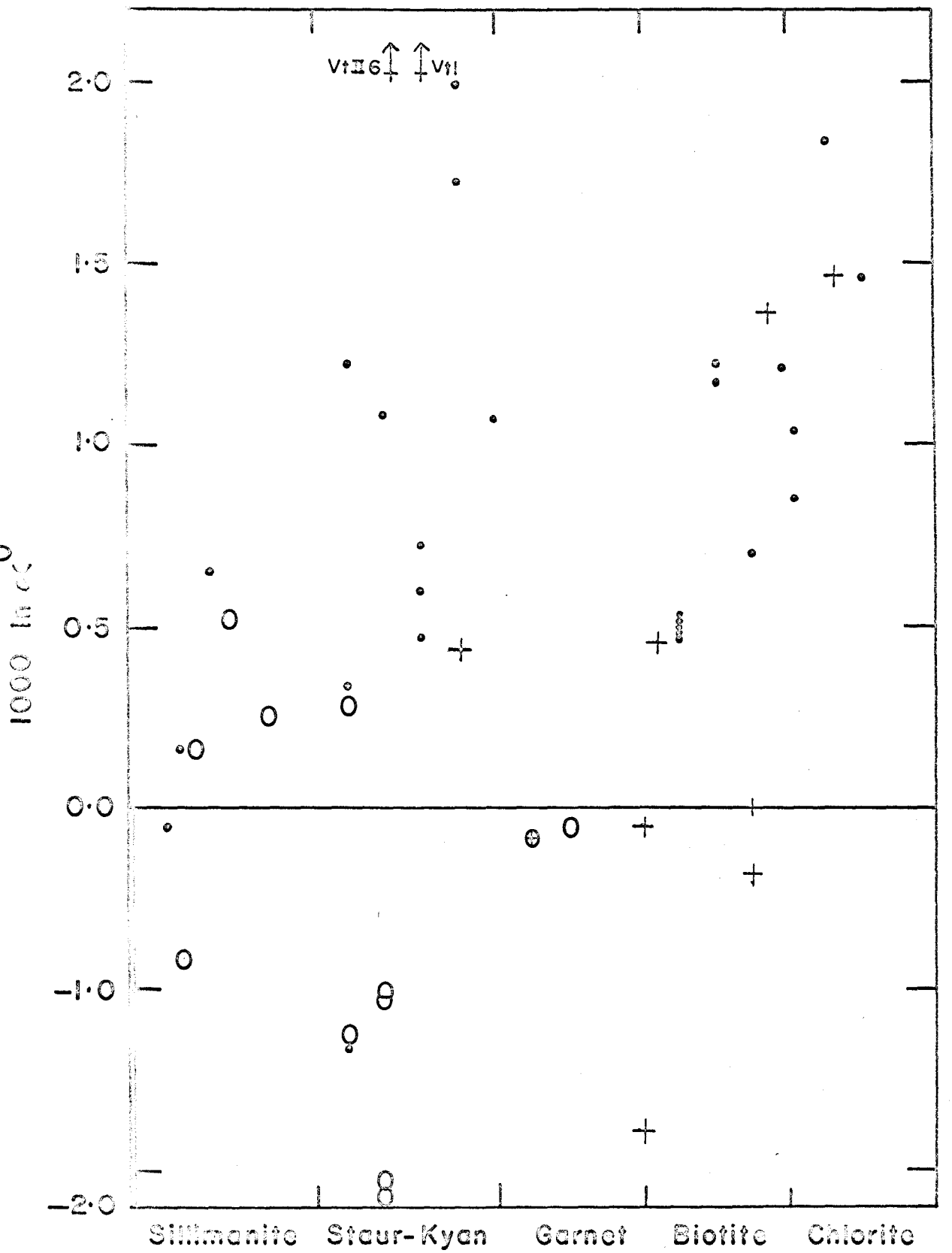
Vt=6
Vt!
2·0
1·5
1·0
0·5
0·0
-1·0
-2·0
1000 ln C^{13}
Sillimanite
Staur-Kyan
Garnet
Biotite
Chlorite

Fig. 17. -- Variation of 1000 ln $\alpha_{D\text{-}Ct}^{C^{13}}$ with 1000 ln $\alpha_{D\text{-}Ct}^{O^{18}}$

- ● Marbles
- ○ Silicate marbles (Mg-silicates>5%)
- \+ Marbles. (After Schwarcz, 1966)
- ⊕ Calcareous schist (After Schwarcz, 1966)

Line A is the reduced major axis line using the selected data (see § 9.2).

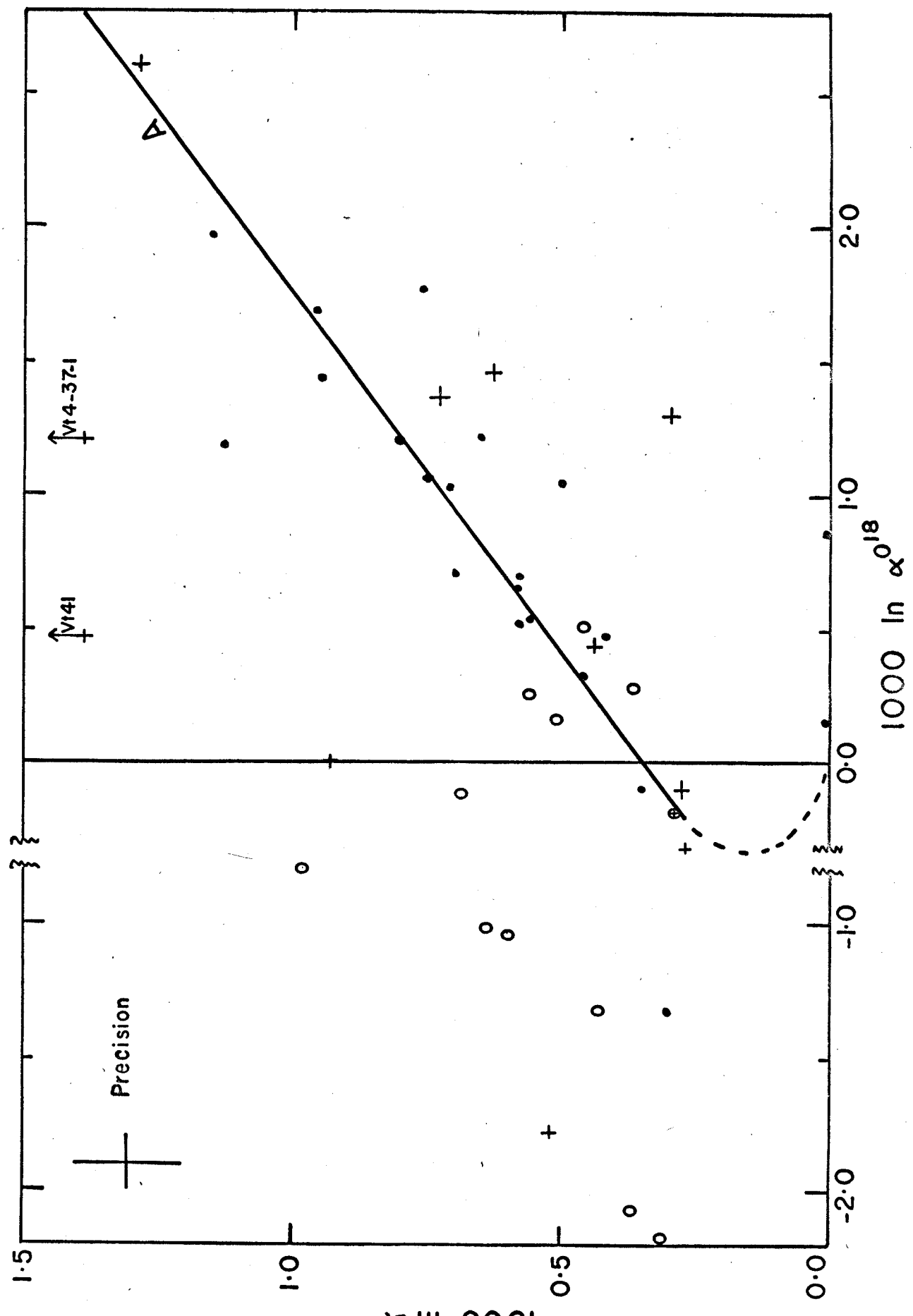
A
Vt4-37-1
Vt141
Precision
1000 ln $\alpha^{C^{13}}$
1000 ln $\alpha^{O^{18}}$
1·5
1·0
0·5
0·0
2·0
1·0
0·0
-1·0
-2·0

Fig. 18. -- Variation of 1000 ln $\alpha^{C^{13}}_{D-Ct}$ with $10^6\ T_s^{-2}$

- ● Marbles
- O Silicate marbles (Mg-silicates>5%)
- \+ Marbles. (After Schwarcz, 1966)
- ⊕ Calcareous schist (After Schwarcz, 1966)

$10^6 T_s^{-2}$ is derived from the solvus thermometer. Line B is the reduced major axis line using the selected data (see § 9.2, where B ≡ S_1).

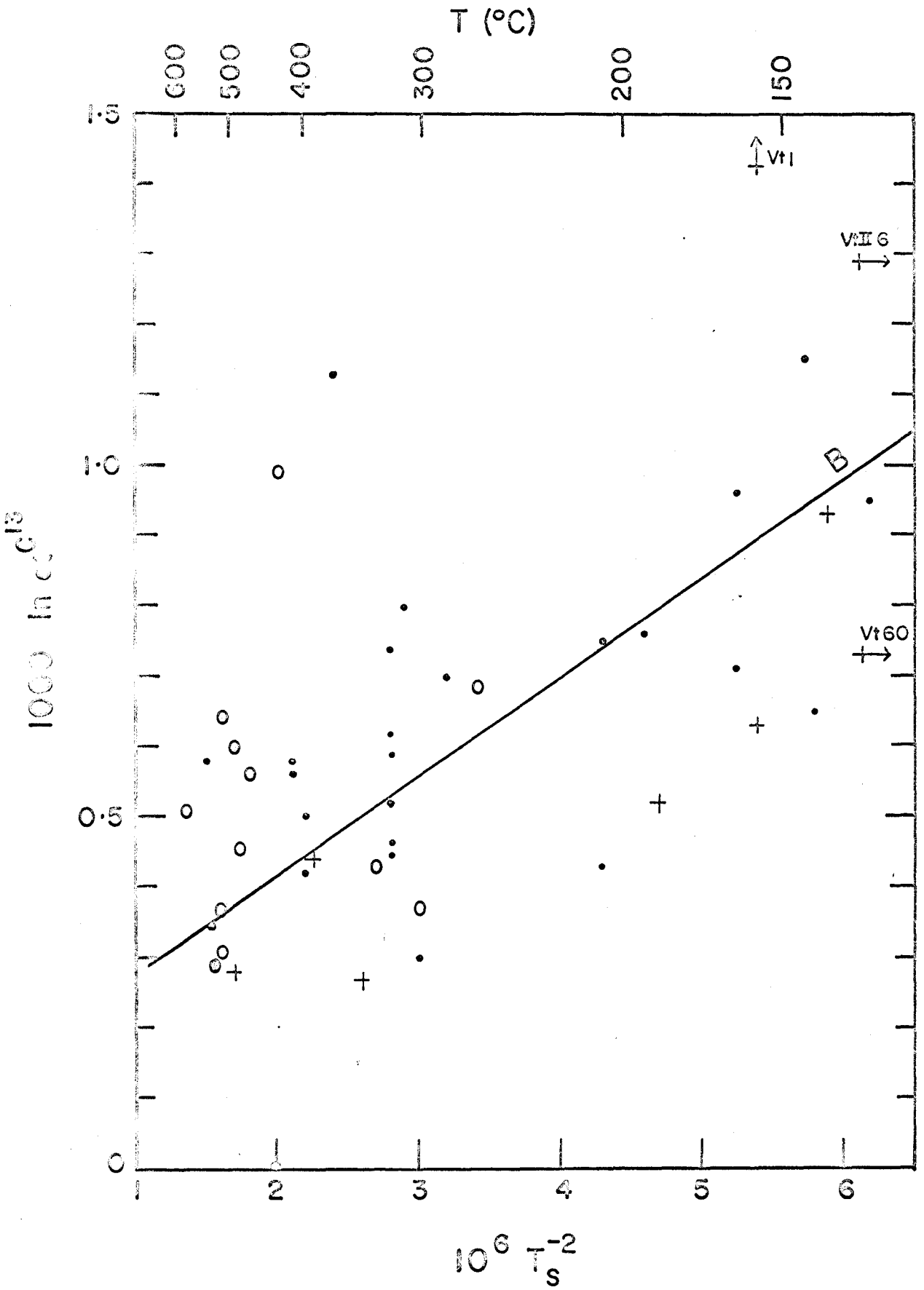
T (°C)
600
500
400
300
200
150
1·5
1·0
0·5
0
Vt1
VtII 6
Vt60
B
1
2
3
4
5
6
$10^6\ T_s^{-2}$

Fig. 19. -- Variation of 1000 ln $\alpha^{O^{18}}_{D-Ct}$ with $10^6 T_s^{-2}$

- ● Marbles
- O Silicate marbles (Mg-silicates>5%)
- \+ Marbles. (After Schwarcz, 1966)
- ⊕ Calcareous schist (After Schwarcz, 1966)

$10^6 T_s^{-2}$ is derived from the solvus thermometer. Line C is the reduced major axis line using the selected data (see § 9. 2, where C ≡ S_1).

Note change in scale on 1000 ln $\alpha^{O^{18}}$ axis at 0.0.

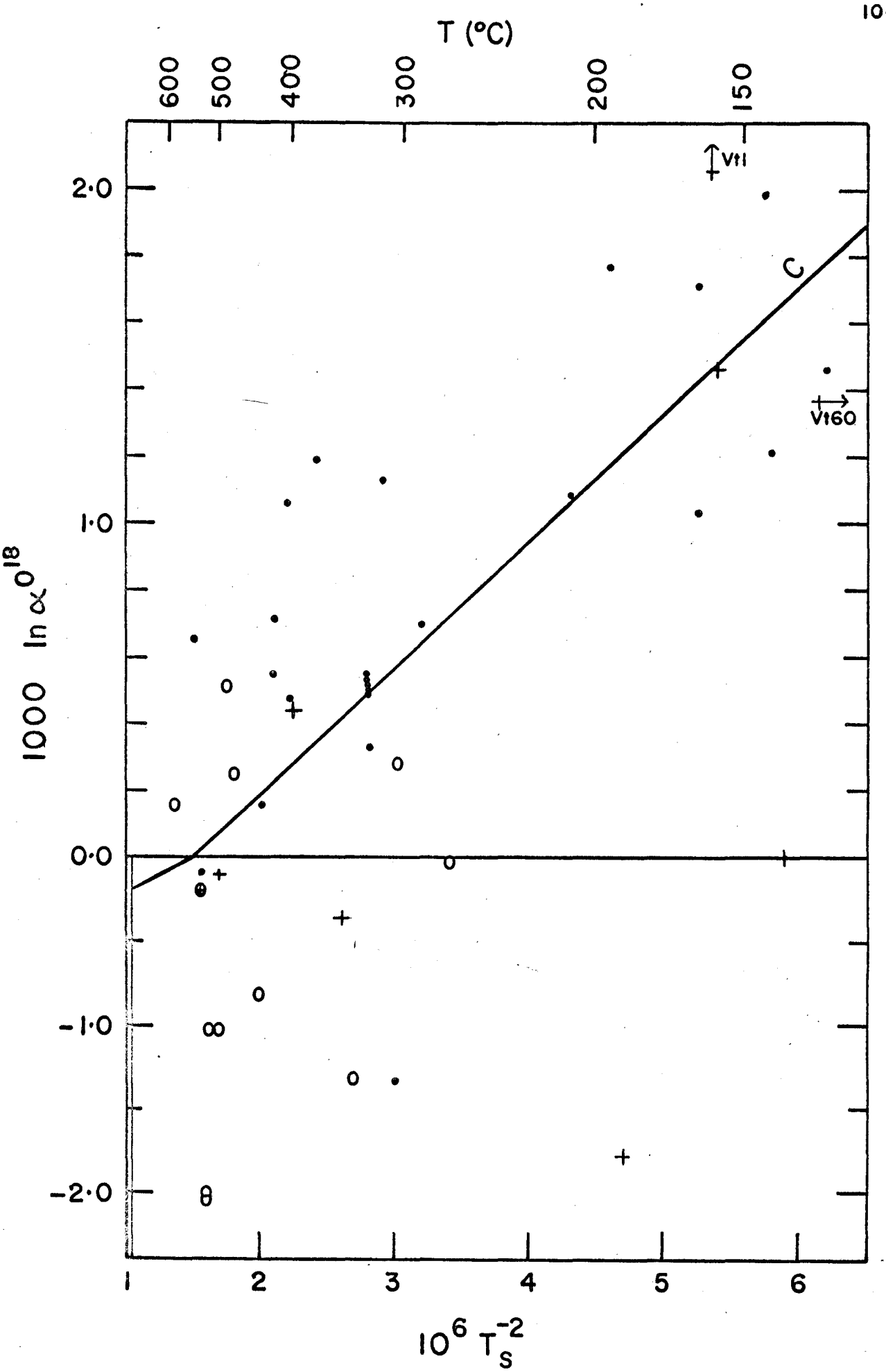
T (°C)
600
500
400
300
200
150
V11
V160
C
2·0
1·0
0·0
-1·0
-2·0
1000 ln α O18
1
2
3
4
5
6
10^6 T_s^-2

7.4 The Grenville Province of South East Ontario

The Grenville Province of S.E. Ontario is composed of a wide variety of igneous rocks, metasediments, amphibolites and metavolcanics. In this part of the Grenville marbles are widespread. Although the metamorphic history is very involved, a broad zonation occurs, as shown on Figure 20, after Lumbers (1964), centered on a N.E.-S.W. trending low of greenschist facies rocks. The metamorphic grade increases to the west, north and east attaining upper amphibolite to granulite facies.

Tectonic patterns are quite complex; faulting and folding evolved over a 300 m.y. period (Lumbers, 1965). Throughout this time various intrusives series were emplaced and many structures are related to the emplacement of the numerous batholithic masses. The sequence of intrusion is: Tudor Volcanics (1310 ± 15 m.y.) - Trondhjemite, Biotite Diorite (1250 ± 25 m.y.) - Mafic Intrusives - Quartz Monzonites (1125 ± 25 m.y.) - Pegmatites and Veins (1050 ± 20 m.y.) (Silver and Lumbers, 1965).

The general regional metamorphic pattern probably was established before the emplacement of the biotite diorite series, one of the earliest intrusive series. In the high grade areas migmatite is common. Contact aureoles are more conspicuous about the intrusives in the low and intermediate grades (Lumbers, 1964).

The marbles in the intermediate and high grade areas yielded plastically. Tectonic thinning and flowage are common features, for example as shown by Evans (1964) in Denbigh Township. The marbles are characteristically medium to coarse grained (2-5 mm. medium grained, $>$ 5 mm. coarse grained), and white to light grey outside the greenschist facies area. Very variable amounts of silicate minerals are

Fig. 20. -- General metamorphic map of part of southeastern Ontario with sample locations. (After Lumbers, 1964; Wynne-Edwards, 1959).

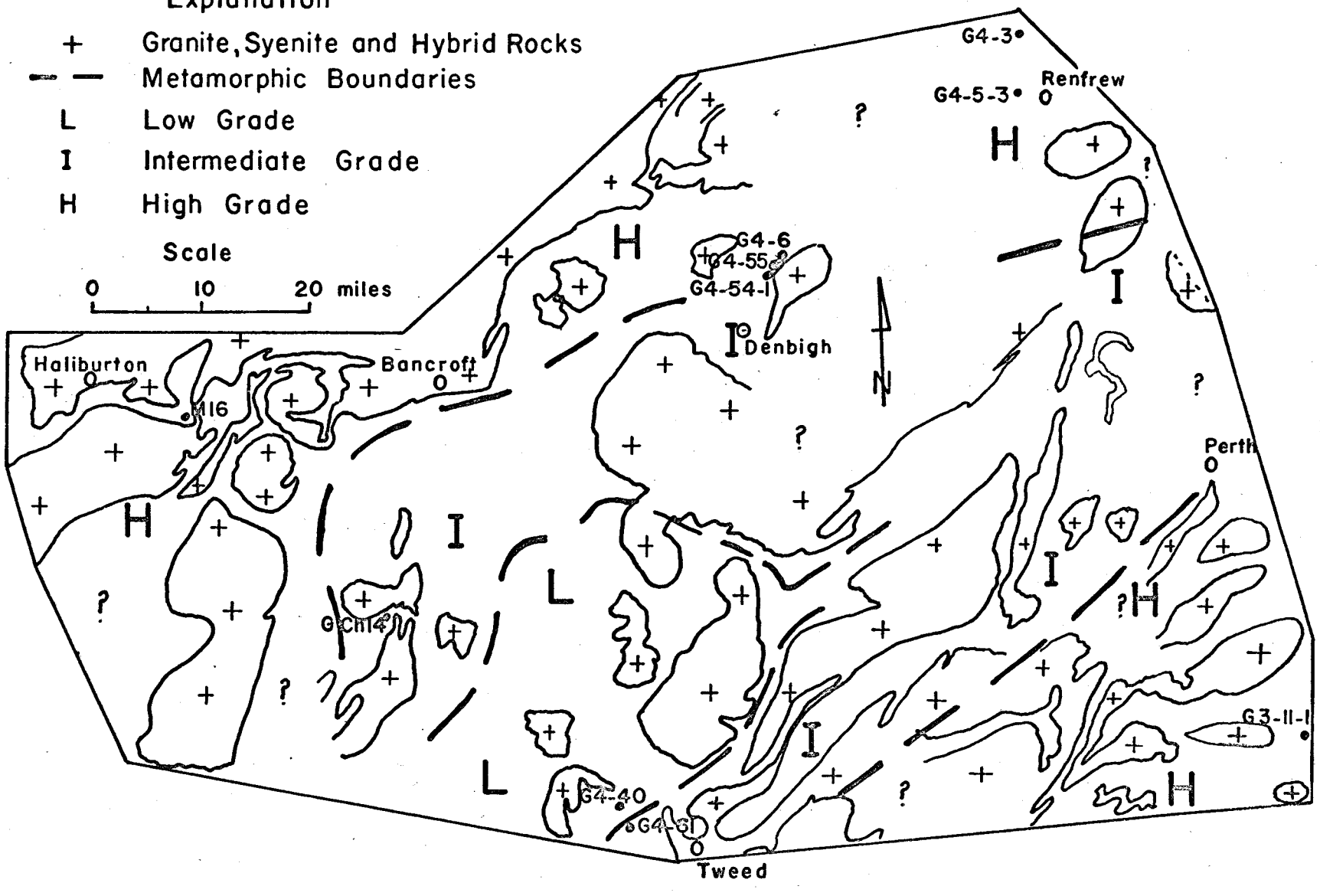
Explanation
+ Granite, Syenite and Hybrid Rocks
Metamorphic Boundaries
L Low Grade
I Intermediate Grade
H High Grade
Scale
0 10 20 miles
G4-3
Renfrew
G4-5-3
G4-6
G4-55
G4-54-1
Denbigh
N
Haliburton
Bancroft
M16
Perth
G3-11-1
G4-40
G4-61
Tweed

present and calc-silicate rocks occur. Common non-carbonate minerals are: phlogopite, biotite, amphibole, forsterite, felspar, chlorite, pyrite and graphite. However, large tracts of the marbles contain less than 5% of non-carbonates. The distribution of coexisting calcite and dolomite appears to be irregular. The graphite distribution is variable and in the higher grade marbles graphite may be segregated into little clots of well crystallized plates a few mm. in size. X-ray diffraction studies of $d_{(002)}$ (French, 1964) indicate that the graphite is ordered in samples G 4-54 and G 5-1 from intermediate and high grade areas respectively.

It is emphasized here that, since the regional metamorphic zonation was established during the early history of the Grenville province, the metamorphic and quench histories of the marbles were both long and complex. Comparison between Grenville and Vermont marbles from a similar temperature environment indicate that the grain size is larger and the mineralogy more variable in the Grenville samples.

The location of the samples is given in Figure 20, with the exception of G 5-1 and -1b from the Seguin River, near Parry Sound, and GLSK described by Shaw et al. (1965). A description of each sample is given in Appendix II with the metamorphic grade inferred from the mineral assemblages described in nearby pelitic rocks. Geological information for the Seguin River area, G 5-1 and -1b, and the Renfrew area, G 4-3, G 4-5-3, is limited and the metamorphic grade is known only very broadly. The isotopic data for all Grenville samples are reported in Table XV.

Table XV

Isotopic Data for Samples from the Grenville Province

Sample No.	δO^{18}_{D} (‰)	δO^{18}_{Ct} (‰)	$10^3 \ln \alpha^{O^{18}}_{DCt}$	δC^{13}_{D} (‰)	δC^{13}_{Ct} (‰)	$10^3 \ln \alpha^{C^{13}}_{DCt}$
G 4-40		23.61			0.87	
G Ch 14	17.90	18.02	-0.12	4.55	3.86	0.69
G 4-61	19.66	20.89	-1.21	12.98	1.28	11.70
G 4-54-1	23.46	22.75	0.70	-1.51	-2.09	0.58
G 4-55	23.25	22.77	0.48	3.55	3.13	0.42
G 4-6	26.35	25.90	0.54	2.56	2.00	0.56
M 16	21.38	21.13	0.25	2.57	2.01	0.56
G 4-5-3	22.93	22.41	0.51	3.66	3.20	0.46
G 4-3	26.29	25.64	0.64	3.83	3.25	0.58
G 5-1	19.98	20.80	-0.80	-0.17	-1.15	0.98
G 5-1b	20.79	20.63	0.16	-0.75	-0.75	0.00
GLSK	23.29	23.13	0.16	0.84	0.33	0.51
G 3-11-1	21.95	22.05	-0.10	5.11	4.76	0.35

7.5 General Analysis of Dolomite-Calcite Pairs

7.5.1 Introduction

From the samples collected, those with textural evidence for more than one generation of calcite or dolomite were avoided. Secondary veins or veinlike calcite are common in the dark meta-limestones from the chlorite zone where extensive recrystallization has not occurred; Vt 3-65 is such a sample. Samples from the biotite and higher zones are more thoroughly recrystallized. The forms of the carbonates are variable: euhedral rhombs, subhedral or anhedral with curved grain boundaries (Appendix II). Dolomite is idioblastic but this is less pronounced in the high grade rocks. Calcites from the high grade assemblages are typically cloudy, in contrast to the clear dolomites (§ 5.3), and may contain blebs of dolomite.

A general presentation of the isotopic and solvus data for the selected samples given in Tables II, XIII, XIV, XV follows. Possible relations between various functions of these parameters are sought in order to reveal any equilibrium relationships. A detailed analysis of certain sets of samples selected to gain confidence in and comprehension of the processes involved comes immediately afterwards.

In the introduction, § 2.2.1, certain properties of isotopic fractionations were reviewed. It was noted that for coexisting phases in equilibrium a relation of the following form should be followed more or less closely:

$$1000 \ln K_{D-Ct} = A T^{-2} + B$$

where A and B are constants. At high temperature $10^3 \ln K \longrightarrow 0$.

For this reason the data given in Tables II, XIII, XIV, XV are presented in terms of the parameters:

1) Figure 15 $1000 \ln \alpha^{C^{13}}_{D\text{-}Ct}$ vs metamorphic grade

2) Figure 16 $1000 \ln \alpha^{O^{18}}_{D\text{-}Ct}$ vs metamorphic grade

3) Figure 17 $1000 \ln \alpha^{C^{13}}_{D\text{-}Ct}$ vs $1000 \ln \alpha^{O^{18}}_{D\text{-}Ct}$

4) Figure 18 $1000 \ln \alpha^{C^{13}}_{D\text{-}Ct}$ vs $10^6 T_s^{-2}$

5) Figure 19 $1000 \ln \alpha^{O^{18}}_{D\text{-}Ct}$ vs $10^6 T_s^{-2}$

From the noted relations between the solvus temperature, T_s, and the metamorphic grade, Figure 4, more complex relations are expected from the high grade samples. If equilibrium is generally preserved a correlation between one or more of these variables may be expected. However, there is no a priori reason why the C-isotopes, O-isotopes, and Mg content should freeze in at the same temperature. Differential quenching will be reflected in an absence of a correlation between one or more of the above relations.

7.5.2 $1000 \ln \alpha^{C^{13}}_{D\text{-}Ct}$ vs Metamorphic Grade

Figure 15 reveals no well-defined relation between the C-isotope fractionation and the metamorphic grade. Nevertheless, the minimum value for the fractionation in a given zone decreases on going from the chlorite to the staurolite-kyanite zone. The considerable spread in the data points could be a consequence of either: (1) equilibrium fractionations being preserved at a temperature less than the metamorphic high; or

(2) some disequilibrium process.

7.5.3 $1000 \ln \alpha^{O^{18}}_{D\text{-}Ct}$ vs Metamorphic Grade

No well defined relation is seen in Figure 16. Both positive and negative O-isotope fractionations are noted. In particular most of the large negative fractionations are given by high-grade calcareous schists. Arguments presented below, § 8.3, indicate that the large negative O-isotope fractionations are disequilibrium values. Excluding these values the minimum value for the fractionation in a given zone again decreases from the chlorite to the sillimanite zone.

7.5.4 $1000 \ln \alpha^{C^{13}}_{D\text{-}Ct}$ vs $1000 \ln \alpha^{O^{18}}_{D\text{-}Ct}$

A marked positive correlation between $1000 \ln \alpha^{C^{13}}_{D\text{-}Ct}$ and $1000 \ln \alpha^{O^{18}}_{D\text{-}Ct}$ is shown in Figure 17 when the large negative O-isotope fractions are excluded. Line A is the regression line using those data points falling in the positive fractionation quadrant. This excellent correlation indicates that, for the majority of marble samples analysed the C- and O-isotope fractionations are closely coupled. The smallest C- and O-isotope fractionations are given by the highest grade rocks. The equation for Line A is:

$$10^3 \ln \alpha^{C^{13}}_{D\text{-}Ct} = 0.373(10^3 \ln \alpha^{O^{18}}_{D\text{-}Ct}) + 0.35 \qquad (21)$$

7.5.5 $\left.\begin{array}{l}(1000 \ln \alpha^{C^{13}}_{D-Ct} \quad vs \quad 10^6 T_s^{-2} \\ (\\ (\\ (\\ (1000 \ln \alpha^{O^{18}}_{D-Ct} \quad vs \quad 10^6 T_s^{-2}\end{array}\right.$

The C-isotope fractionations are plotted against the temperature function, $10^6 T_s^{-2}$, derived from the solvus thermometer and shown in Figure 18, and that for O-isotopes in Figure 19. A rather diffuse positive correlation is observed for carbon and for oxygen, if the large negative fractionations are excluded.

7.5.6 Conclusions

These results now can be conveniently summarized before entering upon a detailed analysis of the data:

1) A strong positive correlation exists between $1000 \ln \alpha^{C^{13}}_{D-Ct}$ and $1000 \ln \alpha^{O^{18}}_{D-Ct}$.
2) Most high grade calcareous schists give large negative oxygen isotope fractionations.
3) Weak correlations appear to be present between the isotopic fractionations and the solvus-derived temperature.
4) Weaker correlations may be present between the minimum isotopic fractionations and the metamorphic grade.
5) A greater range in fractionations is observed for high grade samples.
6) The magnitude of the isotopic fractionations appear to be of the following order:

Grade	1000 ln $\alpha^{C^{13}}_{D-Ct}$	1000 ln $\alpha^{O^{18}}_{D-Ct}$
Greenschist Facies	0.5 - 1.0‰	0.5 - 2.0‰
Upper Amphibolite	0.3 - 0.5‰	0.0 - 0.5‰

VIII. ANALYSIS

8.1 Introduction

Interpretation of the fractionation data necessitates disentangling equilibrium fractionations from disequilibrium ones. In the discussion of equilibrium, § 4.6, no infallible practical criterion was evolved. Nevertheless, consistency between observations was recommended as a good guide, with appeal to laboratory equilibration studies where applicable. For example, the analysis of a set of several coexisting carbonate pairs from a volume of rock sufficiently small that uniformity of physical conditions can be assumed with confidence, should provide an adequate check on such a consistency study (§ 4.6).

Comparisons of the experimental fractionation expressions of Northrop and Clayton (1966) and O'Neil and Epstein (1966) for O-isotopes, § 2.4.6, and for C-isotopes, § 6.3.3, given above with the natural fractionation data shown in Figures 15 to 19 indicate that the natural fractionations may be smaller than the experimental ones by about 1 to 2‰ for oxygen and by 0‰ (at 600°C) to 6‰ (at 300°C) for carbon. Because of the noted inconsistencies between the O-isotope fractionation expressions (1), (5) and (6) discussed above (§ 2.4.6; § 6.4) an alternative calibration will now be sought.

Two groups of isotopic data are now discussed in some detail to (a) establish whether some natural fractionations are consistent with

equilibrium, (b) to determine the nature of possible disequilibrium processes. The first group of samples have C- and O-isotope fractionations that fall on the correlation trend shown in Figure 17 while the second group are calcareous schists with large negative O-isotope fractionations which fall away from line A, Figure 17.

8.2 Consistency Study

8.2.1 Kent Quarry Core, South Dorset, South West Vermont

The broad geological features of S.W. Vermont have been described above (§ 7.2, Fig. 14). The geology of the Dorset area, Equinox Quadrangle, shown in Figure 21, is taken here after Hewitt (1961). The Dorset anticline is composed of a multitude of small isoclinal and recumbent folds (Dale, 1912, Fig. 14). In the Valley Quarry and Plateau Quarry the inferred relict bedding is nearly flat lying because the axial planes are essentially horizontal. Locally the marble is intensely plicated but flow folding is characteristic. There is a thrust fault between the allocthonous Mount Anthony phyllites and the Bascom-Beldens formation (Thompson, 1959). Thrusting was pre-metamorphic.

The Kent, Valley, Plateau and Bennington quarries are all within the Shelburne Marble of the Lower Ordovician (Table XII). Table XII emphasizes the restricted occurrence of hydrous silicate rich rocks immediately above and below the Shelburne. These white to light grey marbles in the biotite zone may contain up to a few percent of non-carbonates: phlogopite, chlorite, actinolite, sericite, quartz, pyrite and graphite. The degree of decarbonation is minor. Locally coarse white calcite veins (width $< 1"$) were observed in the calcite marbles.

Fig. 21. -- Geological sketch map of the South Dorset area, Equinox quadrangle, Vermont. (After Hewitt, 1961, Doll, 1961).

Kent Quarry:	Vt 4 - 11B
Valley Quarry:	Vt 3 - 83 - 3, Vt 4 - 10
Bennington Quarry:	Vt 4 - 12 - 1

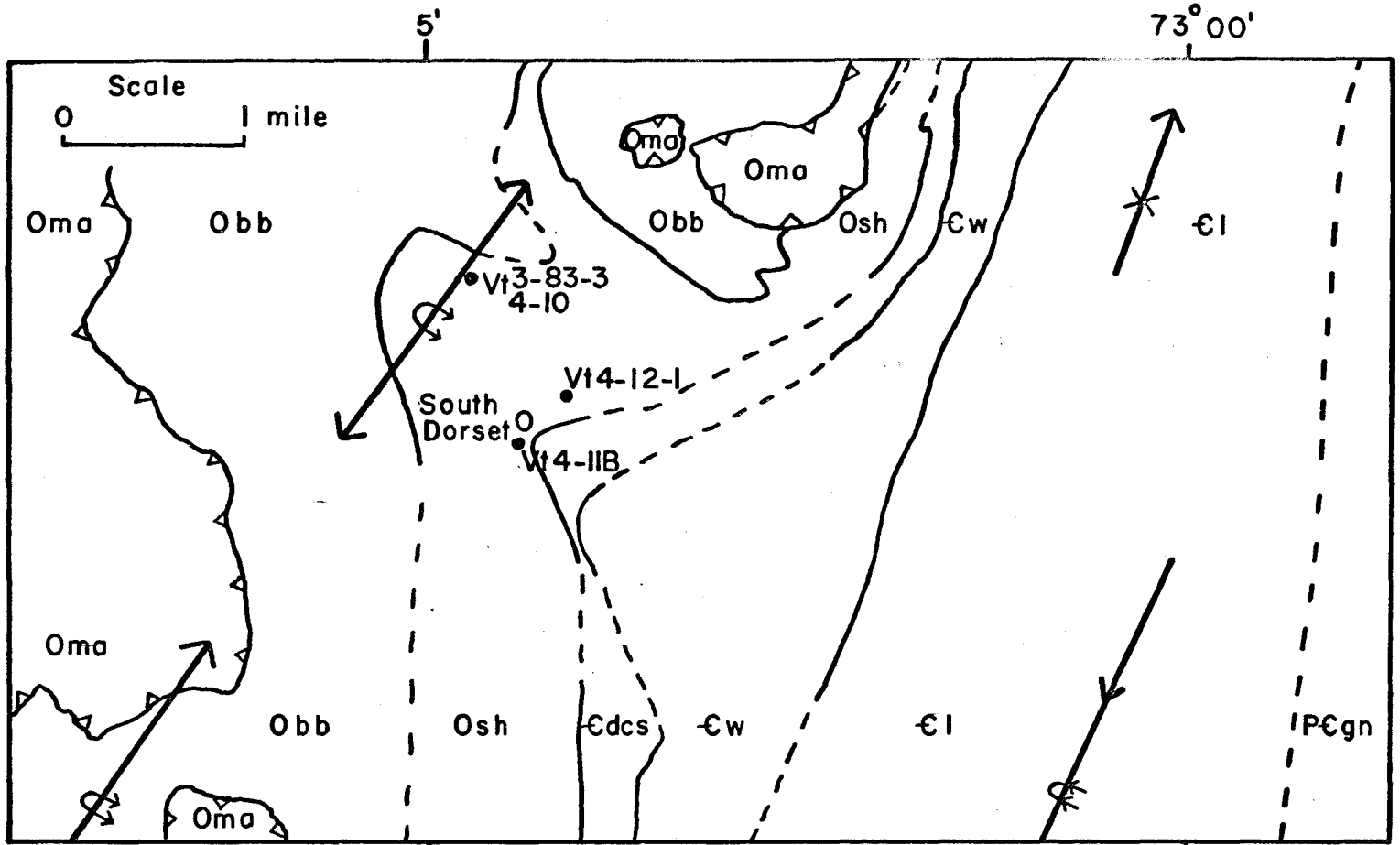

Legend:

Formations

Oma	Mount Anthony	€w	Winooski
Obb	Bascom-Beldens	€l	Lower Cambrian
Osh	Shelburne Marble	P€gn	Mount Holly Complex
€dcs	Danby-Clarendon Springs		

Symbols:

- Fold Axis
- Syncline
- Overturned Syncline
- Overturned Anticline
- Thrust Fault

Vt 4-11B-11 is such a vein calcite from the Kent Quarry. Quartz veins occur in the dolomite beds. The calcite marbles are more thoroughly recrystallized than the dolomite beds.

From Kent Quarry, 17 samples* were taken from an 130 ft. core steeply inclined to the inferred relict bedding. Five of these samples contain more than 1-2% of both calcite and dolomite. Mineral separates were made from about 1-1.5 cm^3. of sample. The $MgCO_3$ content of the calcites, C^{13} and O^{18} analyses of the carbonates are presented in Table XVI and shown in Figures 22 and 23. A description of the samples is given in Appendix II.

8.2.2 $MgCO_3$ Content of Calcites

The five calcites coexisting with dolomite give a single value for their $MgCO_3$ content of 2.85 mol %, σ = 0.09 mol %. The $MgCO_3$ content of the other 12 samples with no detectable dolomite (less than 1-2% dolomite) have contents less than or equal to this same maximum value of 2.85 mol %. Equilibrium partitioning of Mg between coexisting calcite and dolomite apparently was attained and preserved at a single temperature for these five samples. A temperature of 325° ± 25°C is derived from Figure 2 neglecting any pressure correction.

The dotted lines between sample locations, Figure 22, are no more than guides to a minimum value for the maximum Mg gradients present. They signal the small size of the equilibrium systems for Mg in these marbles, which are in thermal (and probably mechanical) equilibrium.

---

* sampled by kind permission of the Green Mountain Marble Company

Table XVI

Kent Quarry Core: Isotopic Data and $MgCO_3$ Content of Calcites

Sample	Depth (feet)	δO^{18}_D (‰)	δO^{18}_{Ct} (‰)	$10^3 \ln \alpha^{O^{18}}_{DCt}$	δC^{13}_D (‰)	δC^{13}_{Ct} (‰)	$10^3 \ln \alpha^{C^{13}}_{DCt}$	$MgCO_3$ (mol %)
Vt 4-11B								
1	2		22.75			0.07		2.25
2	22		22.23			-0.06		2.90
3	36		22.36			0.83		1.40
4	40		22.16			0.79		1.40
5	47		22.23			0.77		1.70
6	59	23.04	22.49	0.54	1.26	0.67	0.59	2.80
7	65		22.50			-0.52		3.00
8	70.5	23.04	22.50	0.53	0.64	0.18	0.46	2.75
9	74	22.83	22.32	0.48	0.79	0.05	0.74	2.95
17	77		22.32			0.12		2.65
10	79		22.59			0.68		2.95
11	89		22.51			0.09		1.25
12	92	23.03	22.50	0.52	0.66	0.04	0.62	2.80
13	101		22.00			-0.15		1.70
14	111.5		21.97			0.10		1.70
15	118.5	22.63	22.09	0.53	1.16	0.64	0.52	2.90
16	128.5		21.83			0.18		1.20

Fig. 22. -- The variation of the $MgCO_3$ content of calcite with position in the Kent quarry core.

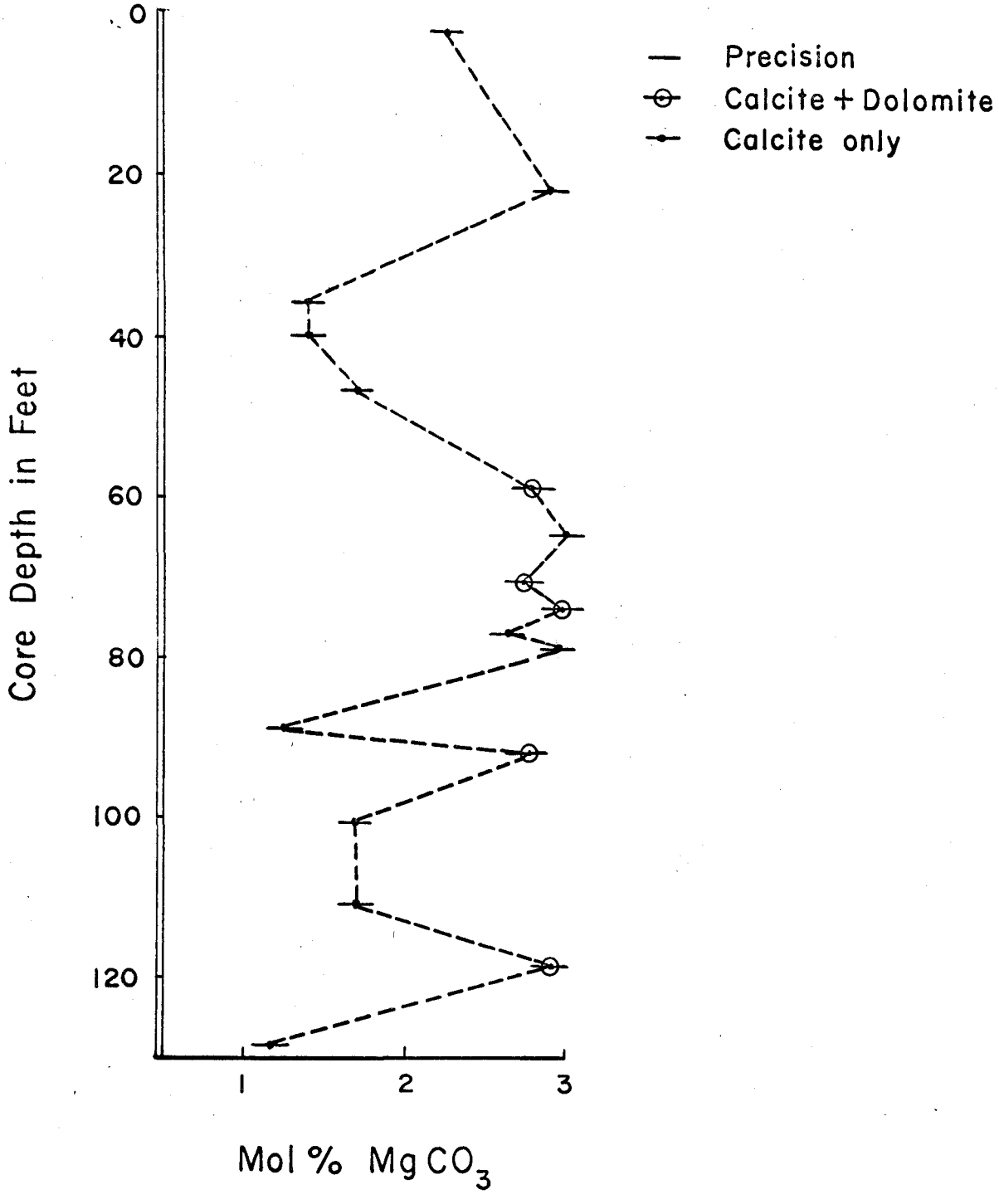
0
20
40
60
80
100
120
Core Depth in Feet
1
2
3
Mol % $MgCO_3$
Precision
Calcite + Dolomite
Calcite only

8.2.3 δO^{18} and δC^{13} Analyses

In Figure 23a the δO^{18}_{Ct} analyses are given with reference to their location in the core. Significant but small variations are noted. The fractionations between dolomite and calcite, also presented in Figure 23a, are seen to give a single value, $\Delta O^{18}_{D-Ct} = 0.53‰$, $\sigma = 0.02‰$, a necessary, but not sufficient indication that O-isotope equilibrium was preserved at a single temperature, as supported by the $MgCO_3$ solvus data.

The C^{13} data, Figure 23b, are a little more irregular. First, more sizeable δC^{13}_{Ct} gradients than those for δO^{18}_{Ct} are observed, presumably reflecting the more restricted size of the C-isotope equilibrium system. The dolomite-calcite fractionations, ΔC^{13}_{D-Ct}, Figure 23b, show a spread which is a little larger than the precision. This perhaps is due to either C-isotope equilibrium being attained on a scale less than the sample size, or preservation of equilibrium fractionations over a range of temperatures - improbable in light of the behaviour of O^{18} and Mg - or to some, as yet, undetected process. The large δC^{13}_{Ct} gradients between sample locations is suggestive, but not proof that the sample size could be greater than the size of the equilibrium system with regard to C^{13}. There is nothing unusual about the O- or C-isotope composition of the coarse vein calcite, Vt 4-11B-11.

Three samples were collected within an inferred single bedding unit over a distance of 100 ft. in Valley Quarry to complete a three dimensional picture of the possible isotopic gradients. These analyses are given in Table XVII and indicate that the isotopic composition for both oxygen and carbon is uniform over this distance within a given unit.

Table XVII

Isotopic Composition of Calcite Along and Across the Inferred Relict Bedding Plane in Valley Quarry, South Dorset, Vermont

Sample No.	δO^{18}_{Ct} (‰)	δC^{13}_{Ct} (‰)	Comments
Vt 4-10-2	21.63	-0.35	Reference sample
Vt 4-10-3-1	21.71	-0.30	12 ft. along inferred relict bedding plane from 10-2
Vt 4-10-4	21.74	-0.31	100 ft. along inferred relict bedding plane from 10-2
Vt 4-10-3-2	22.19	-0.03	4 inches across inferred relict bedding plane from 10-3-1

Fig. 23. -- The variation of (a) δO^{18}_{Ct}, ΔO^{18}_{D-Ct}; (b) δC^{13}_{Ct} and ΔC^{13}_{D-Ct} with position in the Kent quarry core.

Core Depth in Feet
0
20
40
60
80
100
120
Precision
Precision
21.6
22.0
22.4
22.8
δO^{18}_{Ct} (%) SMOW
(a)
ΔO^{18}_{D-Ct}
0.4
0.5
0.6
ΔC^{13}_{D-Ct}
0.4
0.5
0.6
0.7
Precision
Precision
0.8
0.4
0.0
-0.4
δC^{13}_{Ct} (%) PDB
(b)
Core Depth in Feet

Similar isotopic gradients across the sedimentary bedding have been observed by Degens and Epstein (1964) in Muschelkalk limestones. Their maximum gradients are a little greater than those observed here.

In the Kent Quarry and Valley Quarry samples only 1-5% of Mg-silicate minerals are present - chlorite, phlogopite, actinolite - except in two samples, Vt 4-11B-7, with 42% of chlorite plus phlogopite, and Vt 4-11B-2 with 21% of chlorite plus phlogopite. The calcite of Vt 4-11B-7 is isotopically the lightest in C^{13} observed here. However, there is no simple correlation between the isotopic composition and content of Mg-silicates or Mg-silicates plus quartz. Decarbonation through reactions between dolomite and silicates is of minor extent in these marbles. Dolomite-quartz is a common assemblage in the core and adjacent marbles.

The isotopic composition of the marbles, for both O^{18} and C^{13}, is similar to that of diagenetically altered limestones. This is in sympathy with the observed restricted decarbonation in this area, assuming that a fractionation occurs during this process. If a pore fluid phase was present during metamorphism presumably it contained both carbon and oxygen species. However, the significant gradients together with the constancy of the isotopic fractionations throughout the core attests to the lack of an efficient communicating fluid phase, assuming the absence of any kinetic barriers to isotope exchange. This latter assumption is supported by the observed relatively rapid rates of O-isotope exchange between groundwater and calcite (Clayton, 1966).

Consequently, it is possible that the observed variations in δO^{18} and δC^{13} in calcite are largely relict variations inherited from the sedimentary protolith. This does not exclude the partial modification of both the variations and the isotopic composition. Since the isotopic compositions of the marbles are so similar to diagenetically altered limestones, modifications to the latter are presumed to be quite small.

8.2.4 Denbigh Area, Ontario

Three coexisting calcite-dolomite pairs from a 3/4 mile length of a single marble unit, exposed along Highway 41, north-east of Denbigh, fall close to the correlation trend of Figure 17. The geological history of these samples undoubtedly is complex. Interpretation is necessarily less precise.

The marbles are bordered by biotite granodiorite 1/4 mile to the south, and paragneiss to the immediate north. The grade of metamorphism is sillimanite-almandine-muscovite subfacies (Evans, 1964). Traces of phlogopite and graphite mark out complex structural patterns in the medium-grained crystalline white marbles. The distribution of coexisting calcite and dolomite is very irregular. The calcites are cloudy due to probable fine-grained exsolved dolomite (Goldsmith, 1960).

The pertinent data for samples G 4-54-1, G 4-55, G 4-6 are given in Table XVIII. The X-ray data indicate that the calcite compositions for each sample are variable. Similar maximum $MgCO_3$ contents, and O- and C-isotope fractionations are found. These fractionation data are consistent with the preservation of equilibrium at similar temperatures.

Table XVIII

Isotopic and Solvus Data for Denbigh Area, Ontario

Sample	Phase	δO^{18} (‰)	ΔO^{18}_{D-Ct} (‰)	δC^{13} (‰)	ΔC^{13} (‰)	T_s^* (°C)
G 4-54-1	D	23.46	0.71	-1.51	0.58	415
	Ct	22.75		-2.09		110
G 4-55	D	23.25	0.48	3.55	0.42	400
	Ct	22.77		3.13		160
G 4-6	D	26.35	0.55	2.56	0.56	415
	Ct	25.90		2.00		145

* The two temperatures are derived from the two different $MgCO_3$ contents of the calcites, assuming that they represent an equilibrium quench.

However, the fractionations are of the same magnitude as those for the Kent Quarry core, even though the grade of metamorphism was considerably higher. The solvus relations are more involved here. Again, isotopic compositions are similar to diagenetic limestones and there are variations of both δO^{18} and δC^{13} between samples.

8.2.5 Conclusions

The data from the Kent Quarry (Table XIX) and Denbigh area are internally consistent with the preservation of equilibrium for both the partitioning of the cations and the isotopes. If the constancy of the fractionation factors for the two groups of samples is due to processes other than equilibrium, then the same processes must be responsible for the observed general trends shown in Figures 17, 18 and 19.

The relationships between the grade of metamorphism, solvus temperature, and the isotopic fractionations observed in these two sets of data imply that the high grade marbles quenched at a temperature considerably less than the inferred metamorphic high. This relation is well illustrated by the plot of T_s against metamorphic grade (Figure 4).

The disparity between the experimental and natural fractionations indicates that either one or both are not equilibrium fractionations. Considering these natural fractionation data, it is difficult to conceive of disequilibrium processes that would lead, fortuitously, to the observed correlations shown strongly in Figure 17 and weakly in Figures 18 and 19. O-isotope exchange rate experiments and observations on natural carbonate systems argue in support of the greater resistance of dolomite compared with calcite, and carbon compared with oxygen, to

Table XIX

Summary of Isotopic and Solvus Data for the Kent Quarry Core, South Dorset, Vermont

---

1) From the five calcite-dolomite pairs:

(a) $MgCO_3$ = 2.85 mol %, σ = 0.09 mol %, T = 325° ± 25°C.

(b) ΔO^{18}_{D-Ct} = 0.53 ‰, σ = 0.02 ‰.

(c) ΔC^{13}_{D-Ct} = 0.58 ‰, σ = 0.09 ‰.

2) $\frac{d(\delta O^{18})}{dx}$ = 0.00 - 0.13 ‰/ft., mean 0.03 ‰/ft.

3) $\frac{d(\delta C^{13})}{dx}$ = 0.00 - 0.28 ‰/ft., mean 0.06 ‰/ft.

4) $\frac{d(MgCO_3)}{dx}$ = 0.00 - 0.51 mol % $MgCO_3$/ft.

mean 0.11 mol % $MgCO_3$/ft.

---

exchange in the metamorphic and sedimentary temperature environments (Northrop, 1964; O'Neil and Epstein, 1966; Degens and Epstein, 1964; § 2.4.6). Thus, it is improbable that calcite and dolomite would be affected similarly by post-metamorphic processes. An equilibrium interpretation of many of the natural marble fractionations is favoured.

The observed δO^{18} and δC^{13} gradients between nearby samples reflects the limited size of the equilibrium system, and is smaller for C^{13} than O^{18} (see Table XIX: 2,3). The absence of a good communicating pore fluid is proposed. This may be related to the restricted extent of decarbonation.

8.3 Systems with Large Negative Oxygen Isotope Fractionations

8.3.1 Introduction

It was noted above (§ 7.5.3) that most of the large negative O-isotope fractionations were given by high grade calcareous schists. These samples, Vt 4-35-1a, -1b, -2a, -2b, G 5-1, exhibit both petrographic features characteristic of dedolomitization and light O-isotope compositions. However, some other samples, GLSK, M 16, G 4-5-3, whose mineralogy is indicative of dedolomitization, exhibit neither negative O-isotope fractionations nor O-isotope lightening. To elucidate the possible mechanisms of attainment of these large negative O-isotope fractionations a set of marble and calcareous schists, Vt 4-35, -1a, -1b, -2a, -2b, -5, which are closely related spatially, are now analysed in more detail.

8.3.2 Cavendish Formation Samples (Staurolite-Kyanite Zone)

The general geology of the Chester dome area was summarized above, § 7.3. The four Cavendish formation samples, Vt 4-35, -1a, -1b, -2a, -2b are from two cores taken from a single hand specimen: -1a and -2a are from the same carbonate rich schist band but 5 inches apart, while -1b and -2b are from a carbonate poor schist, immediately adjacent to -1a and -2a respectively. Vt 4-35-5 is from a massive marble unit (non-carbonate < 5%), 4 feet across the foliation from Vt 35-1 and -2. The mineralogy and mode of the five samples are recorded in Appendix II. It is noted that hydrous silicates are abundant in the schists and marbles, more commonly in the former. The isotopic data are given in Table XIV and presented diagrammatically in Figure 24. The data are essentially identical for Vt 4-35 -1a and -2a, and for -1b and -2b, and subsequently will be referred to as -1a and -1b respectively. Some pertinent features of these samples are summarized and contrasted in Table XX.

There can be no doubt that these different large negative O-isotope fractionations coupled with the uniformity of δO^{18}_{Ct} between -1a and -1b are indicative of disequilibrium. The C-isotope fractionations are consistent with equilibrium. On the other hand, the marble Vt 4-35-5 has concordant C- and O-isotope fractionations (Fig. 17) and probably concordant relations between the isotope fractionations and T_s (Figs. 18 and 19). As inferred from its position in Figures 4 and 15, the quench temperature was considerably lower than the metamorphic maximum.

Fig. 24. -- The isotopic composition of the samples Vt 4 - 35 - 1a, -1b, -2a, -2b, -5 from the Chester dome area.

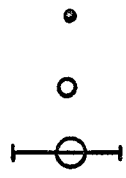

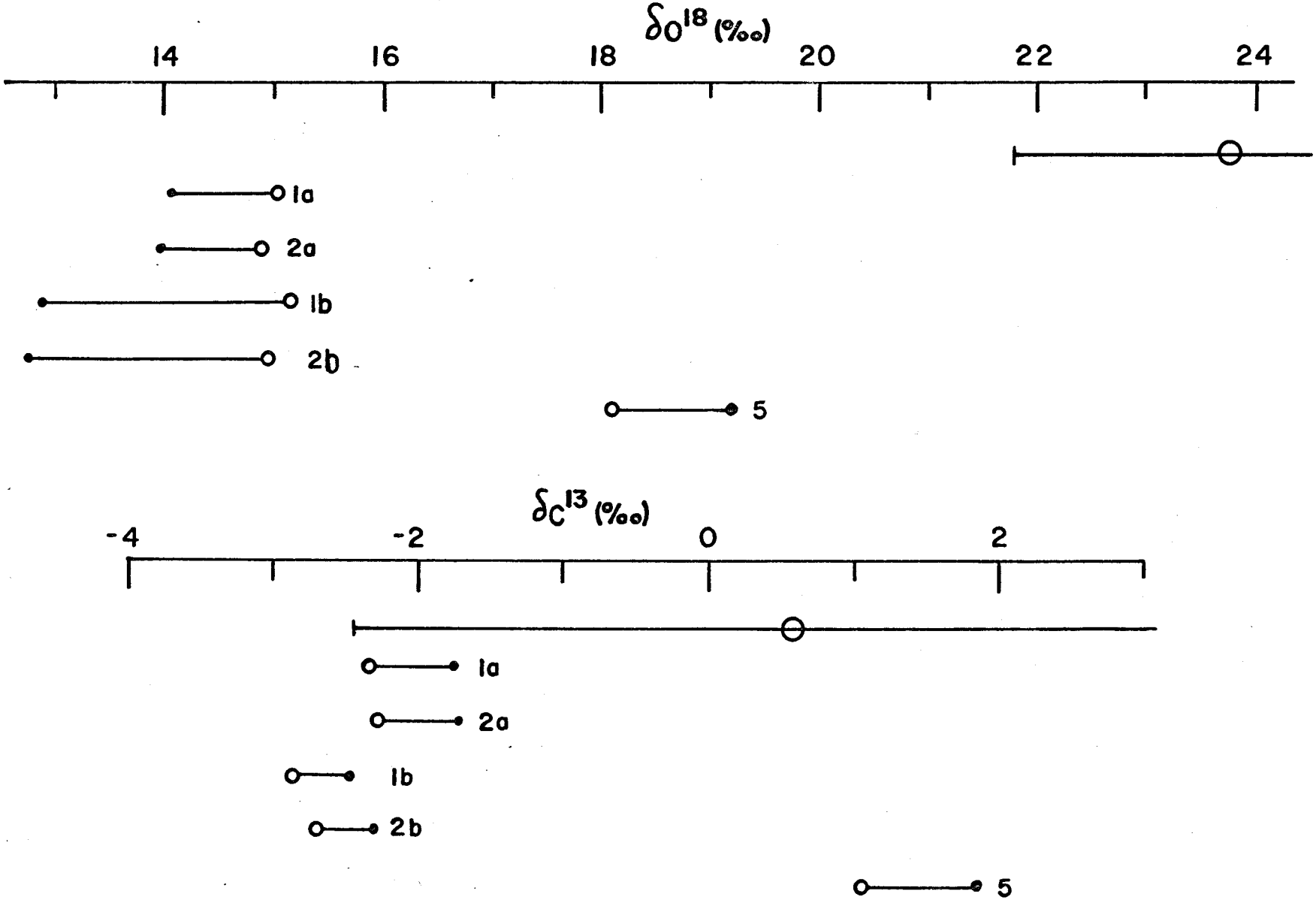
δO^{18} (‰)
14
16
18
20
22
24
1a
2a
1b
2b
5
δC^{13} (‰)
-4
-2
0
2
1a
2a
1b
2b
5

Table XX

Summary and Contrast of Data for Vt 4-35 -1a, -1b and -5

Vt 4-35-1a	Vt 4-35-1b	Vt 4-35-5
1) Calcareous rich schist	Calcareous poor schist	Marble
2) δO^{18} very light compared to limestone	δO^{18} very light compared to limestone	δO^{18} a little lighter than limestone
3) δC^{13} light but in limestone range	δC^{13} light but in limestone range	δC^{13} in limestone range
4) ΔO^{18} negative, large	ΔO^{18} negative, large	ΔO^{18} positive
5) ΔC^{13} positive	ΔC^{13} positive	ΔC^{13} positive
6) T_s = 510°, 450°C	T_s = 520°, 430°C	T_s = 210°C
7) δO^{18}_{Ct} similar to that in -1b	δO^{18}_{Ct} similar to that in -1a	δO^{18}_{Ct} much heavier than that in -1a or -1b

If only one carbonate phase exchanges, or both at different rates, then their fractionation may, in general, either increase or decrease during retrogradation. Calcite is more susceptible to exchange than dolomite (§ 2.4.6). The resultant dolomite-calcite fractionation is dependent upon: (1) the relative exchange rates of the carbonates; (2) the exchange temperature; (3) the isotopic composition of the exchange medium relative to the carbonates; (4) the chemical composition of this medium; (5) the relative proportions of exchanging carbonate to medium.

Assuming that the dolomite was essentially inert to retrograde exchange, then the O-isotope compositions of the calcites have become heavier by about +1.0‰ and + 2.0‰ in Vt 4-35 -1a and -1b respectively, assuming that ΔO^{18}_{D-Ct} (equilibrium) $\simeq$ 0.0‰ at 520°C. Such an O-isotope shift could result from exchange with an isotopically heavier water rich fluid common to both -1a, -1b and an oxygen reservoir. The large difference between δO^{18}_{D} in -1a and -1b possibly supports the assumption that the dolomite was relatively inert to exchange. Without knowing either the temperature of calcite exchange or the isotopic composition of the exchange medium, little more can be said about the nature of the process. It is noted that not all calcareous schists give obvious disequilibrium O-isotope fractionations.

Although large negative O-isotope fractionations are considered indicative of O-isotope disequilibrium, other partial exchange processes could result in fractionations that are less conspicuously disequilibrium. The nature of the exchange medium is very critical. This effect is the more important because the quench temperature may be so variable and un-

predictable. The working rule is proposed that all fractionation data which do not correlate with either the other isotope fractionation or T_s be treated as disequilibrium, until proven otherwise. Some discordant but equilibrium fractionations may be sacrificed in this process.

These negative O-isotope fractionations are particularly characteristic of samples, both marbles and schists, which come from the Chester dome area. Although the nature of the processes producing these effects is not known, other retrograde phenomena, e.g. chlorite haloes about garnets, are conspicuous in this region.

8.4 Variations of Isotopic Composition with Metamorphic Grade

In Figure 25 δC^{13}_D and δO^{18}_D are plotted against the metamorphic grade. Different symbols are given to Grenville and Vermont samples. The average isotopic composition of diagenetically altered limestone and its range is included for reference. In the upper half of Figure 25 neither a variation of δC^{13}_D with grade nor a significant deviation from the limestone range is noted. The isotopic composition of the one greenschist facies Grenville calcite, G 4-40 (Table XV), also falls into this general pattern. As noted by Craig (1953) Grenville marbles tend to be heavy in C^{13}.

In the lower half δO^{18}_D of samples from the Chester dome area are observed to fall below the limestone range. However, in contrast the high grade Grenville samples cluster around the limestone range. These Chester dome samples are now analysed in more detail.

Fig. 25. -- The variation of δC^{13}_{D} and δO^{18}_{D} with metamorphic grade.

Samples in the chlorite and biotite zones are approximately in their relative positions within the zone.

● Vermont dolomites

○ Grenville dolomites

⊢—⊖—⊣ Average limestone and its range.

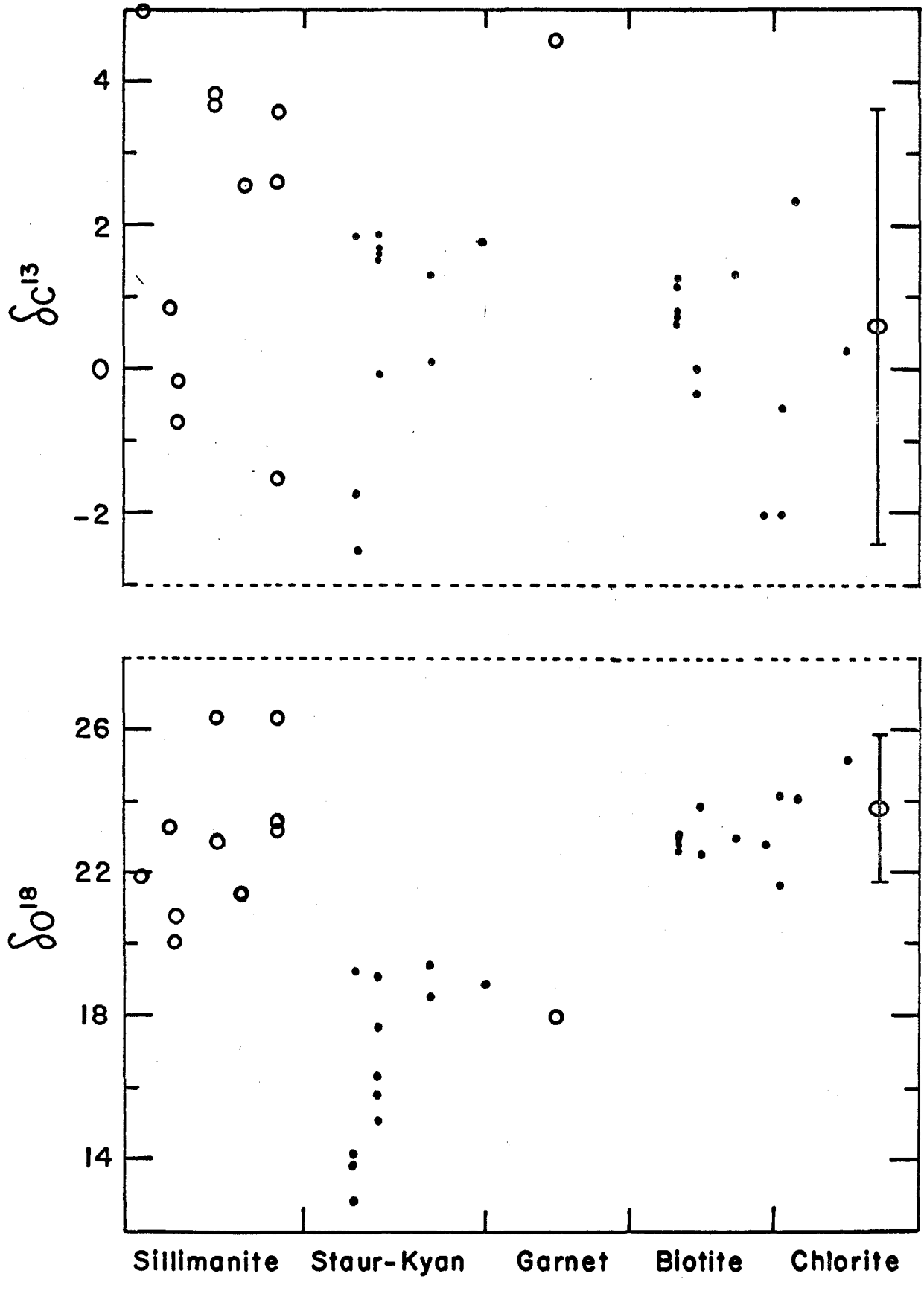
4
2
0
-2
δC^{13}
26
22
18
14
δO^{18}
Sillimanite
Staur-Kyan
Garnet
Biotite
Chlorite

8.5 Samples with Light O-Isotope Compositions

All samples from the Chester dome area are lighter in oxygen than average limestone or low grade Vermont marbles (Figure 25). Dedolomitization has occurred in many of these Vermont samples as well as in some Grenville samples, which display no conspicuous O-isotope lightening. Dedolomitization reactions are of the form:

$$\text{Dolomite} + \text{silicate} \longrightarrow \text{Mg silicate} + \text{calcite} + CO_2$$

For example:

$$2CaMg(CO_3)_2 + SiO_2 \longrightarrow Mg_2SiO_4 + 2CaCO_3 + 2CO_2$$

$$3CaMg(CO_3)_2 + KAlSi_3O_8 + H_2O \longrightarrow KMg_3AlSi_3O_{10}(OH)_2 + 3CaCO_3 + 3CO_2$$

$$3CaMg(CO_3)_2 + KAlSi_3O_{10}(OH)_2 \longrightarrow KMg_3AlSi_3O_{10}(OH)_2 + 3CaCO_3 + 3CO_2 + Al_2O_3$$

These reactions yield calcite plus the Mg-silicate and, in all the samples with more than a few percent of Mg-silicates, calcite is more abundant in the silicate rich layer. Much of the forsterite in the Grenville samples is serpentinized.

In Figures 26 and 27 the C- and O-isotope compositions of the dolomites for all samples with petrographic evidence for dedolomitization are plotted against the percent of Mg-silicates present, using the data presented in Tables XIV, XV and Appendix II. Many of these samples are mineralogically banded, Mg-silicate-rich carbonate-poor, and Mg-silicate-poor carbonate-rich. Therefore, the modes should be considered only as estimates to within 5 or 10% or so. The isotopic composition of the dolomite was chosen as the other parameter because: (1) only carbonates have been isotopically analysed; (2) prior to any possible retro-

Fig. 26. -- Variation of δC^{13}_{D} with modal abundance of Mg-silicates (wt %).

- ● Dolomites from the Chester dome area, Vermont.
- ○ Dolomites from the Grenville province.
- ▷ Average isotopic composition of limestone.

The dashed line is the trend shown by the Chester dome samples.

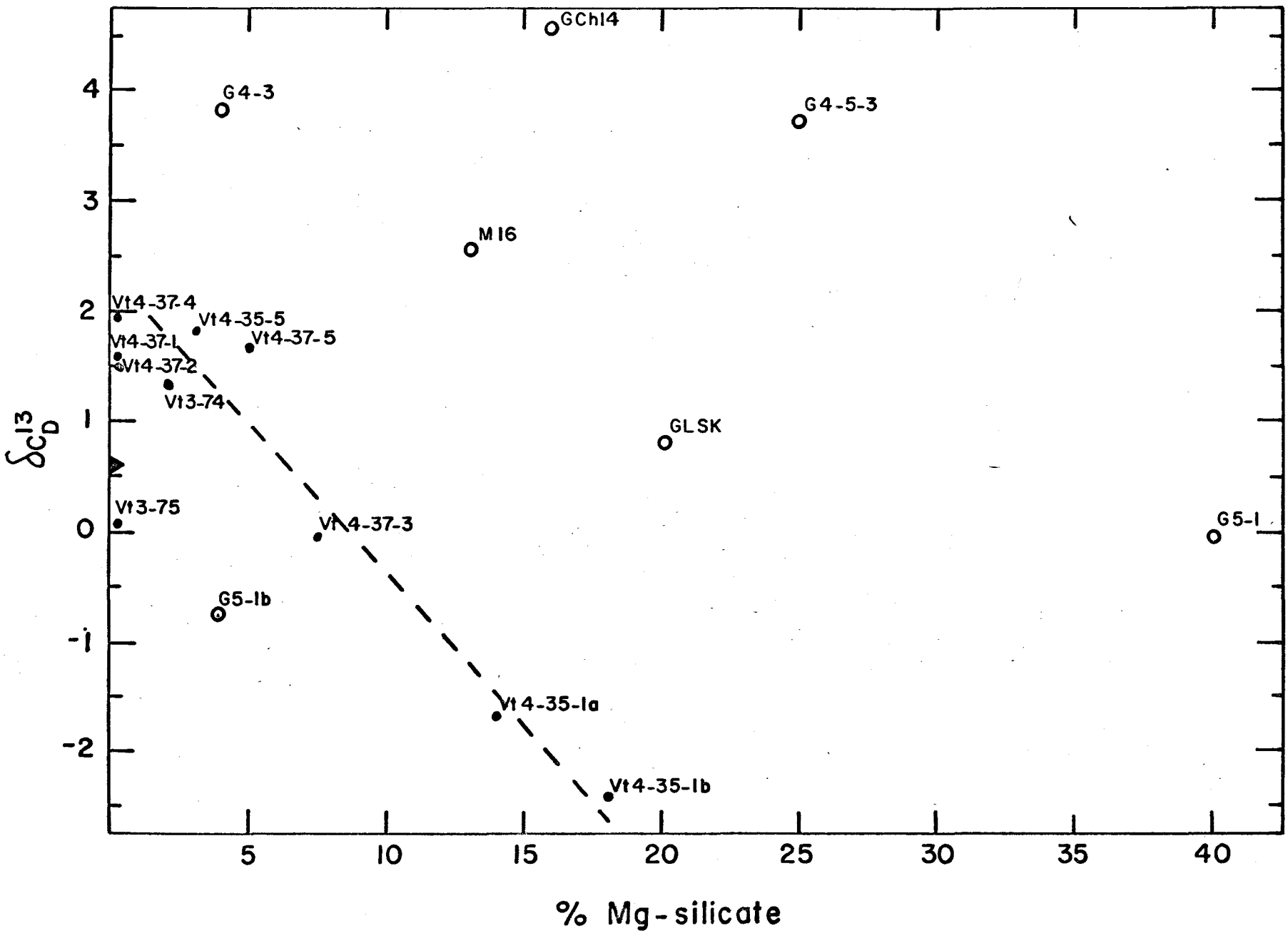
GChl4
G4-3
G4-5-3
M16
Vt4-37-4
Vt4-35-5
Vt4-37-1
Vt4-37-5
Vt4-37-2
Vt3-74
GLSK
Vt3-75
Vt4-37-3
G5-1
G5-1b
Vt4-35-1a
Vt4-35-1b
4
3
2
1
0
-1
-2
5
10
15
20
25
30
35
40
δC^{13}_{D}
% Mg-silicate

Fig. 27. -- Variation of δO^{18}_{D} with modal abundance of Mg-silicates (wt %).

- ⊙ Dolomites from the Chester dome area, Vermont.
- O Dolomites from the Grenville province.
- ▷ Average isotopic composition of limestone.

The dashed curve is the trend shown by the Chester dome samples.

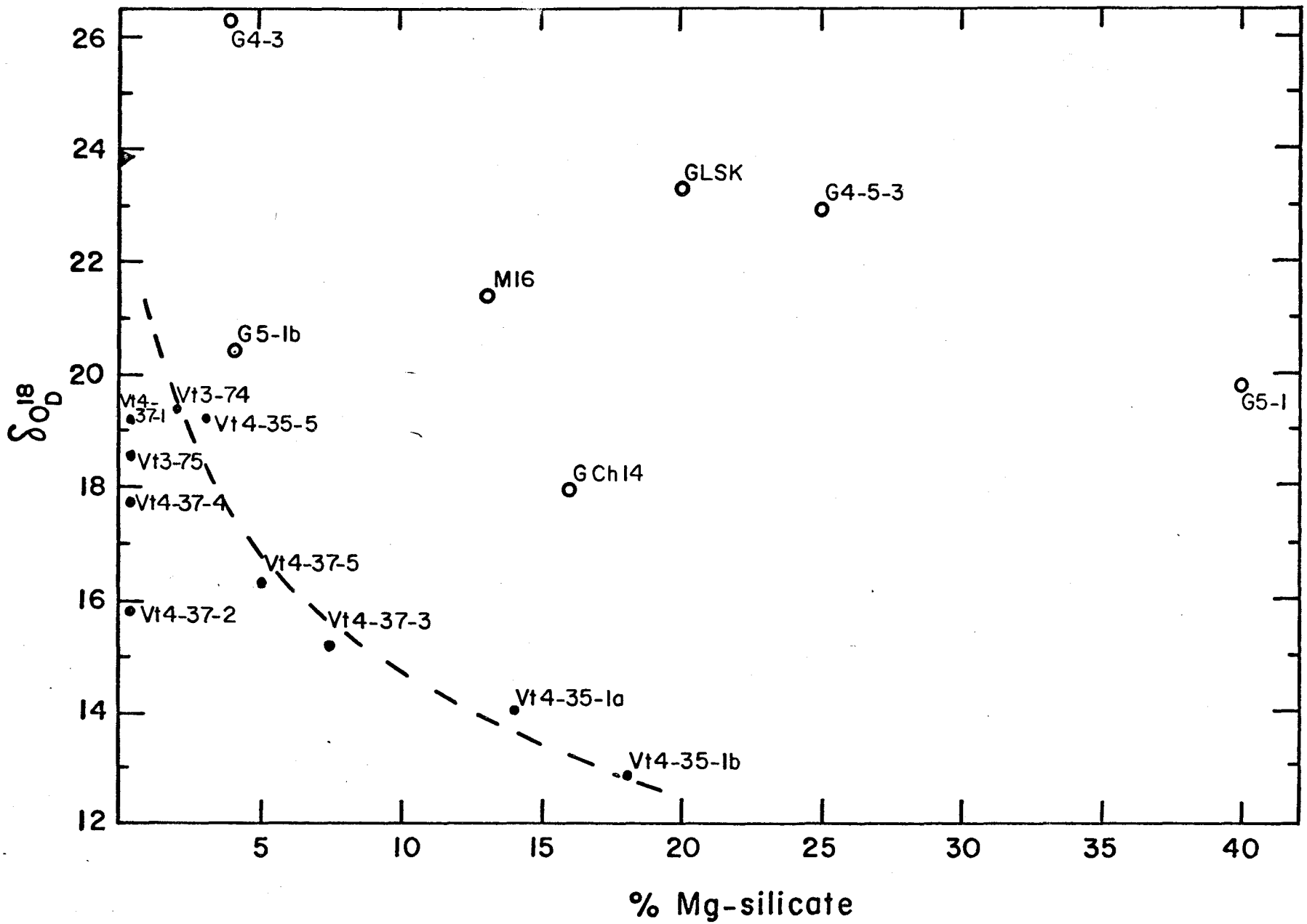
G4-3
GLSK
G4-5-3
MI6
G5-Ib
G5-I
Vt4-37-I
Vt3-74
Vt4-35-5
Vt3-75
GCh14
Vt4-37-4
Vt4-37-5
Vt4-37-2
Vt4-37-3
Vt4-35-Ia
Vt4-35-Ib
26
24
22
20
18
16
14
12
5
10
15
20
25
30
35
40
δO^{18}_D
% Mg-silicate

gradation, the isotopic composition of the total carbonate should have been similar to that of dolomite at these high temperatures, assuming that the dolomite was essentially inert to retrograde exchange. Some marbles from the Chester dome area are included: Vt 3-74, 3-75, 4-37-1, -2, -3, -4, -5.

A trend is noted for $\delta\, O_D^{18}$ and $\delta\, C_D^{13}$ vs. modal percent of Mg-silicates in both Figures 26 and 27 for the Chester dome samples. The isotopically lightest samples are more silicate rich. The $\delta\, O_D^{18}$ values for the marbles cluster around 18 to 20‰, which is 2 to 3‰ lighter than the average limestone value. These samples have undergone a certain degree of O-isotope exchange which is not directly associated with dedolomitization.

The variations in $\delta\, C_D^{13}$ for the Chester dome samples give a similar trend. However, there is no distinct difference between the range of isotopic compositions and the marine carbonate range, $\delta\, C^{13} = +\, 0.6 \pm 3‰$ (Fig. 25). The slopes of both trends are similar:

$$\frac{d(\delta\, O_D^{18})}{dZ} \simeq -\, 0.35‰/\% \;;\quad \frac{d(\delta\, C_D^{13})}{dZ} \simeq -\, 0.25‰/\%$$

where Z = the modal abundance of Mg-silicates (wt.%). All these Vermont samples come from the Cavendish formation as exposed around the Chester dome. Consequently they probably had a similar geological history, except for differing degrees of dedolomitization.

The Grenville samples show no such systematic variation. This may be a consequence of the variety of environments which these samples represent or to some other processes.

Various processes, either singly or in combination, could have produced the observed trends for the Chester dome samples. For O-isotopes these are:

1) Exchange

   (a) between carbonates and isotopically lighter silicates with little communication across the foliation between layers with different silicate contents. Shales typically have $\delta O^{18}_{rock} \simeq 16.0‰$, range 14.2 to 18.2‰, while pelitic schists tend to be about 2‰ lighter (Taylor and Epstein, 1962c; Taylor et al., 1963; Garlick, 1964).

   (b) with some non-carbonate medium whose isotopic composition is buffered externally to the system.

Some such exchange process is required to produce the isotopically light marbles.

2) Decarbonation. The mechanisms for such reactions are not known; they are sensitive to the environmental conditions. At equilibrium for metamorphic temperatures, CO_2 is isotopically heavier than the carbonates with respect to oxygen and possibly carbon (Northrop and Clayton, 1966; O'Neil and Epstein, 1966). If the liberated CO_2 tends to be in equilibrium with the carbonates then progressive isotopic lightening occurs to an extent dependent on the degree of decarbonation and the fractionation factor for the process. They are not necessarily equilibrium processes.

In thermal decomposition experiments with dolomite Sharma and Clayton (1965) report a fairly large kinetic isotope effect, which decreases with increase in temperature. The decomposition results in the concentration of O^{18} in the liberated CO_2.

For carbon isotopes, the variations between samples may be essentially those inherited from the protolith. However the following processes may have affected the Chester dome rocks to produce the observed trends:

1) Exchange with organic carbon, with the more shaley limestone originally being more carbonaceous.
2) Decarbonation: as for oxygen.

Again for C^{13}, whatever the process the communication across the foliation apparently was limited.

From the number and nature of these samples no definite conclusions can be drawn here about which process was dominant. A combination of these processes seems probable because the final isotopic compositions of the carbonates in the marble and associated calcareous schist are dissimilar. Preservation of such processes is dependent on the degree and efficiency of the exchange processes between neighbouring systems with different mineral proportions. Compared with the Chester dome area, the Grenville samples are isotopically heavier in both oxygen and carbon (Fig. 25). If similar processes to those in the Chester dome area operated in the Grenville, then possibly more effective exchange processes have smoothed out the differences between the marbles and

silicate-marbles. The coarser grain size of the Grenville marbles suggests that more extensive recrystallization occurred.

G 4-61, from a contact aureole talc deposit, has an exceptionally large C^{13}/C^{12} ratio for the dolomite, $\delta C_D^{13} = 13.0‰$, together with a large negative O-isotope fractionation. This is indicative of disequilibrium processes. This finale to exchange and decarbonation reactions attests to the variety of these processes.

Although a detailed analysis in the different areas will be necessary to determine the dominant processes producing disequilibrium O-isotope fractionations and isotopic lightening, the consequences of these results add confidence to the interpretation of many natural fractionations, especially from marbles, as equilibrium values.

IX. ISOTOPIC GEOTHERMOMETRY

9.1 Introduction

With the confidence gained from the previous discussion, the natural isotopic data, portrayed in Figures 15, 16, 17, 18 and 19, can be reconsidered with profit. Neglecting those data now known to be disequilibrium and appreciating that many high grade assemblages quench at a temperature less than the maximum, lines such as Line B and Line C on Figures 18 and 19 can be estimated visually. These consistencies and trends in the relationships between the C- and O-isotope fractionations and the $MgCO_3$ solvus data from marbles and some calcareous schists are most readily explicable in terms of an equilibrium model.

A calibration of both the C- and O-isotope fractionations as a function of temperature is sought. In the carbonate system, the $MgCO_3$ solvus thermometer is the only quantitative thermometric property available at present. Any calibration via the solvus thermometer demands that at least one of the isotopic fractionations quenched concordantly with it.

9.2 Derivation of Carbon and Oxygen Isotope Fractionation Expressions

The correlations noted in § 7.5.6 now can be applied to the derivation of probable fractionation expressions for C- and O-isotopes between coexisting dolomite and Mg-calcite. All the data shown on Figures 17, 18 and 19 cannot be employed indiscriminantly during this

operation. The following factors were considered and methods used in selecting suitable dolomite-calcite pairs:

1) All large negative O-isotope fractionations were rejected.
2) The plot of 1000 ln $\alpha^{C^{13}}_{D-Ct}$ vs. 1000 ln $\alpha^{O^{18}}_{D-Ct}$ (Figure 17) was used to select samples which had attained both C- and O-isotope equilibrium.
3) The remaining pairs were plotted as 1000 ln α_{D-Ct} vs. $10^6\ T_s^{-2}$, where $10^6\ T_s^{-2}$ was derived from the solvus thermometer. Those calcites composed of two Mg-calcites were plotted as two points. The high grade pairs with a large isotopic fractionation and high $MgCO_3$ content, which fall away from the trend (1000 ln $K = A\ T^{-2} + B$), were discarded.
4) The five Kent Quarry core samples were given special significance because of their concordant Mg, C- and O-isotope partitioning (§ 8.2.3, Table XIX). The solvus data for these samples is uncomplicated, with well defined high angle back-reflections.

The analysis of all the samples is reported in Table XXI.

These operations probably have selected those samples which most closely approached concordant quenching of Mg, C- and O-isotope partitioning. They fall about a line with small dispersion in 1000 ln $\alpha^{C^{13}}_{D-Ct}$, 1000 ln $\alpha^{O^{18}}_{D-Ct}$, $10^6\ T_s^{-2}$ space. Fifty percent of the calcite-dolomite pairs were rejected in this way. Those pairs selected are given in Table XXI and shown on Figures 28 and 29. The reduced major axis line (Miller and Kahn, 1962) fitted to these data, and shown in Figures 28 and 29 as Line S_1, give the fractionation expressions

Table XXI

Selection Analysis of Samples with Concordant Mg, C- and O-Isotope Fractionations*

Sample No.	Large Neg. ΔO^{18}	ΔO^{18} vs. ΔC^{13}	ΔC^{13} vs. $10^6 T_s^{-2}$	ΔO^{18} vs. $10^6 T_s^{-2}$	Selected
Vt3-51		Y	Y	Y	Y
Vt3-48					
Vt4-29		Y	Y	Y	Y
Vt3-65			Y		
Vt3-47		Y	Y	Y	Y
Vt4-23		Y	Y	Y	Y
Vt3-83-3		Y			
Vt4-12-1					
Vt4-11B (5)		Y	Y	Y	Y
Vt4-35-1a (2)	X				
Vt4-35-1b (2)	X		Y		
Vt4-35-5		Y	Y	Y	Y
Vt4-37-1					
Vt4-37-2	X				
Vt4-37-3		Y	Y	Y	Y
Vt4-37-4		Y	Y	Y	Y
Vt4-37-5	X		Y		
Vt3-74		Y	Y	Y	Y
Vt3-75		Y	Y	Y	Y
Vt3-76			Y		
GCh 14			Y		
G4-54-1		Y	Y	Y	Y
G4-55		Y	Y	Y	Y
G4-6		Y	Y	Y	Y
M16				Y	
G4-5-3		Y			
G4-3		Y			
G5-1	X				
G5-1b				Y	
GLSK				Y	
G3-11-1		Y	Y	Y	Y
Vt 26 (HPS)		Y	Y	Y	Y
VtII 36 (HPS)		Y	Y	Y	Y

* Samples with a large negative ΔO^{18}_{D-Ct} are marked: X

Samples with probable concordant relations are marked: Y

Fig. 28. -- Variation of 1000 ln $\alpha^{C^{13}}_{D-Ct}$ with $10^6 T_s^{-2}$ for the selected data.

Line S_1 is the reduced major axis line using all the selected data points. Line S_2 is the line using only the greenschist facies data points.

• Marble (Mg-silicates < 5%).

o Silicate Marble (Mg-silicates > 5%).

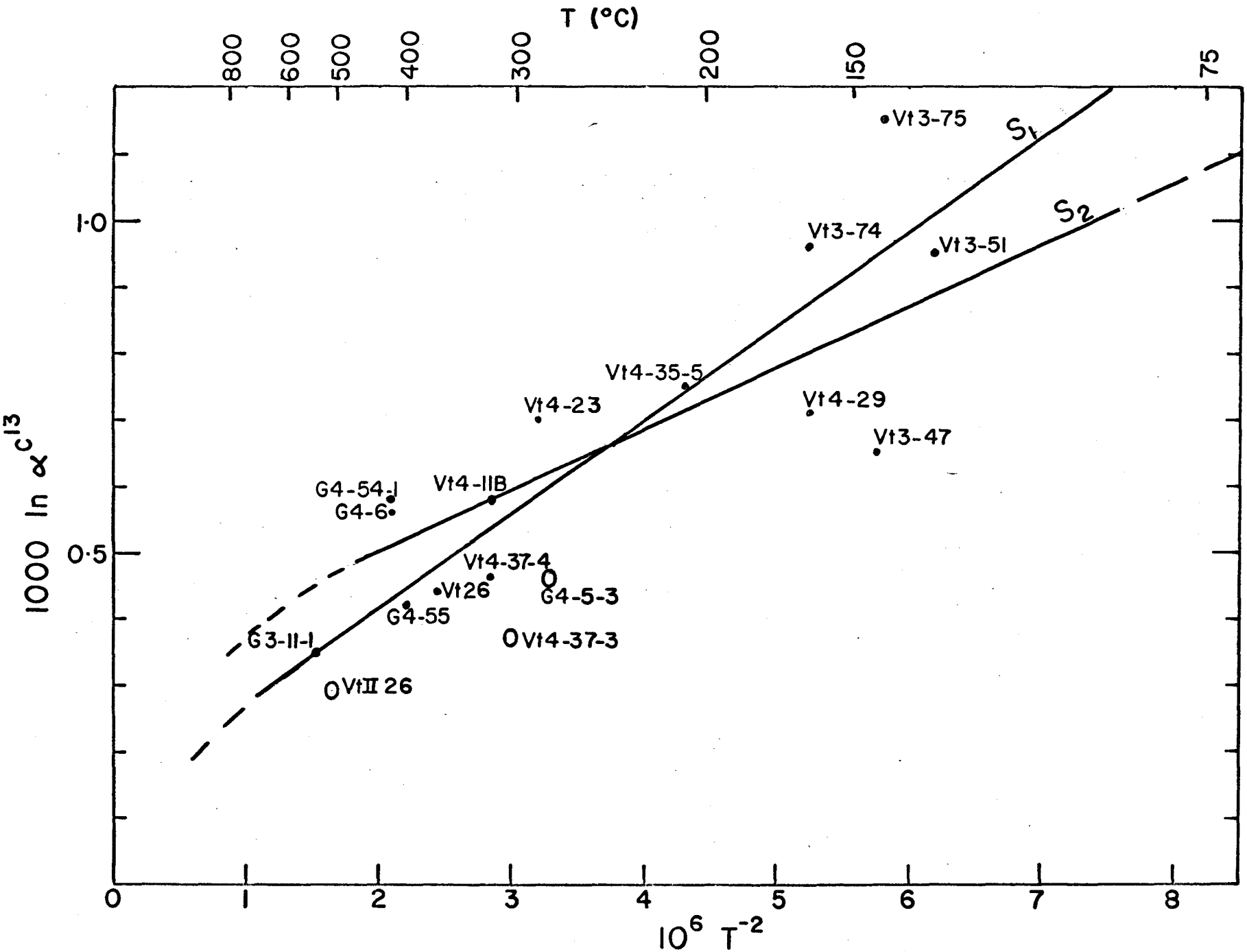
T (°C)
800
600
500
400
300
200
150
75
Vt3-75
S1
S2
Vt3-74
Vt3-51
Vt4-35-5
Vt4-23
Vt4-29
Vt3-47
G4-54-1
G4-6
Vt4-11B
Vt4-37-4
Vt26
G4-5-3
G4-55
G3-11-1
Vt4-37-3
VtII 26
1000 ln αC13
1·0
0·5
0
1
2
3
4
5
6
7
8
10^6 T^-2

Fig. 29. -- Variation of 1000 ln $\alpha_{D\text{-}Ct}^{O^{18}}$ with $10^6 T_s^{-2}$ for the selected data.

Line S_1 is the reduced major axis line using all the selected data points. Line S_2 is the line using only the greenschist facies data points.

- • Marble (Mg - silicates < 5%).
- o Silicate marble (Mg - silicates > 5%).

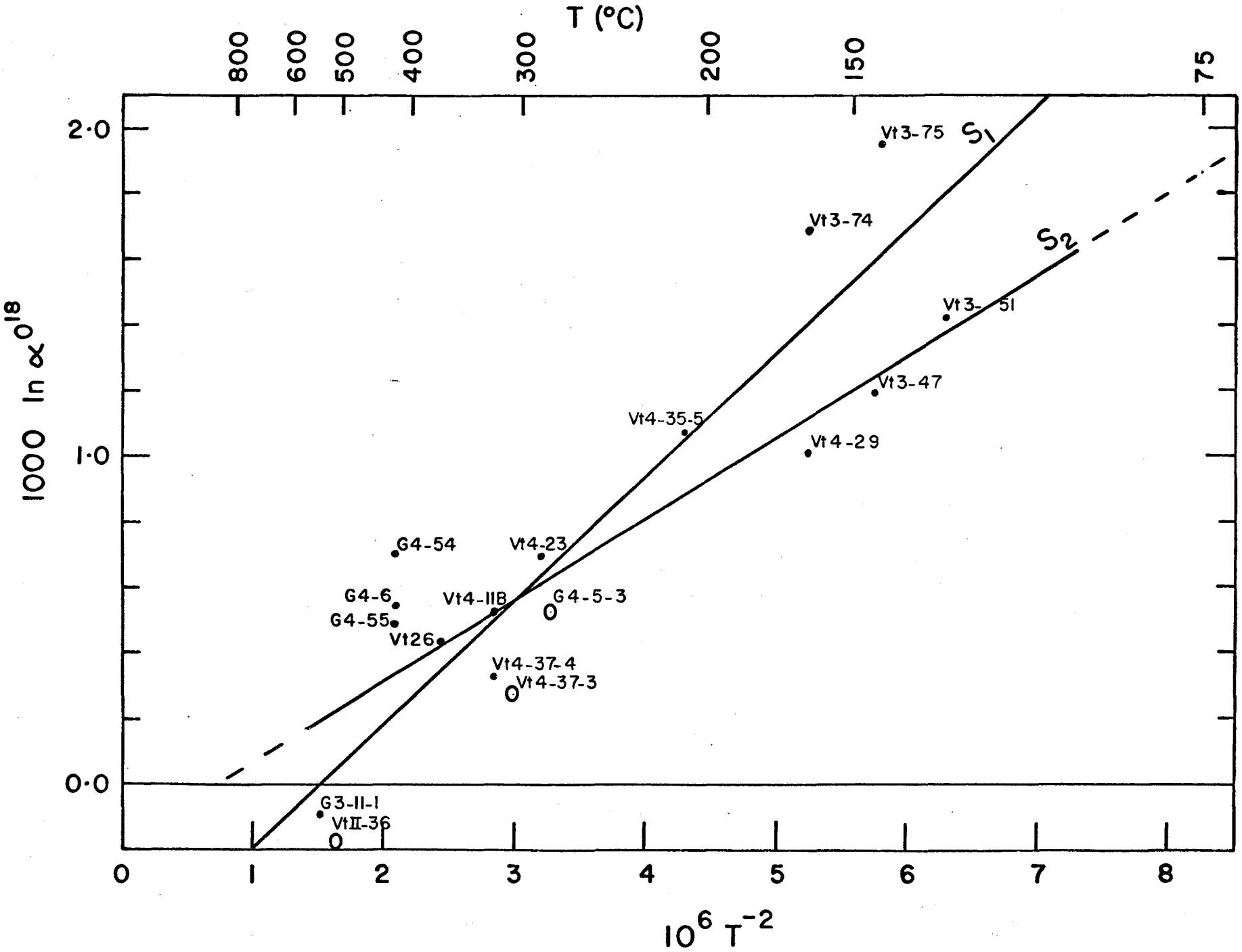
T (°C)
800
600
500
400
300
200
150
75
2·0
1·0
0·0
1000 ln $\alpha^{O^{18}}$
Vt3-75
S1
Vt3-74
S2
Vt3-51
Vt3-47
Vt4-35-5
Vt4-29
G4-54
Vt4-23
G4-6
Vt4-118
G4-5-3
G4-55
Vt26
Vt4-37-4
Vt4-37-3
G3-II-1
VtII-36
0
1
2
3
4
5
6
7
8
$10^6 T^{-2}$

$$1000 \ln \alpha^{C^{13}}_{D\text{-}Ct} = 0.14 \ (10^6 \ T^{-2}) + 0.14 \qquad (22)$$

$$1000 \ln \alpha^{O^{18}}_{D\text{-}Ct} = 0.38 \ (10^6 \ T^{-2}) - 0.58 \qquad (23)$$

It should be appreciated that the above procedure is not considered to be the most satisfactory method of determining the isotopic fractionation expressions because the $MgCO_3$ content of the calcite is a geologically determined property. Independent experimental calibration of each thermometer is the most satisfactory method. However, the calibration of each isotopic fractionation expression has not been performed simply upon those samples displaying a consistent relation between that fractionation and $10^6 \ T_s^{-2}$. The relationship with the other isotopic fractionation has been considered in the selection procedure, reducing the uncertainties in distinguishing concordant equilibrium isotope-solvus relations.

In Figures 17, 28 and 29 the greatest dispersion in the data is in the Figures 28 and 29. This is a consequence of the problems associated with deriving a temperature from the $MgCO_3$ content of the calcite. Uncertainties in the fractionation expressions (22) and (23) arise on four major accounts:

1) Pressure: the effect of pressure is undoubtedly more influential on the $MgCO_3$ solubility than on the C- or O-isotope fractionations. This affects both high and low quench-temperature samples. Vt 3-74 and 3-75 are high grade samples from the Chester dome area which apparently re-equilibrated at a lower temperature. The calcites of both samples have a higher $MgCO_3$ content than chlorite zone samples

with a similar isotopic fractionation (Figs. 28 and 29). If this is an effect of pressure, then Vt 3-74 and 3-75 quenched in a higher pressure environment than that in the chlorite zone of West Vermont. Lines (22) and (23) should then be closer to, for example, Vt 3-47, 3-51 at this temperature, since these samples crystallized at pressures closer to those used in the experimental determination of the solvus (see § 5.1.4). The difference in pressure between the two regions is estimated to be about 5 kb., using the extrapolated solvus data and assuming that the observed differences in T_s are wholly a result of pressure differences.

2) Exsolution phenomena are prevalent in the high grade samples which have not recrystallized at a much lower temperature.

3) Chemical analyses of a few Mg-calcites give appreciably higher $MgCO_3$ contents than given by the X-ray technique (Table III). If all this extra dolomite was in solution in the calcite then $10^6 T^{-2}$ should be smaller for those calcites which have remained closed systems during and since ex-solution. Again, the effect of pressure must be considered before deriving a temperature from the chemical analysis for $MgCO_3$.

4) The derived fractionation expressions are linear relations. The lines shown on Figures 17, 28 and 29 must be curves at least at the high temperature end because $1000 \ln K \longrightarrow 0$ as $T \longrightarrow \infty$.

Lines S_2 on Figures 28 and 29 are the natural expressions derived from the greenschist facies data only, in the temperature range 135° to 325°C. These expressions are:

$$1000 \ln \alpha^{C^{13}}_{D\text{-}Ct} = 0.09\ (10^6\ T^{-2}) + 0.32 \qquad (25)$$

$$1000 \ln \alpha^{O^{18}}_{D\text{-}Ct} = 0.25\ (10^6\ T^{-2}) - 0.20 \qquad (26)$$

In $1000 \ln \alpha^{C^{13}}_{D\text{-}Ct}$, $1000 \ln \alpha^{O^{18}}_{D\text{-}Ct}$, $10^6\ T_s^{-2}$ space, the greenschist fractionation and solvus data fall about a line with less dispersion than that displayed by all the selected data (Table XXI). The $MgCO_3$ content of these calcites is known with greater certainty because the high angle back-reflections are sharp well-defined single peaks. Uncertainties in the extrapolation of the solvus are critical in introducing a possible consistent calibration error. However, the pressure correction for these samples is probably minimal. Interestingly, the fractionation trend noted by Northrop and Clayton (1966) from their synthesis reactions, using magnesite + calcite as starting materials, for the temperature range 500° to 700°C, falls in between the fractionations given by expressions (23) and (26) at these temperatures and deviates by less than 0.2‰ from both lines.

In the absence of independent calibration, the derived fractionation expressions are a compromise considered to be good guides to the order of magnitude of the equilibrium fractionation expressions. The expressions (22) and (23), and (25) and (26) are presented as possible alternative calibrations. At present, there appears to be no way to choose between them. Both have their associated uncertainties.

The fractionation expressions for O-isotopes determined experimentally by Northrop and Clayton (1966) and O'Neil and Epstein (1966), and from an empirical relation by O'Neil (1963) (see § 2.2.3) are presented in Figure 30 as Lines NC, OE and O, respectively; that for carbon isotopes, determined earlier (§ 6.3), as Line D in Figure 31. The natural fractionation expressions are included for comparison as Lines S_1 for (22) and (23) and Line S_2 for (25) and (26). The disparity between the natural and experimental fractionation expressions is conspicuous. It is noted that O'Neil's empirical expression is quite closely followed by Line S_2, and by Line S_1 at higher temperatures. The interpretation of the dolomite-calcite fractionation at room temperature, determined from the extrapolated regions of these lines, is open to question.

Both expressions (23) and (26) indicate the presence of a cross-over in the O-isotope fractionation expression; for (23) at about 550°C and for (26) at about 875°C. Samples G 3-11-1 and Vt II 36, both with small negative O-isotope fractionations, may, therefore, be equilibrium fractionations. Petrographic relations are consistent with equilibrium; but, Vt II 36 is a calcareous schist with 35% biotite plus chlorite and the carbonate is isotopically very light: $\delta O_D^{18} = 10.8‰$, $\delta C_D^{13} = -6.2‰$.

9.3 Discordant Relations

It was noted that 50% of the samples were rejected during the selection operation because they did not have apparent concordant C- and O-isotope and $10^6 T_s^{-2}$ relations (Table XXI). One third of these samples have large negative O-isotope fractionations, showing that they have suf-

Fig. 30. -- The dolomite - calcite O-isotope fractionations determined experimentally and from the natural data.

Line OE from O'Neil and Epstein (1966).

Line NC from Northrop and Clayton (1966).

Line S_1 from this work; all selected data.

Line S_2 from this work; greenschist facies data.

Line O from O'Neil (1963).

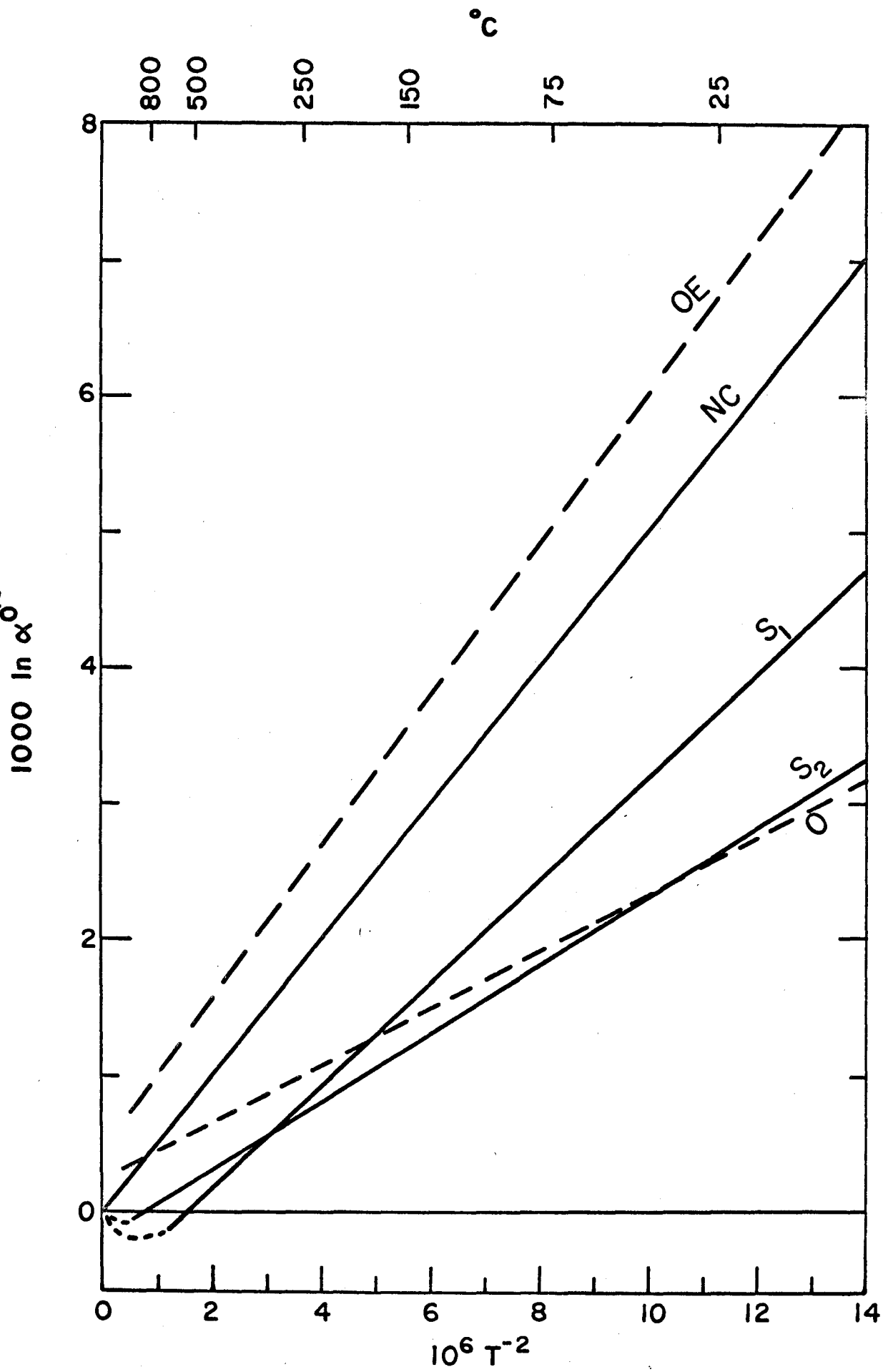
°C
800
500
250
150
75
25
8
6
4
2
0
1000 ln $\alpha_{O^{18}}$
OE
NC
S_1
S_2
O
0
2
4
6
8
10
12
14
$10^6\ T^{-2}$

Fig. 31. -- The dolomite-calcite C-isotope fractionations determined experimentally and from the natural data.

Line D — from this work (experimental).

Line S_1 — from this work; all selected data.

Line S_2 — from this work; greenschist facies data.

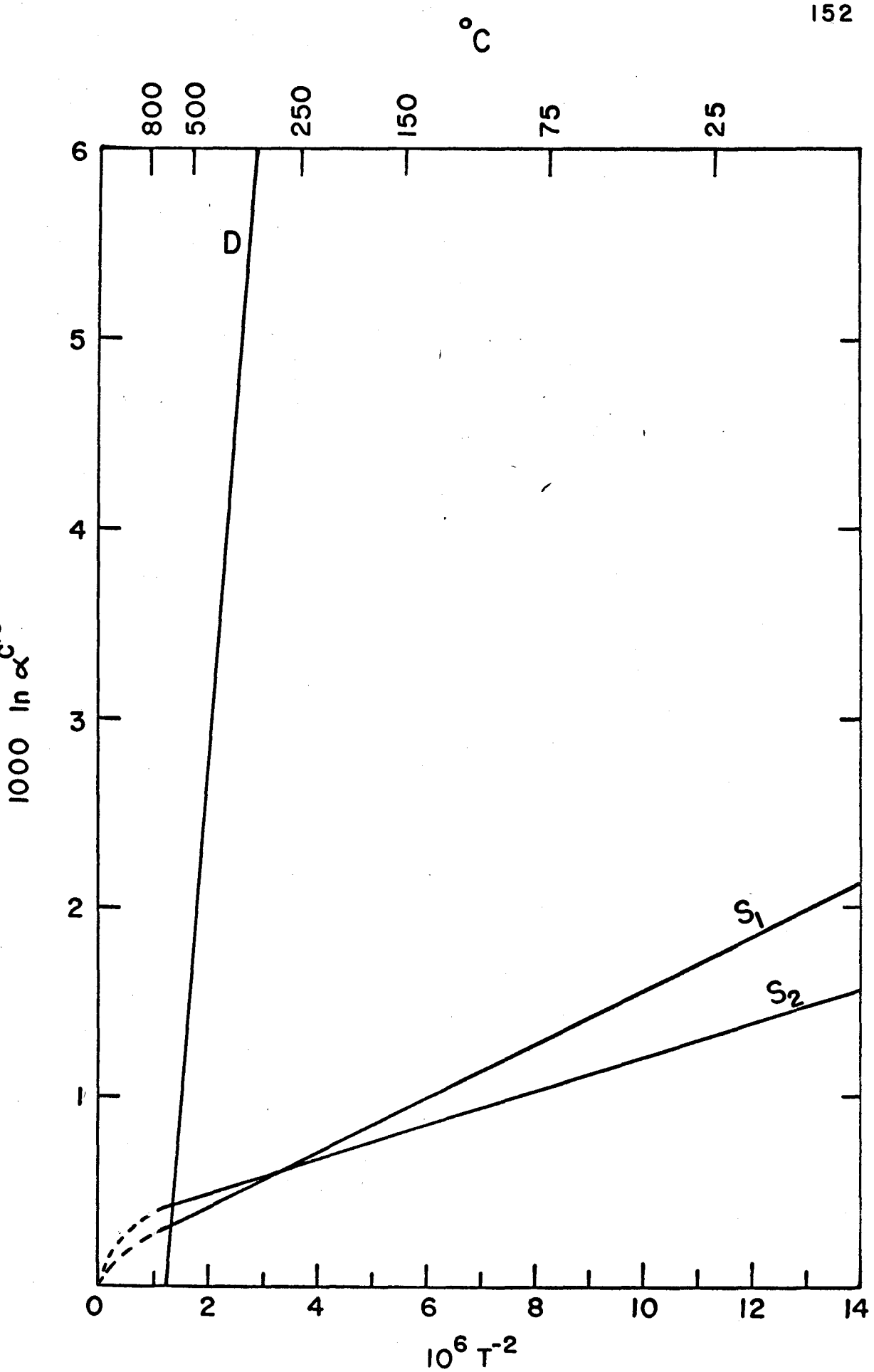
°C
800
500
250
150
75
25
6
5
4
3
2
1
0
2
4
6
8
10
12
14
D
S1
S2
1000 ln αC13
10^6 T^-2

fered conspicuous partial O-isotope exchange (§ 8.3). The remaining samples fall into two groups:

1) Low grade samples: Vt 3-48 is a black meta-limestone which has both a disequilibrium C-isotope fractionation and a calcite with a very low $MgCO_3$ content. There is little evidence for recrystallization. Although this sample comes from the upper chlorite zone (Fig. 14), neither cation nor C-isotope equilibrium was attained.

Vt 3-65 from the chlorite zone has textural evidence for more than one generation of calcite. It is observed to have discordant O-isotope fractionation relations with both the C-isotopes and the solvus thermometer. However, the C-isotope fractionation and the solvus relations are concordant. It is concluded that the O-isotope fractionation is probably not an equilibrium value.

Vt 3-83-3 and Vt 4-12-1 both come from South Dorset (Fig. 21). The $MgCO_3$ content of these calcites are similar to those observed from the Kent Quarry suite, Vt 4-11B. Nevertheless, Vt 3-83-3 has concordant C- and O-isotope relations suggesting a lower temperature equilibration. Vt 4-12-1 is probably in isotopic disequilibrium. The reasons for these differences are not known.

2) High grade samples: the discordant relations observed in some marbles from the Chester dome area indicate that oxygen or oxygen and carbon isotope exchange occurred which resulted in disequilibrium but positive fractionations. Carbon appears to be more resistant to retrograde exchange. Many Grenville samples may preserve one concordant relation but, nevertheless exhibit significant retrograde exchange. Many of these samples apparently give lower quench temperatures for the isotopic thermo-

meters than that given by the maximum solvus temperature. One interpretation is that carbon and oxygen exchanged between minerals to a lower temperature than Mg. Alternatively, the high $MgCO_3$ content of the calcite may not represent an equilibrium quench.

9.4 Dolomite-Calcite Geothermometers

Isotopic thermometers are inherently more sensitive at lower temperatures than at high temperatures, in antithesis to solvus thermometers. Comparison of the dolomite-calcite fractionation expressions derived earlier, (22) and (23), and (25) and (26), with other established isotopic geothermometers such as the quartz-magnetite or quartz-calcite thermometers emphasize their relative insensitivity. Nevertheless, the presence of three potential thermometers in a single mineral pair is an attractive feature, together with the wide occurrence, and different structural behaviour of marbles compared with schists and gneisses.

From the previous analysis of the solvus and isotopic data the observed geothermometric relations are summarized and possible criteria for selecting equilibrated samples noted:

A. Marbles and Calcareous Schists

1) The maximum solvus temperature correlates well with the metamorphic grade for many samples.

2) Samples from areas where adjacent pelitic schists have conspicuously suffered retrogradation may, but not necessarily will, give anomalous oxygen, or oxygen and carbon isotope fractionations.

3) Most marbles and silicate-marbles give concordant C- and O-isotope relations (Figure 17), except where 2) applies. However, the relationships between the solvus data, the O- and C-isotope fractionations and the metamorphic grade indicate that many high grade samples quench at a temperature considerably less than T_{max} (Figures 4, 15 and 16). There is commonly no textural evidence for retrogradation.

4) No working criterion has been found to select a high grade rock which will yield an isotopic or solvus temperature close to T_{max}, except by looking at one of the thermometric properties. However, marbles associated with calcareous schists may re-equilibrate to lower temperatures.

5) Rocks showing textural evidence for disequilibrium, such as calcite veins filling fractures, give discordant O- and C-isotope fractionations (Schwarcz, 1966; § 9.3).

6) Some samples from the chlorite zone give C-isotope fractionations that are apparently too small for equilibrium fractionations e.g. Vt 3-48, Vt 69. T_s and the O-isotope thermometer give temperatures consistent with the chlorite zone in some cases.

B. General

1) Significant discordancy between all three thermometric properties is probably the exception except where (a) subsequent exchange disturbs the fractionation in high grade rocks, and (b) C-isotope equilibrium was not attained (§ 9.3).

2) The sample size should be kept as small as possible, especially when measuring C-isotope fractionations in low grade assemblages.

9.5 Comparison of Geothermometers

A direct comparison can be made between these carbonate geothermometers and the other geothermometers present in Vt II 36, a calcareous schist (Schwarcz, 1966). The temperatures derived from the three dolomite-calcite thermometers (they are not strictly all independent here) are compared in Table XXII with the quartz-calcite and quartz-magnetite isotopic thermometers of O'Neil and Clayton (1964). The five thermometers give similar temperatures, except those using (25) and (26), with the dolomite-calcite isotopic thermometers giving the highest temperatures. If these are all concordant equilibrium fractionations, then the calibration of the dolomite-calcite isotopic thermometers may be too high by 50° to 100°C. Dolomite-quartz is present in this assemblage. It becomes unstable above about 550° to 600°C, with $P_{CO_2} = P_{total} \geqslant 2$ kb. (Bowen, 1940).

Some Leadville Limestone carbonate-quartz assemblages can be exploited for an indirect comparison (Engel et al., 1958). Two samples, LV 4 (coexisting quartz-calcite), and LV 569 (coexisting quartz-dolomite) are closely related assemblages in the Gilman mine. LV 4 is adjacent to the ore body; LV 569 is about 50 feet away and down the presumed temperature gradient. Engel et al., present evidence that a large amount of hydrothermal fluid of relatively uniform O-isotope composition was in contact with the recrystallized minerals. Assuming that LV 4 and LV 569 were both in isotopic equilibrium with the common fluid, a quartz-calcite

and an inferred dolomite-calcite temperature can be derived from these assemblages. It is not suggested here that LV 4 and LV 569 were in thermal equilibrium with one another. These temperatures are reported in Table XXII. They are not similar. Although LV 569 gives the lower temperature as expected, such a temperature difference seems unreasonable.

A less direct comparison is given by the geothermometric results of Garlick (1964) on pelitic schists in New England, using the quartz-magnetite isotopic thermometer. The results are presented in Figure 32, where the temperature range for the metamorphic zones deduced by Garlick (biotite zone up to orthoclase zone) are plotted against those from this work. The temperature range for the chlorite zone is taken after McNamara (1965). He deduced the possible temperature conditions by arguments based on: (a) quartz segregations; (b) anatase-rutile transition; (c) synthesis fields for muscovite, chlorite, kaolinite. These temperatures must be considered as approximate. Dashed Line A, Figure 32, is the concordant temperature line. The points on Figure 32 were arrived at, either by comparing the temperatures from nearby samples, for example in the Chester dome area, or from samples close to an isograd, for example the biotite isograd near Middlebury, Vermont. The tentative Line B emphasizes that the carbonate temperatures are a little lower than the reference temperatures.

The deviations at high temperatures are not considered to be significant because calibration problems are most critical there. However, discrepancies in the biotite and chlorite zones may be significant.

Table XXII

Comparison of Geothermometers

Sample No.	Mineral	δO^{18} (‰)	δC^{13} (‰)	T (°C)	Method
Vt II 36	Calcite	10.99	-6.46	640	D-Ct-O^{18} (23)
(Schwarcz, 1966;	Dolomite	10.80	-6.17	disequilibrium	D-Ct-O^{18} (26)
O'Neil and				635	D-Ct-C^{13} (22)
Clayton, 1964)				disequilibrium	D-Ct-C^{13} (25)
				525	Solvus
	Quartz	12.60		560	Qtz-Ct
	Magnetite	2.0		600	Qtz-Mt
Leadville Lst.					
LV 4	Calcite	13.4		345	Qtz-Ct
	Quartz	16.1			
LV 569	Dolomite	15.6		105	D-Ct-O^{18} (23)
	Quartz	16.2		60	D-Ct-O^{18} (26)
	Calcite*	13.5			

* Inferred isotopic composition of Ct, using LV 4, ΔO^{18}_{Qtz-Ct} = 2.7‰

Fig. 32. -- Comparison of the carbonate thermometers with other reference thermometers.

The reference thermometer is taken after the results of Garlick (1964) and McNamara (1966).

Line A is the concordant temperature line.

Line B is the comparative line.

○ Temperatures derived from both the carbonate and reference thermometers.

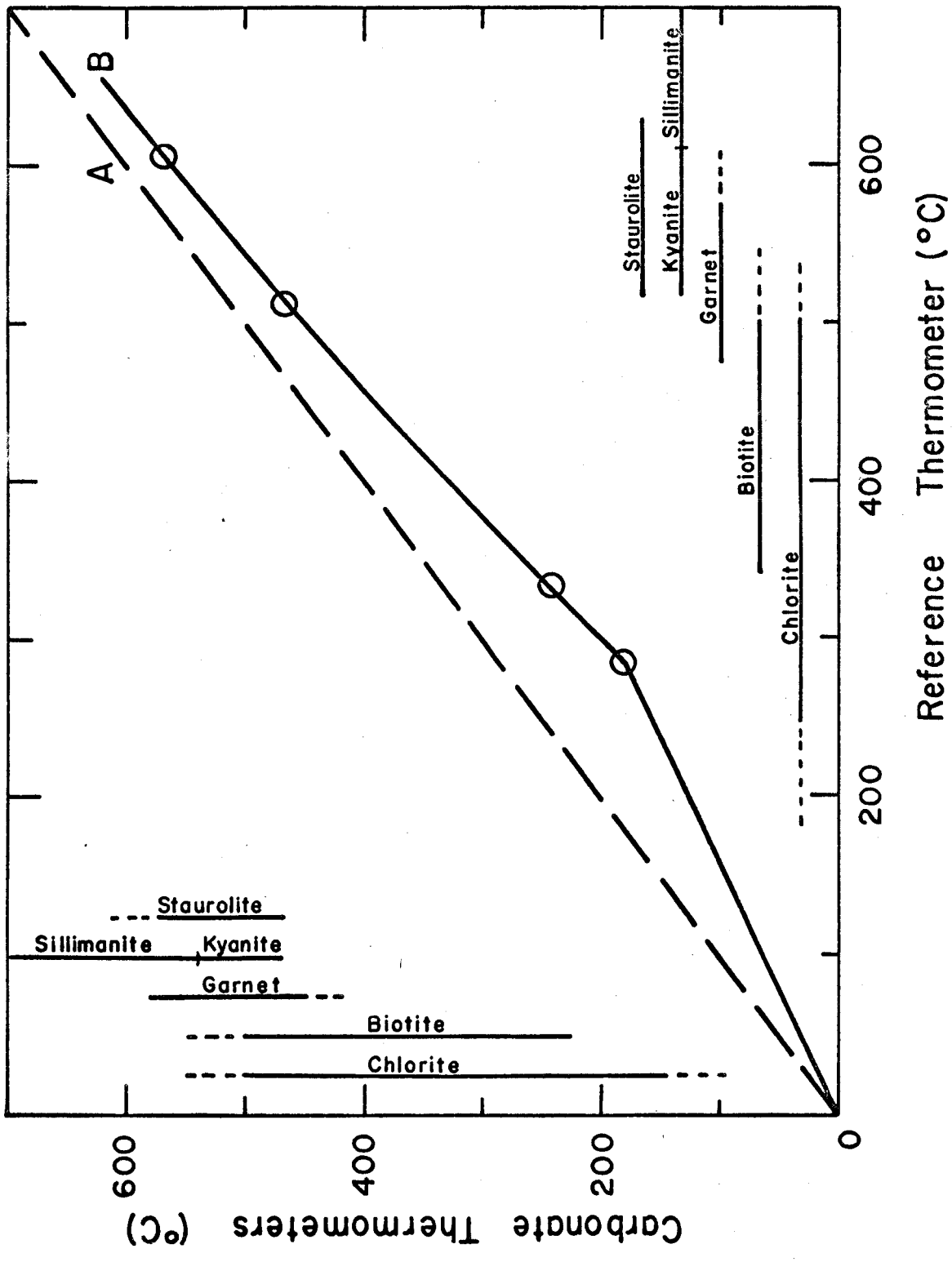
Carbonate Thermometers (°C)
0
200
400
600
Reference Thermometer (°C)
0
200
400
600
A
B
Staurolite
Sillimanite
Kyanite
Garnet
Biotite
Chlorite
Staurolite
Sillimanite
Kyanite
Garnet
Biotite
Chlorite

Garlick's lowest temperature sample, T_{Q-Mt} = 375°C (C518), comes from the biotite zone about 8 miles due east, and, hence up grade from samples Vt 4-29, 3-47, 3-48 which straddle the biotite isograd, near Middlebury, Vermont (Doll, 1961). Reactions between phases in the greenschist facies are, in general, more pressure sensitive than reactions at higher grades because of the nature of reaction surfaces at lower pressures. The lower temperature observed for the biotite isograd ($T \simeq 225°C$) near Middlebury compared with that inferred for the Dalradian ($T \simeq 300°C$) could be a consequence of the difference in pressure between the two areas, assuming, as seems reasonable from Figure 2, that the error in the extrapolated solvus is small. The pressure range for the Dalradian greenschist facies of Scotland was estimated at: 3-5 kb. (McNamara, 1965). This must be considered only as a possibility because the reactions taking place at the biotite isograd are not known specifically and may not be equivalent to each other. Also, the location of the isograd is dependent on physical properties other than P and T, such as the fluid composition.

The general thermometric properties of calcite-dolomite assemblages seem to be reasonably well established. Satisfactory resolution of the conflict between the experimental and geological (solvus) calibration of these thermometers is essential before pursuing any detailed geothermometry in this system.

9.6 Conclusions

This analysis implies that a certain confidence can be placed in much of the isotopic fractionation data from carbonates. Excluding samples with conspicuous textural disequilibrium, there does not appear

to be a good criterion available for distinguishing, in high grade rocks, a retrograde re-equilibrated assemblage from a sample which quenched at the maximum metamorphic temperature. Some calcareous schists preserve a high temperature equilibrium fractionation, but there is always the problem of possible subsequent O-isotope exchange in such samples. It was noted previously by Taylor and Epstein (1962b, p. 692) that 'there is evidence that the degree to which re-equilibration takes place during metamorphism varies from rock to rock and even from mineral to mineral in the same rock'. This statement is borne out by this study.

The geological interpretation of the retrograde temperatures is a problem beyond the scope of this study. Nevertheless it is worth noting the broad similarities between this thermal phenomena and those observed in A^{40} and Sr^{87} studies in metamorphic rocks (e.g. by Wasserburg et al., 1964; Hurley et al., 1962). Quench phenomena are multivariant functions - depending on mineral type, size, imperfections, structural behaviour, etc. - and may record some geological event such as uplift and cooling history rather than the peak of metamorphic activity.

X. SUMMARY AND CONCLUSIONS

This research set out to establish whether calcite and dolomite in metamorphic assemblages preserve equilibrium C- and O-isotope fractionations. An a posteriori argument using the natural fractionation data was applied to demonstrate, with some confidence, that many assemblages preserve an equilibrium fractionation for both C- and O-isotopes and for the partitioning of Mg. Equilibrium was tested for by obtaining consistent fractionations from a set of carbonate pairs with variations in the isotopic composition of the carbonates between samples. The volume of rock was sufficiently small that uniformity of physical conditions could be assumed with confidence.

Quench phenomena are characteristically complex in amphibolite facies marbles. This is illustrated both by the variations in isotopic and solvus quench relations between adjacent samples, and in the unpredictability of the quench temperature relative to the metamorphic maximum. Some marbles from the Chester dome area, Vermont, exhibit the largest difference between the metamorphic peak and the final quench temperature, about 350°C, although these rocks had a shorter metamorphic history than Grenville province marbles by a factor of about six. The larger grain size of the Grenville marbles may be one of the several critical factors controlling retrograde re-equilibration (Grenville: 2 to 3 mm.; Vermont: 0.3 to 1 mm., for a similar grade).

The solvus thermometer correlates well with the metamorphic grade for many samples although a lower than maximum temperature is recorded from high grade marbles. Calibration of the isotopic geothermometers using both C- and O-isotope fractionations concordant with the solvus thermometer gave, in the temperature range 130° to 550°C, the expressions:

$$1000 \ln \alpha^{C^{13}}_{D\text{-}Ct} = 0.14(10^6 T^{-2}) + 0.14 \qquad (22)$$

$$1000 \ln \alpha^{O^{18}}_{D\text{-}Ct} = 0.38(10^6 T^{-2}) - 0.58 \qquad (23)$$

These equations are considered to be good estimates of the equilibrium fractionation expressions. Calibration is least satisfactory at high temperatures. The effect of pressure on the solvus thermometer and the intervention of exsolution processes introduce uncertainties in the high grade samples. The variation of $\alpha_{CO_2\text{-carbonate}}$ (for acid decomposition) with the calcite composition may introduce an error of 0.1 to 0.2‰ in the O-isotope composition of the high Mg-calcites or calcite plus exsolved dolomite. Modified relations for (22) and (23) are presented in § 9.2 using only the greenschist facies samples. High angle diffraction maxima are sharp for these samples. However, possible uncertainties in the solvus extrapolation may cause a consistent calibration error.

The high Mg-calcites of variable composition are cloudy. Blebs of dolomite in calcite are occasionally observed but micro- or cryptoexsolved dolomite probably is present in these cloudy calcites (Goldsmith, 1962). These features are consistent with a thermodynamic model for the

calcite-dolomite binary system. This model assumes that none of the structure-sensitive thermodynamic properties such as G have a discontinuity between ordered dolomite and calcite, with an absence of long range order. Delineation of the metastable-unstable boundary, the spinodal point, shows that the high Mg-calcites possibly were unstable and spontaneously decomposed under near surface P,T conditions. The calibration of the fractionation with the solvus thermometer is valid if the Mg-calcite composition measured is a relict from the high temperature quench. Considering all these things, the observed fractionation trends shown in Figures 18 and 19 are reasonable.

Neither of the derived fractionation expressions are very temperature sensitive. However, the well defined relation between $10^3 \ln \alpha^{C^{13}}_{D-Ct}$ and $10^3 \ln \alpha^{O^{18}}_{D-Ct}$ ((21) and Fig. 17) is a powerful test for concordant equilibrium, attained at a semi-quantitatively known temperature.

Examination of a suite of samples from the biotite zone has shown that, although equilibrium was attained at a single temperature for Mg, C- and O-isotopes, the size of the exchange equilibrium system was quite limited, less than a few feet, across the inferred relict bedding. Decarbonation is insignificant in these rocks. The absence of a pore fluid may be responsible for the lack of a mechanism for extensive equilibration. The isotopic composition of the marbles is similar to that of diagenetically altered limestone. The application of isotopic fractionations as a test for equilibrium gains power when combined with the isotopes used as tracers to give information on the size of the equilibrium system or exchange processes.

There is no general variation in the isotopic composition of marbles with metamorphic grade (Fig. 25). However, all high grade samples from the Chester dome area are appreciably lighter in O^{18} than limestones. This is probably a consequence of a combination of processes: decarbonation and exchange with an oxygen reservoir. Isotopic studies of exchange processes and decarbonation reactions in high temperature assemblages should throw some light on to the nature of these processes. The exploratory results of this study in the Chester dome and Grenville indicate that a detailed analysis will be necessary. Moreover, complications arising from exsolution phenomena, variability in apparent quench temperature of adjacent samples and retrograde exchange of some phases are problems which must be contended with.

The relationship between the quench temperature and the thermal and geological history of the samples requires further exploration.

Laboratory equilibration studies must play a dominant role in the development of the isotopic thermometers. Although the equilibrium dolomite-calcite C-isotope fractionation has not been satisfactorily calibrated in the laboratory experiments of this work, a greater understanding of the problems associated with partial exchange experiments has been achieved. Until these problems are resolved completely caution must be applied to the application of the results of incomplete exchange experiments to the interpretation of natural fractionation data.

APPENDIX I

1. Hydrothermal Experiments

1.1 Composition of Typical Initial Charge

H_2O	83.5 mg.
$CaCl_2$(sol)	16.4 mg.
NH_4Cl	6.7 mg.
NH_4HCO_3	5.1 mg.
$CaCO_3$	65.0 mg.
$CaMg(CO_3)_2$	65.0 mg.

where $CaCO_3$ is: (1) H-calcite; (2) L-calcite; or (3) 42.8 mg. H-calcite plus 22.2 mg A-calcite.

1.2 NH_4HCO_3 Correction

The NH_4HCO_3 added to each run changes the initial dolomite-calcite fractionation through exchange. This has been corrected for by assuming that the addition of NH_4HCO_3 is equivalent to the addition of a certain number of moles of $CaCO_3$ with the isotopic composition of NH_4HCO_3. The amount of $CaCO_3$ added in this way, in a given run, is calculated by material balance. For example:

(1) Initial composition

$$\delta_{total} = (\text{C-atom }\%_{Ct})\ \delta_{Ct} + (\text{C-atom }\%_{D})\ \delta_{D} + (\text{C-atom }\%_{NH_4HCO_3})\ \delta_{NH_4HCO_3}$$

e.g. for CtD III:

$$\delta_{\text{total}} = (0.4571)(8.80) + (0.4972)(2.94) + (0.0457)(-25.80)$$

$$\delta_{\text{carbonate}} = 4.31‰$$

$$\delta_{\text{Ct + D}} = 5.73‰$$

(2) Final composition

$$\delta_{\text{total}} = (0.4790)(5.31) + (0.5210)(4.29)$$

$$\delta_{\text{Ct + D}} = 4.76‰$$

(3) Amount of NH_4HCO_3 exchanged is given by X where

$$(0.6500)(8.80) + (0.7065)(2.94) + \left(\frac{X}{79}\right)(-25.80) = (1.36 + X)(4.76)$$

$$X = 0.0468 \text{ moles}$$

$$= 4.3 \text{ mg.}$$

The intial isotopic composition of the calcite is corrected accordingly.

APPENDIX II

Sample Localities and Description of Analysed Specimens

1. Southwestern Vermont

Abbreviations: Qtz = quartz; Phl = phlogopite; Act = actinolite; Op = opaques.

Vt 3-51 Loc.: Middlebury quadrangle, 3.5 miles W. of Middlebury on U.S. 125 Highway. Ordovician Burchards formation. Chlorite zone. D = 41%, Ct = 52%, Qtz = 7%, Op = tr. Chemically separated. Black fine grained meta-limestone weathering with buff patches. D in 0.01 mm. brown subhedral rhombs associated with anhedral Ct. Qtz in 0.01 mm. subangular grains.

Vt 3-48 Loc.: Middlebury quadrangle. 0.25 mile W. of New Haven Junction on U.S. 17 Highway. Ordovician Bascom formation. Chlorite zone D = 30%, Ct = 57%, Qtz = 12%, Op = 1%. Chemically separated. Black fine grained meta-limestone. D in 0.04 mm. euhedral rhombs in finer grained Ct-Qtz matrix. Ct in 0.02 mm. anhedral grains. Qtz subangular 0.01 mm. grains.

Vt 4-29 Loc.: Middlebury quadrangle, 1 mile E. of Weybridge along Otter Creek. Ordovician Beldens formation. Chlorite zone. D = 76%, Ct = 27%, Qtz = 6%, Op = 1%. Chemically separated. Grey fine grained meta-limestone. D in euhedral rhombs, 0.02 mm. Ct in interstitial, elongate blebs parallel to bedding. Qtz subrounded, 0.02 mm. Pyrite euhedral.

Vt 3-65 Loc.: Bomoseen quadrangle. 1.1 mile E. of Hortonville. Ordovician Hortonville formation. Chlorite zone. D = 45%, Ct = 52%, Qtz = 2%, Op = 1%. Chemically separated. Fissile blue-grey meta-limestone with veinlets of Ct. D in 0.01 mm. brown euhedral to subhedral rhombs associated locally with graphite (?). Ct is anhedral, interstitial, 0.01 mm., and locally coarser grained or veining (0.4 mm.). Qtz subangular relict clastic grains, 0.15 mm. Relict lamination shown by more D rich layers.

Vt 3-47 Loc.: Middlebury quadrangle, 0.7 mile E. of New Haven Junction on U.S. 17 Highway. Ordovician Burchards formation. Biotite zone. D = 47%, Ct = 42%, Qtz = 8%, Phl = 2%, Op = 1%. Chemically separated. Blue-grey meta-limestone. D and Ct equigranular subhedral in 0.1 mm. grains. Qtz subrounded 0.1 mm. Phl evenly distributed but not elongate parallel.

Vt 4-23 Loc.: Brandon quadrangle, Landon quarry, 3 miles S. 15 E. of Brandon. Ordovician Shelburne formation. Biotite zone. D = 4%, Ct = 96%, Qtz = tr, Sericite = tr, Op = tr. White marble with intricately plicated dolomite beds up to 2 mm. thick which weather buff colour. D in elongate blebs up to 1 mm. in subhedral twinned Ct matrix. Ct equant 0.3 mm.

Vt 4-11B Loc.: Equinox quadrangle, Kent quarry, South Dorset. Ordovician Shelburne formation. White and grey banded marbles. Biotite zone.

	D(%)	Ct(%)	Qtz(%)	Phl+Act(%)	Chl(%)	Op(%)	Depth (ft.)
1		95	2		3		2
2		72	6	8	14	tr	22
3		97	1	2			36
4		98	1	1			40
5		99	tr	1		tr	47
6	2	98	tr	tr			59
7		53	3	4	38	2	65
8	4	85	1	2	8	tr	70.5
9	14	82	1	2	1	tr	74
17		96	1		3	tr	77
10		98	2	tr		tr	79
11		100					89
12	80	13	1	5		1	92

Vt 4-11B (continued)

	D(%)	Ct(%)	Qtz(%)	Phl+Act(%)	Chl(%)	Op(%)	Depth (ft.)
13		95	2		3	tr	101
14		97	1		2	tr	111.5
15	6	93	tr	1			118.5
16		98	2		tr		128.5

D in 0.2 to 0.5 mm. subhedral grains in D rich layers parallel to inferred relict bedding. D-Qtz coexist stably. Ct in 0.2 to 0.4 mm. anhedral grains except in Vt 4-11B-11 where Ct is coarsely crystalline vein, 1.5 cm. crystals. Chlorite in bent wavy streaks parallel to inferred relict bedding. Qtz in 0.25 mm. subrounded grains. Pyrite grains up to 0.5 mm.

Vt 3-83-3 Loc.: Equinox quadrangle, Valley quarry, South Dorset. Ordovician Shelburne formation. Biotite zone.
D = 80%, Ct = 5%, Qtz = 12%, Phl+Sericite = 3%, Op = tr.
Massive grey dolomite bed weathering to buff colour. Patches of Qtz-Ct in finer grained D-Qtz matrix with about 1% Ct. Phyllosilicates in matrix. Ct in 0.2 mm. anhedral grains. Qtz in 0.3 mm. anhedral rounded grains associated with Ct-Qtz patches. D subhedral, 0.1 mm. D-Qtz coexist.

Vt 4-10-2, -3-1, -3-2, -4, Valley Quarry.
Ct = 96%, Qtz = 2%, Act+Sericite + 2%, Op = tr
White marble with faintly greenish streaks of actinolite. Ct in 0.3 mm. anhedral grains. Actinolite fibres parallel to inferred relict bedding.

Vt 4-12-1 Loc.: Equinox quadrangle, Bennington quarry, South Dorset. Ordovician Shelburne formation. Biotite zone.
D = 17%, Ct = 71%, Qtz = 10%, Phl+Sericite = 3%, Op = tr.
White banded marble. D 0.2 mm. subhedral. Ct 0.3 mm. anhedral. Quartz 0.3 mm. rounded. D-Qtz coexist. D-Ct richer layers and Ct-Qtz richer layers.

2. Southeastern Vermont

Vt 3-76 Loc.: Wilmington quadrangle, 2 miles S. 20 W. of Whitingham, Cambrian (?) Cavendish formation, Sherman Marble. Garnet or Staurolite-Kyanite zone. D = 63%, Ct = 34%, Qtz = tr, Phl = 2%. Cream coloured marble. D subhedral to anhedral, 0.5 mm. Ct elongate interstitial blebs, 3 mm. long. D weakly idioblastic. Ct richer layers parallel to foliation. Qtz anhedral, 0.1 mm. D-Qtz coexist.

Vt 3-74 Loc.: Ludlow quadrangle, 1 mile S. of Felchville on U.S. 106 Highway. Cambrian (?) Cavendish formation. Staurolite-Kyanite zone. D = 71%, Ct = 26%, Qtz = 1%, Phl = 2%, Microcline = tr. Buff dolomitic marble. D anhedral with curved grain boundaries. D and Ct equigranular, anhedral 0.3 mm. D strongly twinned. Ct-Qtz rich layers not associated with Phl. D-Qtz coexist. Ct-Qtz layers parallel to foliation.

Vt 3-75 Loc.: Saxtons River quadrangle, on Vermont State Highway 35, 0.7 miles S. of Williams River, Grafton Gulf. Cambrian (?) Cavendish formation. Staurolite-Kyanite zone. D = 88%, Ct = 3%, Qtz = 3%, Phl = 1%, Microcline = 5%. White dolomitic marble. D 0.4 mm. anhedral. Ct 0.4 mm. anhedral, interstitial. Ct-microcline-Qtz rich layers parallel to foliation. D strongly twinned. D-Qtz coexist.

Vt 4-37 Loc.: Ludlow quadrangle, 0.5 mile S. of Amsden by Black River. Cambrian (?) Cavendish formation. Staurolite-Kyanite zone.

	D(%)	Ct(%)	Qtz(%)	Phl(%)
1	94	3	2	1
2	93	4	3	tr
3	6	86		8
4	76	22	2	tr
5	69	26		5

Buff marbles with white Ct rich bands. D and Ct anhedral with curved interfaces, D convex, equigranular 0.3 mm. except Vt 4-37-3. This has D(0.3 mm.) rich layers adjacent to Phl rich layers and coarse Ct, 2 mm.

Vt 4-35 Loc.: Ludlow quadrangle, Duttonsville Gulf, 3 miles N. of Gassetts. Cambrian (?) Cavendish formation. Staurolite-Kyanite zone.

	D(%)	Ct(%)	Qtz(%)	Phl+Act.(%)
1a, 2a	53	33	tr	14
1b, 2b	34	48	tr	18
5	70	25	2	3

Vt 4-35-1a and -2a are from the same schist band but 5 inches apart. Vt 4-35-1b and -2b are from the adjacent schist band ½ inch below. Vt 4-35-5 is from a massive marble unit 4 feet across the foliation from Vt 4-35-1a and -1b.

Vt 4-35-1a and -1b: Calcareous schist. D. anhedral, equant, 0.3 mm. Ct in carbonate rich layers is anhedral, 0.3 mm. Ct in silicate rich layers is anhedral elongate, 1 mm. Ct is more abundant than D in silicate rich regions. Some Ct are locally cloudy. Act is restricted to silicate bands. Phl occurs both in silicate bands and in carbonate richer regions. D-Qtz coexist.

Vt 4-35-5: Buff dolomitic marble. D and Ct anhedral, equigranular, 0.3 mm. Phl rich and Qtz rich layers parallel to foliation. D-Qtz coexist.

3. Grenville Province Samples

Abbreviations: Phl = phlogopite, Fo = forsterite, Serp = serpentine.

G Ch-14 Loc.: Chandos Twp., 2.5 miles E. of Lasswade on road. Lower (?) Amphibolite facies.
D = 70%, Ct = 14%, Phl = tr, Fo + Serp = 16%.
White dolomitic marble with 2 to 4 mm. bands of Ct plus Fo. D anhedral, 0.5 to 1 mm. Ct anhedral, interstitial, 0.4 mm. D weakly idioblastic. Ct restricted to Fo rich bands. Ct probably produced by dedolomitization. Fo strongly serpentinized. Ct cloudy.

G 4-54-1 Loc.: Denbigh Twp., 1 mile N.E. of Hydes Creek on Highway 41. Sillimanite-muscovite-almandine subfacies (Evans, 1964).
D = 94%, Ct = 4%, Phl + Fo = 2%, Pyrite = tr.
White marble. D anhedral, 2 to 2.5 mm. Ct anhedral, interstitial, 0.2 mm. Ct cloudy. Fo partially serpentinized. Pyrite euhedral, 0.2 mm.

G 4-55 Loc.: Denbigh Twp., 0.4 mile N.E. of Hydes Creek on Highway 41. Sillimanite-muscovite-almandine subfacies.
D = 96%, Ct = 3%, Fo = 1%, Graphite = tr.
Grey marble. D anhedral, curved interfaces, 1 to 1.5 mm. Ct anhedral, interstitial, 0.2 mm. Ct cloudy and with odd bleb of D in no specific orientation.

G 4-6 Loc.: Griffith Twp., 1.2 miles N.E. of Hydes Creek on Highway 41. Sillimanite-muscovite-almandine subfacies.
Grey marble. D anhedral, 2 to 2.5 mm. Ct anhedral, interstitial, 0.2 mm.
D = 96%, Ct = 2%, Fo = 1%, Pyrite + Graphite = 1%.
Grey marble. D anhedral, 2 to 2.5 mm. Ct anhedral, interstitial, 0.2 mm. Fo with only trace of serpentinization.

M 16 Loc.: Monmouth Twp., Boundary between Lots 13-14, Con.XIV. Collected by H.S. Armstrong. Upper Amphibolite facies.
D = 37%, Ct = 50%, Phl + Fo + Chondrodite = 13%.
Coarse white marble with buff chondrodite rich bands, 1 to 2 cm. wide. D subhedral, with ragged outlines and intergrown with D. D 1.5 to 2 mm. Ct interstitial to D and silicates and in anhedral blebs, 3 mm. Ct restricted to silicate layers. Partial serpentinization of Fo. Ct cloudy. Trace of Phl.

G 4-5-3 Loc.: Renfrew Co., Horton Twp., 0.5 mile N.E. of Payne. Upper Amphibolite facies.
D = 31.%, Ct = 44%, Fo + Phl 25%, Op = tr.
D and Ct anhedral, equigranular, with curved grain boundaries, 0.5 mm. Ct is cloudy but margins tend to be clearer. Fo strongly serpentinized.

G 4-3 Loc.: Renfrew Co., Ross Twp., 1.5 miles E. of Haley Station. Upper Amphibolite facies.
D = 6%, Ct = 85%, Phl = 4%, Fo = 4%, Op = 1%.
Grey marble. Ct anhedral, 2 to 3 mm. D anhedral, interstitial, 0.4 mm. Ct with ragged boundaries and intergrown with Ct. Ct is cloudy with odd bleb of D. Phl and Fo rich layers.

GLSK Loc.: Pontefract Twp., Pontiac Co., Gibb Lake, Quebec. Upper Amphibolite facies.
D = 36%, Ct = 44%, Phl = tr, Fo + Serp = 20%.
White marble with abundant brown grains of serpentinized Fo. Marble is adjacent to the phlogopite zone of the zoned skarn (Shaw et al., 1965). D anhedral, clear, 2 to 3 mm. Ct anhedral, cloudy, 3 mm. A few large composite grains of Ct contain blebs of exsolved D (Shaw et al., 1965, Fig. 5). Fo is strongly serpentinized.

G 5-1 Loc.: Parry Sound District, Seguin River, E. side of bridge. Upper (?) Amphibolite facies.
D = 35%, Ct = 36%, Fo + Phl = 29%, Spinel = tr.
White marble with abundant grains of Fo and porphyroblasts of Phl (2 cm.). D and Ct equigranular, anhedral, 3 to 4 mm. with curved interfaces. Ct is cloudy. Blebs of D seen in a few grains.

G 5-1b Loc.: Parry Sound District, Seguin River, W. side of the river. Upper (?) Amphibolite facies.
D = 59%, Ct = 37%, Phl + Fo = 4%
Coarse white marble with irregular Fo bands. D and Ct equigranular, anhedral, 3 to 4 mm. D generally clear. Ct cloudy. Fo is partially serpentinized.

G 3-11-1 Loc.: Leeds Co. Bastard Twp., 0.8 mile S. 20 E of Philipsville. Granulite facies.
D = 32%, Ct = 66%, Serpentine = 2%.
White marble. D and Ct anhedral, equigranular, 0.5 mm. Ct is cloudy. Few irregular blebs of D in Ct. Patches of serpentine after Fo (?).

G 4-40 Loc.: Madoc Twp., 1 mile N. on Highway 62 from Madoc. Greenschist facies.
Black banded recrystallized meta-limestone. Ct with little Qtz and Pyrite. No D.

G 4-61 Loc.: Madoc Twp., 1 mile S. 70 E. of Madoc, old Talc quarry. Contact aureole in Greenschist facies.
White banded D-Ct-Tremolite-Talc rock.

BIBLIOGRAPHY

ANDERSON, A.T. and CLAYTON, R.N. (1966) Equilibrium oxygen isotope fractionation between minerals in igneous, meta-igneous, and metasedimentary rocks. Am. Geoph. Union Meeting, Washington, 212.

AVERBACH, B.L., FLINN P.A. and COHEN, M. (1954) Solid solution formation in the gold-nickel system. Acta Met. 2, 92.

BAIN, G.W. (1933) The Vermont marble belt. 16th Int. Geol. Cong Guidebook 1, p. 75-80.

BELL, P.M. (1963) Aluminum silicate system: Experimental determination of the triple point. Science, 139, No. 3539, 1055.

BIGELEISEN, J. and MAYER, M.G. (1947) Calculation of equilibrium constants for isotopic exchange reactions. J. Chem. Phys. 15, 261.

BOTTINGA, J. (1963) Oxygen isotopes in geology. M.Sc. Thesis, University of British Columbia.

BOWEN, N.L. (1940) Progressive metamorphism of siliceous limestone and dolomite. J. Geol. 48, 225.

BUNTON, C.A., CRAIG, D.P. and HALEVI, E.A. (1955) The kinetics of isotopic exchange reactions. Trans. Faraday Soc., 51, 196.

CADY, W.M., ALBEE, A.L. and MURPHY, J.F. (1962) Bedrock geology of the Lincoln Mountain quadrangle, Vermont. U.S. geol. Survey Quadrangle Map, GQ-164.

CHANG, L.L.Y. (1965) Subsolidus phase relations in the systems $BaCO_3$-$SrCO_3$, $SrCO_3$-$CaCO_3$, and $BaCO_3$-$CaCO_3$. J. Geol. 73, 346.

CHAVE, K. E. (1954) Aspects of the biogeochemistry of magnesium: 2. Calcareous sediments and rocks. J. Geol. 62, 587.

CLARK, S.P. (1961) A redetermination of equilibrium relations between kyanite and sillimanite. Amer. J. Sci. 259, 641.

CLAYTON, R.N. and EPSTEIN, S. (1958) The relationship between O^{18}/O^{16} ratios in coexisting quartz, carbonate and iron oxides from various geological deposits. J. Geol. 66, 352.

CLAYTON, R.N. (1959) Oxygen isotope fractionation in the system calcium carbonate-water. J. Chem. Phys. 30, 1246.

CLAYTON, R.N. and DEGENS, E.T. (1959) Use of carbon isotope analysis for differentiating fresh water and marine sediments. Bull. Assoc. Am. Petr. Geol. 43, 890.

CLYATON, R.N. (1961) Oxygen isotope fractionation between calcium carbonate and water. J. Chem. Phys. 34, 724.

CLAYTON, R.N. (1963) Oxygen isotope geochemistry: thermometry of metamorphic rocks. Studies in Analytical Geochemistry, (ed. D.M. Shaw), p.42. The Royal Society of Canada Special Publications, No. 6. University of Toronto.

CLAYTON, R.N. (1965) Personal communication.

CLAYTON, R.N. (1966) Oxygen isotope exchange in rock-water systems. Am. Geoph. Union Meeting, Washington, 203, 1966.

CRAIG, H. (1953) The geochemistry of the stable carbon isotopes. Ceochim. et Cosmochim. Acta. 3, 53.

CRAIG, H. (1957) Isotopic standards for carbon and oxygen, and correction factors for the mass spectrometric analysis of carbon dioxide. Geochim. et Cosmochim. Acta. 12, 133.

CRAIG, H. (1961) Standards for reporting concentrations of deuterium and oxygen-18 in natural waters. Science 133, 1833.

DALE, T.N. (1912) The commercial marbles of western Vermont. U.S. Geol. Survery Bull. 521, 170 pp.

DEGENS, E.T. and EPSTEIN, S. (1964) Oxygen and carbon isotope ratios in coexisting calcites and dolomites from recent and ancient sediments. Geochim. et Cosmochim. Acta. 28, 23.

DOLL, C.G. (1961) Geologic map of Vermont. Vt. Geol. Survey.

ENGEL, A.E.J., CLAYTON, R.N. and EPSTEIN, S. (1958) Variations in isotopic composition of oxygen and carbon in Leadville limestone (Mississippian, Colorado) and its hydrothermal and metamorphic phases. J. Geol. 66, 374.

EPSTEIN, S., BUCHSBAUM, R., LOWENSTAM, H and UREY, H.C. (1951) Carbonate-water isotopic temperature scale. Bull. Geol. Soc. Am. 62, 417.

EPSTEIN, S., BUCHSBAUM, R., LOWENSTAM, H. and UREY, H.C. (1953) Revised carbonate-water isotopic temperature scale. Bull. Geol. Soc. Am. 64, 1315.

EPSTEIN, S., GRAF, D.L., and DEGENS, E.T. (1964) Oxygen isotope studies on the origin of dolomites. Isotopic and Cosmic Chemistry, dedicated to H.C. Urey 70th Birthday (eds. H. Craig, S.L. Miller and G.R. Wasserburg), p. 188. North Holland, Amsterdam.

EVANS, A.M. (1964) Geology of Ashby and Denbigh Townships. Ontario Dept. Mines, Geol. Rept. No. 26.

FEIGL, F. (1958) Spot tests in inorganic analysis. 5th Edition. Elsevier, Amsterdam.

FOWLER, P. (1950) Stratigraphy and structure of the Castleton area, Vermont. Vt. Geol. Survey, Bull. 2, 83 pp.

FRENCH, B.M. (1964) Graphitization of organic material in a progressively metamorphosed Precambrian iron formation. Science, 146, 917.

FRIEDMAN, G.M. (1959) Identification of carbonate minerals by staining methods. Jour. Sedimentary Petrology, 29, 87.

FRIEDMAN, I. and HALL, W.E. (1963) Fractionation of O^{18}/O^{16} between coexisting calcite and dolomite. J. Geol. 71, 238.

FROST, A.A. and PEARSON, R.G. (1961) Kinetics and mechanisms. 2nd Edition. John Wiley, New York.

GARLICK, G.D. (1964) Oxygen isotope ratios in coexisting minerals of metamorphic rocks. Ph.D. Thesis. California Institute of Technology.

GOLDSMITH, J.R., GRAF, D.L. and JOENSUU, O.I. (1955) The occurrence of magnesian calcites in nature. Geochim. et Cosmochim Acta 7, 212.

GOLDSMITH, J.R. and GRAF, D.L. (1958) Relations between lattice and composition of the Ca-Mg carbonates. Am. Mineral. 43, 84.

GOLDSMITH, J.R. (1960) Exsolution of dolomite from calcite. J. Geol. 68, 103.

GOLDSMITH, J.R. and GRAF, D.L. (1960) Subsolidus relations in the system $CaCO_3$-$MgCO_3$-$MnCO_3$. J. Geol. 68, 324.

GOLDSMITH, J.R. and HEARD, H.C. (1961) Subsolidus phase relations in the system $CaCO_3$-$MgCO_3$. J. Geol. 69, 45.

GOLDSMITH, J.R. (1962) Private communication to H.P. Schwarcz.

GOLDSMITH, J.R., GRAF, D.L., WITTERS, J. and NORTHROP, D.A. (1962) Studies in the system $CaCO_3$-$MgCO_3$-$FeCO_3$: 1. phase relations; 2. a method for major-element spectrochemical analysis; 3. compositions of some ferroan dolomites. J. Geol. 70, 659.

GRAF, D.L. and GOLDSMITH, J.R. (1955) Dolomite-magnesian calcite relations at elevated temperatures and CO_2 pressures. Geochim. et Cosmochim. Acta 7, 109.

GRAF, D.L. and GOLDSMITH, J.R. (1958) The solid solubility of $MgCO_3$ in $CaCO_3$. A revision. Geochim. et Cosmochim. Acta 13, 218.

GROSS, M.G. and TRACEY, J.I. (1966) Oxygen and carbon isotopic composition of limestones and dolomites, Bikini and Eniwetok atolls. Science, 151, No. 3714, 1082.

GUGGENHEIM, E. A. (1959) Thermodynamics (4th ed.) North Holland, Amsterdam.

HARDY, H.K. (1953) A "sub-regular" solution model and its application to some binary alloy systems. Acta Metallurg. 1, 202.

HARKER, R.I. and TUTTLE, O.F. (1955) Studies in the system CaO-MgO-CO_2: Part 2. Limits of solid solution along the binary join $CaCO_3$-$MgCO_3$. Amer. J. Sci. 253, 274.

HAUL, R. A.W. and STEIN, L.H. (1955) Diffusion in calcite crystals on the basis of isotopic exchange with carbon dioxide. Trans. Far. Soc. 51, 1280.

HEWITT, P.C. (1961) The Geology of the Equinox Quadrangle and vicinity, Vermont. Vt. Geol. Survey, Bull. 18, 83pp.

HOERING, T.C. (1961) The physical chemistry of isotopic substances. Ann. report of the Director of the Geophysical Laboratory, 203.

HOLM, J.L. and KLEPPA, O.J. (1966) The thermodynamic properties of the aluminium silicates. Submitted to J. Phys. Chem.

HURLEY, P.M., HUGHES, H., PINSON, W.H. and FAIRBAIRN, H.W. (1962) Radiogenic argon and strontium diffusion parameters in biotite at low temperatures obtained from Alpine fault uplift in New Zealand. Geochim. et Cosmochim. Acta 26, 67.

JAMES, H.L. and CLAYTON, R.N. (1962) Oxygen isotope fractionation in metamorphosed iron formations of the Lake Superior region and in other iron-rich rocks. Petrologic Studies: A Volume to Honor A.F. Buddington Geol. Soc. Amer., 217.

JOY, H.W. and LIBBY,W F. (1960) Size effects among isotopic molecules. J. Chem. Phys. 33, 1276.

KEITH, M.L. and WEBER, J.N. (1964) Carbon and oxygen isotopic composition of selected limestones and fossils. Geochim. et Cosmochim. Acta 28, 1787.

LERMAN, A. (1965) Paleoecological problems of Mg and Sr in biogenic calcites in light of recent thermodynamic data. Geochim. et Cosmochim. Acta. 29, 977.

LONG, J.V.P. and AGRELL, S.O. (1965) The cathodo-luminescence of minerals in thin section. Min. Mag. 34, Tilley Volume, 318.

LOWENSTAM, H.A. (1963) Biologic problems relating to the composition and diagenesis of sediments. In The Earth Sciences, Ed. T.W. Donnelly, p. 137. University of Chicago.

LUMBERS, S.B. (1964) Preliminary report on the relationship of mineral deposits to intrusive rocks and metamorphism in part of the Grenville province of southeastern Ontario. Ontario Dept. Mines, Preliminary Report,1964-4.

LUMBERS, S.B. (1965) Personal communication.

McCREA, J.M. (1950) On the isotopic chemistry of carbonates and a paleo-temperature scale. J. Chem. Phys. 18, 849.

McKINNEY, C.R., McCREA, J.M., EPSTEIN, S., ALLEN, H.A. and UREY, H.C. (1950) Improvements in mass spectrometers for the measurement of small differences in isotope abundance ratios. Rev. Sci. Instr. 21, 724.

McNAMARA, M. (1965) The lower greenschist facies in the Scottish Highlands. Geol. Fören. Förh. 87, 347.

MILLER, R.L. and KAHN, J.S. (1962) Statistical analysis in the Geological sciences. John Wiley, New York.

MOREY, G.W. (1962) The action of water on calcite, magnesite and dolomite. Am. Mineral. 47, 1456.

NEWTON, R.C. (1966) Kyanite-sillimanite equilibrium at 750°C. Science, 151, No. 3715, 1223.

NIER, A.O. (1947) A mass spectrometer for isotope and gas analysis. Rev. Sci. Instr. 18, 398.

NORTHROP, D.A. (1964) Oxygen isotope fractionations in systems containing dolomite. Ph.D. Thesis, University of Chicago.

NORTHROP, D.A. and CLAYTON, R.N. (1966) Oxygen-isotope fractionations in systems containing dolomite. J. Geol., 74, 174.

O'NEIL, J.R. (1963) Oxygen isotope fractionation studies in mineral systems. Ph.D. Thesis, University of Chicago.

O'NEIL, J.R. and CLAYTON, R.N. (1964) Oxygen isotope geothermometry. Isotopic and Cosmic Chemistry, dedicated to H.C. Urey 70th Birthday (eds. H. Craig, S.L. Miller and G.T. Wasserburg), p.157. North Holland, Amsterdam.

O'NEIL, J.R. and TAYLOR, H.P. (1965) The oxygen isotope chemistry of felspars. Am. Geoph. Union Meeting, Washington.

O'NEIL, J.R. and TAYLOR, H.P. (1966) Oxygen isotope equilibrium between muscovite and water. Am. Geoph. Union Meeting, Washington, 212.

O'NEIL, J.R. and EPSTEIN, S. (1966) Oxygen isotope fractionation in the system dolomite-calcite-CO_2. Science, 152, No. 3719, 198.

PRIGOGINE, I. and DEFAY, R. (1954) Chemical thermodynamics. Longmans, London.

ROSENBERG, P.E. (1963) Subsolidus relations in the system $CaCO_3$-$FeCO_3$. Am. Jour. Sci. 261, 683.

ROSENBERG, P.E. and HOLLAND, H.D. (1964) Calcite-dolomite-magnesite stability relations in solutions at elevated temperatures. Science, 145, No. 3633, 700.

SCHWANDER, H. (1953) Bestimmung des relativen Sauerstoffisotopen - Verhaltnisses in Silikatgesteiner und - Mineralien; Geochim. et Cosmochim. Acta 4, 261.

SCHWARCZ, H.P. and CLAYTON, R.N. (1965) Oxygen isotopic studies of amphibolites. Can. J. Earth Sci. 2, 72.

SCHWARCZ, H.P. (1966) Oxygen and carbon isotopic fractionation between coexisting metamorphic calcite and dolomite. J. Geol. 74,38.

SHARMA, T. and CLAYTON, R.N. (1965) Measurement of O^{18}/O^{16} ratios of total oxygen from carbonates. Geochim. et Cosmochim. Acta, 29, 1347.

SHARMA, T., MUELLER, R.F. and CLAYTON, R.N. (1965) O^{18}/O^{16} ratios of minerals from the iron formations of Quebec. J. Geol. 73, 664.

SHAW, D.M., MOXHAM, R.L., FILBY, R.H. and LAPKOWSKY, W.W. (1963) The petrology and geochemistry of some Grenville skarns. Part 2. Geochemistry. Can. Mineralogist, 7, 578.

SHAW, D.M., SCHWARCZ, H.P. and SHEPPARD, S.M.F. (1965) The petrology of two zoned scapolite skarns. Can. J. Earth Sci. 2,577.

SILVER, L.T. and LUMBERS, S.B. (1965) Geochronologic studies in the Bancroft-Madoc area of the Grenville Province, Ontario, Canada. Geol. Soc. Am. Annual Meeting, Kansas City, 153.

SILVERMAN, S.R. (1951) The isotope geology of oxygen. Geochim. et Cosmochim. Acta 2, 26.

SKEHAN, J.W. (1961) The Green Mountain anticlinorium in the vicinity of Wilmington and Woodford, Vermont. Vt. Geol. Survey, Bull. 17, 159pp.

TAKENOUCHI, S. and KENNEDY, G.C. (1964) The binary system H_2O-CO_2 at high temperatures and pressures. Am. Jour. Sci. 262, 1055.

TAUBE, H. (1954) Use of oxygen-isotope effects in the study of hydration of ions. J. Phys. Chem. 58, 523.

TAYLOR, H.P. and EPSTEIN, S. (1962a) Relationship between O^{18}/O^{16} ratios in coexisting minerals of igneous and metamorphic rocks, Part 1: Principles and experimental results. Bull. Geol. Soc. Am. 73, 461.

TAYLOR, H.P. and EPSTEIN, S. (1962b) Relationship between O^{18}/O^{16} ratios in coexisting minerals of igneous and metamorphic rocks, Part 2: Applications to petrologic problems. Bull. Geol. Soc. Am. 73, 675.

TAYLOR, H.P. and EPSTEIN, S. (1962c) Oxygen isotope studies on the origin of tektites. J. Geophys. Res. 67, 4485.

TAYLOR, H.P., ALBEE, A.L. and EPSTEIN, S. (1963) O^{18}/O^{16} Ratios of coexisting minerals in three assemblages of kyanite-zone pelitic schist. J. Geol. 71, 513.

TAYLOR, H.P. and COLEMAN, R.G. (1965) O^{18}/O^{16} Ratios of coexisting minerals in glaucophane-bearing metamorphic rocks. Geol. Soc. Am. Annual Meeting, Kansas City, 170.

THODE, H.G., MONSTER, J. and DUNFORD, H.B. (1961) Sulphur isotope geochemistry. Geochim. et Cosmochim. Acta. 25, 159.

THODE, H.G., SHIMA, M., REES, C.E. and KRISHNAMURTY, K.V. (1965) Carbon-13 isotope effects in systems containing carbon dioxide, bicarbonate, carbonate, and metal ions. Can. Jour. Chem. 43, 582.

THOMPSON, J.B. (1952) Southern Vermont; Guidebook for field trips in New England. Geol. Soc. Am., 65th annual meeting, 14.

THOMPSON, J.B. (1959) Stratigraphy and structure in the Vermont Valley and the eastern Taconics between Clarendon and Dorset. New England Intercoll. Geol. Conf., Guidebook, 51st Annual Meeting, pp. 71-87.

TUTTLE, O.F. (1949) Two pressure vessels for silicate-water studies. Bull. Geol. Soc. Am. 60, 1727.

UREY, H.C. (1947) The thermodynamic properties of isotopic substances. J. Chem. Soc., 562

UREY, H.C., LOWENSTAM, H., EPSTEIN, S.and McKINNEY, C.K. (1951) Measurement of paleotemperatures and temperatures of the Upper-Cretaceous of England, Denmark, and the southeastern United States. Bull. Geol. Soc. Am. 62, 399.

WASSERBURG, G.J., ALBEE, A.L. and LANPHERE, M.A. (1964) Migration of radiogenic strontium during metamorphism. J. Geophys. Res., 69, 4395.

WEBER, J.N. (1964) Oxygen isotope fractionations between coexisting calcite and dolomite. Science, 145, No. 3638, 1303.

WEILL, D.F. (1966) Stability relations in the Al_2O_3-SiO_2 system calculated from the solubilities in the Al_2O_3-SiO_2-Na_3AlF_6 system. Geochim. et Cosmochim. Acta 30, 223.

WYART, J., CURIEN, H. and SABATIER, G. (1961) Exchanges isotopiques des atomes d'oxygène dans les silicates et mécanisme d'interaction eau-silicate. Cursillos y Conferencias Fasc. VIII, Instituto "Lucas Mallada," C.S.I.C. (Espana),27.

WYART, J. and SABATIER. (1961) Echange des atomes dans les felspeths. Action de l'eau. Cursillos y Conferencias Fasc. VIII, Instituto "Lucas Mallada", C.S.I.C. (Espana), 23.

WYNNE-EDWARDS, H.R. (1959) Westport map area, Ontario. Geol. Survey Canada, Map 28-1959.

ZEN, E. (1960) Metamorphism of Lower Paleozoic rocks in the vicinity of the Taconic Range in west-central Vermont. Am. Mineral. 45, 52.